AN ABSTRACT OF THE DISSERTATION OF

Daiki Matsuda for the degree of Doctor of Philosophy in Microbiology presented on January 27, 2004.

Title: Two New Roles for the TYMV tRNA-like Structure: Translation Enhancement and Repression of Minus Strand Synthesis

Abstract approved:

Redacted for Privacy

Theo W. Dreher

Some positive-strand RNA plant viruses possess a transfer RNA-like structure (TLS) at the 3´-terminus of their genomic RNAs. The closest mimicry to tRNA is exhibited by the valylatable TLSs from tymoviruses and furo-like viruses, which are able to interact with key cellular tRNA enzymes: [CTP, ATP]:tRNA nucleotidyltransferase (CCA NTase), valyl-tRNA synthetase (ValRS), and translation elongation factor 1A (eEF1A). In this thesis, I report the discovery of two new roles of the *Turnip yellow mosaic tymovirus* TLS, in translation enhancement (Chapter 2) and repression of minus strand initiation (Chapter 4).

Placement of the 3´-terminal 109 nts of TYMV RNA in a luciferase reporter RNA with a generic 5´-UTR enhanced translation by about 20–fold in cowpea protoplasts. Exhibiting a synergistic relationship with the 5´-cap, the 3´-translation enhancement was largely dependent on the aminoacylatability of the TLS and apparently on eEF1A interaction. In the presence of the 5´-UTR from genomic TYMV RNA, translation of both the overlapping proteins p69 and p206 was strongly dependent on a 5´-cap structure, and was enhanced by the 3´-enhancer. These in vivo results contradict the proposed model in which translation initiation of p206, but not p69, is cap-independent and TLS-dependent (Barends et al. Cell 112(2003):123-9).

In vitro experiments with a partially purified preparation of TYMV replicase have investigated the phenomenon of minus strand repression. Interaction of purified eEF1A•GTP specifically with the valylated TLS decreased the template activity for

minus strand to near-background levels. eEF1A•GTP acts by making the 3′-CCA minus strand initiation site unavailable to the replicase. The influence of eEF1A in simultaneously enhancing translation and repressing minus strand synthesis can be considered a regulation that ensures robust translation early in the infection and that offers a coordinated transition from translation to replication.

Previously shown to be critical for TYMV infectivity, a valylatable TLS was investigated for its role in the replication and infectivity of the bipartite *Peanut clump pecluvirus*. A valylatable TLS provided a small competitive advantage in protoplasts and whole plants. The advantage was more apparent in protoplasts than in whole plants, and more so in the replication protein-encoding RNA1 than in the trans-replicating RNA2.

Two New Roles for the TYMV tRNA-like Structure:

Translation Enhancement and Repression of Minus Strand Synthesis

by

Daiki Matsuda

A DISSERTATION

submitted to

Oregon State University

in partial fulfillment of
the requirements for the
degree of

Doctor of Philosophy

Presented January 27, 2004

Commencement June 2004

Doctor of Philosophy dissertation of Daiki Matsuda

presented on January 27, 2004

APPROVED:

Redacted for Privacy

Major Professor, representing Microbiology

Redacted for Privacy

Head of the Department of Microbiology

Redacted for Privacy

Dean of Graduate School

I understand that my dissertation will become part of the permanent collection of Oregon State University libraries. My signature below authorizes release of my dissertation to any reader upon request.

Redacted for Privacy

Daiki Matsuda, Author

ACKNOWLEDGEMENTS

CONTRIBUTION OF AUTHORS

A. Takagi assisted some of the plasmid constructs used in Chapter 2.

L. Bauer and K. Tinnesand assisted with construction of transcription vectors used in Chapter 3.

W-W. Chiu assisted with data collection in Chapter 3.

Dr. P. Dunoyer assisted with data collection, and equally contributed to Chapter 5.

Dr. O. Hemmer and Dr. C. Fritsch helped designing experiments and writing of Chapter 5.

TABLE OF CONTENTS

TABLE OF CONTENTS (Continued)

TABLE OF CONTENTS (Continued)

LIST OF FIGURES

LIST OF TABLES

LIST OF ABBREVIATIONS

AARS	aminoacyl-tRNA synthetase
Bis	Bis-acrylamide
BSA	Bovine serum albumin
CCA-NTase	[CTP, ATP]:tRNA nucleotidyl transferase
CP	coat protein
DMSO	Dimethylsulfoxide
DNA	Deoxyribonucleic acid
EDTA	Ethylene-diamene-tetracetic acid
eEF1A	eukaryotic elongation factor 1A
EtOH	Ethanol
HSP	heat shock protein
IRES	internal ribosomal entry site
kb	kilobase
kDa	kilodalton
MMC	mannitol-MES-calcium
mRNA	messenger RNA
nt	nucleotide
OP	overlapping protein (TYMV p69)
ORF	open reading frame
PABP	poly(A) binding protein
PCBP	poly(C) binding protein
PAGE	polyacrylamide gel eletrophoresis
PEG	polyethylene glycol
PCR	polymerase chain reaction
RdRp	RNA-dependent RNA polymerase
RP	replication protein
RNA	ribonucleic acid
SDS	sodium dodecylsulfate
TE	10 mM Tris-HCl, 1 mM EDTA
3′-TE	lucteovirus translation element
tRNA	transfer-RNA
TLS	tRNA-like structure
UTR	untranslated region
UPSK	upstream pseudoknot
UV	Ultraviolet
YT	Yeast tryptone broth
AMV	*Alfalfa mosaic alfamovirus*
BMV	*Brome mosaic bromovirus*
BSBV	*Beet soil-borne pomovirus*
BYDV	*Barley yellow dwarf luteovirus*

CMV	*Cucumber mosaic cucumovirus*
ELV	*Erysimum latent tymovirus*
EMV	*Eggplant mosaic tymovirus*
IPCV	*Indian peanut clump pecluvirus*
KYMV	*Kennedya mosaic tymovirus*
OYMV	
PCV	*Peanut clump pecluvirus*
PMTV	*Potato mop-top pomovirus*
TBSV	*Tomato busy stunt tombusvirus*
TCV	*Turnip crinkle virus*
TMV	*Tobacco mosaic tobamovirus*
TYMC	*Turnip yellow mosaic tymovirus*, Corvallis strain
TYMV	*Turnip yellow mosaic virus*
SBWMV	*Soil-borne wheat mosaic furovirus*
SHMV	*Sunn-hemp mosaic tobamovirus*

To my father and mother

Two New Roles for the TYMV tRNA-like Structure:
Translation Enhancement and Repression of Minus Strand Synthesis

Chapter 1 <u>INTRODUCTION</u>

Since the discovery of *Turnip yellow mosaic virus* (TYMV) in the mid 1940's (Markham and Smith, 1946), TYMV has been one of the best-studied positive-strand RNA viruses. The terminal region of the 3′-untranslated region (UTR) of TYMV RNA folds into a tRNA-like structure (TLS) (Rietveld et al., 1982; Dumas et al., 1987), which possesses a valine identity and other tRNA characteristics (Haenni et al., 1982; Mans et al., 1991; Dreher et al., 1992). Despite extensive efforts dedicated to research on the TYMV TLS in view of its remarkable structural and functional mimicry to tRNA, its role on the virus lifecycle has not been fully elucidated.

In this thesis, the studies with TYMV have uncovered two new roles for the TLS, adding to a single previously known role in TYMV biology. The new roles implicate an early involvement in the infection, regulating genome translation (Chapter 2 and 3) and the transition to minus strand synthesis and the onset of RNA replication (Chapter 4). Chapter 5 is given to the study of another TLS-carrying virus, the bipartite *Peanut clump virus* (PCV). PCV was of interest because of its unusual TLS based on the design of the TYMV TLS, and because of the unusual difference in predicted TLS functionality between the two genomic RNAs. The effects of valylation mutations in the TLS of each genome component were tested on virus replication and infection.

General characteristics of TYMV and PCV biology are explored in the first section of the Introduction, followed by a review of TLSs from plant viruses. Finally, the viral strategies for gene expression and the transition from translation to minus strand synthesis are discussed for positive strand RNA viruses. The literature review below, mainly focused on recent reports, introduces the current research interests that are relevant for the study of the roles of the TYMV TLS discussed in the later chapters.

1.1   General characteristics of TYMV and PCV

TYMV (type species of the genus *Tymovirus*) and PCV (type species of the genus *Pecluvirus*) are two viruses whose genomic RNAs possesses related valine-charging TLSs. The two viruses, however, are different in many aspects. While TYMV is a monopartite RNA virus, PCV is bipartite. The TYMV genomic RNA exhibits strong cis-

preferential replication, so that defective TYMV RNAs are not likely to be rescued by co-inoculation of helper RNA in protoplasts (Weiland and Dreher, 1993). On the other hand, being bipartite, PCV supports replication in trans of RNA2 by the replication protein expressed from RNA1. The different effects of engineered non-valylatable TLSs in cis-replicating and trans-replicating RNAs of PCV are discussed in Chapter 5 (Matsuda, et al., 2000).

The amazing similarity of TLSs between distantly related viruses is not limited to tymoviruses and pecluviruses (Fig. 1.2.A and B). In addition to the genus *Pecluvirus*, other fungus transmitted rod-shaped viruses (Furo-like viruses: *Furoviruses* and *Pomoviruses*) carry valine-charging TLSs in their genomic RNAs (Goodwin and Dreher, 1998). Moreover, *Sunn-hemp mosaic tobamovirus* (SHMV, also known as the cowpea strain of *Tobacco mosaic virus*) posesses a valine-accepting TLS like the TYMV TLS (Meshi et al., 1981; Dreher and Goodwin, 1998). All these observations suggest the occurrence of molecular recombination between different families of viruses in the course of evolution. Interestingly, the structural features in the 3´-untranslated region (UTR) are often not conserved among closely related viruses. In the family *Tymoviridae*, the presence of a TLS in the genomic RNA is restricted to the genus *Tymovirus*, with marafiviral and maculaviral genomic RNAs typically being polyadenylated (Martelli et al., 2002). Likewise, *Pecluviruses*, *Furoviruses*, and *Pomoviruses* have TLSs at the 3´-termini of their genomic RNAs whereas the RNAs of *Beneviruses* terminate with poly(A) tails, although *Beneviruses* are also fungus transmitted rod-shaped viruses and amino acid sequence comparisons reveal close relationships (Herzog et al., 1994b; Wesley et al., 1994; Shirako and Wilson, 1999).

1.1.1   TYMV and Tymoviruses

1.1.1.1   TYMV genome organization and expression of the viral proteins

The genomic RNA of TYMV is single-stranded, plus sense, and 6319 nts in length (Morch et al., 1988) including the 3´-terminal A that is absent from most virion RNAs but is rapidly added at the start of an infection (see later). A second RNA

synthesized during the course of the infection is the coat protein (CP) subgenomic RNA, whose sequence is identical to the 3´-terminal 695 nts of the genomic RNA. Both genomic and subgenomic RNAs are 5´ capped with ^{m7}GpppN structures (Briand et al., 1978; Guilley and Briand, 1978). The genomic RNA contains three open reading frames (ORFs) encoding viral proteins p69 (also called overlapping protein, OP), p206 (replication protein, RP) and coat protein (CP), while CP expression is silenced in the genomic RNA (Fig. 1.1A).

(A) TYMV genomic RNA (6319 nts)

(A) PCV genomic RNAs

RNA1 (5897 nts)
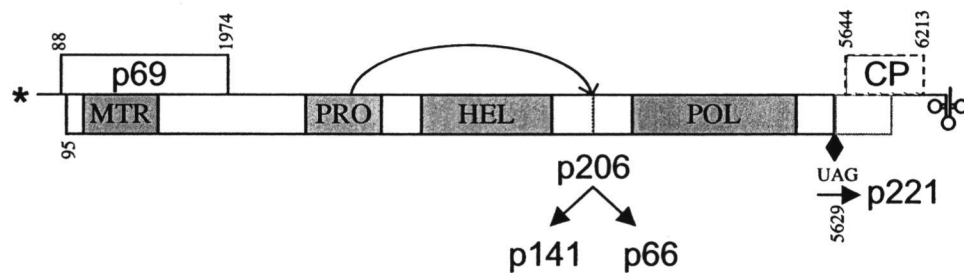
RNA2 (4504 nts)
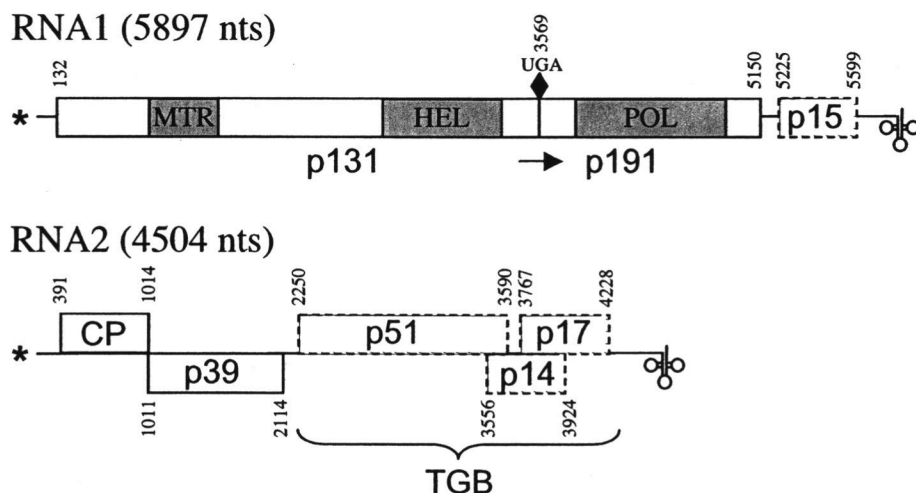
Fig. 1.1 Genome organization of TYMV and PCV

Fig. 1.1 Genome organization of TYMV and PCV

The genomic map of *Turnip yellow mosaic virus* (A) and *Peanut clump virus* (B) are shown with ORFs and their initial and terminal nucleotide numbers. The 5′-^{m7}GpppG cap is depicted with *, and the TLSs with cruciforms placed at the 3′-termini. The ORFs that are not directly expressed from the genomic RNAs are indicated by the dotted boxes. The positions of ribosomal readthrough of stop codons are designated with filled diamonds. **(A)** The 6319 nt-long genomic RNA of TYMV has three ORFs encoding p69 (overlapping protein, OP), p206 (replication protein, RP) and CP (coat protein). p206 includes four domains (shaded): methyltransferase-like (MTR), protease (PRO), helicase-like (HEL) and RNA-dependent RNA polymerase (POL). The protease domain is responsible for the co-translational cleavage in cis of p206 to form p141 and p66. The C-terminal extension of p206 is achieved by readthrough of UAG to produce p221 whose function is not known. **(B)** PCV genomic RNA1 and RNA2 are shown with the ORFs indicated. Translation of ORF131 containing MTR and HEL domains can be C-terminally extended to yield p191 by readthrough of UGA. While p131 and p191 can be expressed from RNA1, p15 (cysteine-rich replication enhancer protein and viral suppressor of RNAi) is only expressed from a subgenomic RNA. RNA2, 4503 nts in length, has five ORFs: CP, p39 (function unknown), and the triple gene block (TGB) proteins, p51, p14 and p17. TGB is involved in cell-to-cell movement of the virus.

Elucidation of the complete TYMV genome sequence (Morch et al., 1988) and establishment of an infectious TYMV cDNA clone (Weiland and Dreher, 1989) have enabled studies on the role of each viral protein in viral proliferation. The only essential protein required to support virus replication in protoplasts is p206. Amino acid sequence comparisons with replication proteins from other positive strand RNA viruses revealed that p206 has the following four domains (Koonin and Dolja, 1993): (from the N-terminus) methyltransferase-like, protease, helicase-like, and polymerase. The methyltransferase-like domain is thought to be required for methylation of the 5´-cap structure of the viral RNA. The papain-like cysteine protease domain is responsible for co-translational self-cleavage of p206 into 141 kDa and 66 kDa proteins (Rozanov et al., 1995; Bransom et al., 1996). The helicase-like domain demonstrating ATPase and GTPase activity binds RNA in a non-specific manner (Kadare et al., 1996), but no helicase activity has been demonstrated. The polymerase domain is the conserved domain that resides in the 66 kDa portion of p206 and possesses the Gly-Asp-Asp (GDD) motif, which serves in the catalytic site of the RNA-dependent RNA polymerase (RdRp). The amber stop codon of ORF-206 may be suppressed at low efficiency, with translation further extended to produce a 221 kDa protein (Fig. 1.1A). However, the extended C-terminal portion has been found to be non-essential for replication and infection of the virus (Bransom et al., 1995).

By altering the AUG start codon of ORF69 to AAG in the genomic RNA (the resulting TYMV RNA was named TYMC-69AAG), the absence of p69 production was confirmed in rabbit reticulocyte lysate using [³H]leucine. TYMC-69AAG replicated in Chinese cabbage protoplasts to low levels relative to wild-type TYMV as indicated by Western blotting to detect CP and Northern analysis detecting both genomic and subgenomic RNA (Weiland and Dreher, 1989). Interestingly, CP accumulation in protoplasts was at wild-type levels for a mutant with a UGA stop codon introduced at nucleotide 139, resulting in production of only the N-terminal 16 amino acid residues of p69 (Bozarth et al., 1992). This mutant, designed to interrupt p69 translation but retain normal ribosome behavior around the AUG initiation codon, failed to induce local lesions

or systemic symptoms in Chinese cabbage and turnip plants, although CP was detected in initially inoculated areas of the leaf (Bozarth et al., 1992). The same results were obtained from other nonsense mutant RNAs (UGA introduced at nucleotide 178 and at both 178 and 224). The failure to support efficient replication of TYMC-69AAG could be due to disruption of the plus strand promoter, alteration of p206 translation initiation, and/or an interfering effect of proteins initiated at downstream AUGs of ORF69. Alternatively, these results suggest that the N-terminal 16 amino acid residues of p69 are important for efficient viral replication in protoplasts, and the rest of the downstream residues are required for virus movement. Very recent studies have identified p69 as the viral suppressor of RNA interference (Dr. S-W. Ding, personal communication), suggesting that the low RNA accumulation of TYMC-69AAG in protoplasts may be due to absence of silencing suppressor activity.

ORF69 starts 7 nts upstream of ORF206, and thus overlaps almost entirely with it. The translation initiation mechanism of p206 has not been completely elucidated. The leaky ribosome scanning of the upstream (ORF69) AUG is supported by its rather weak initiation context and by increased expression of ORF206 (downstream AUG) in reticulocyte lysate from TYMV-69AAG RNA (Weiland and Dreher, 1989). Removal of the upstream AUG allows more ribosomes to access the ORF206 AUG. On the other hand, removal of ORF206 expression by the equivalent mutation of the initiation codon resulted in increased p69 expression. This result cannot be explained by the simple leaky scanning by ribosomes moving in the 5′ to 3′ direction on the mRNA because events at the downstream AUG appear to affect those at the upstream AUG. Recently, using an in vitro wheat germ translation system, translation initiation of p206 has been proposed to occur in a cap-independent and TLS-dependent manner (Barends et al., 2003). This unusual scheme may need further examination since in vivo experimental results in Chapter 3 of this thesis are in direct conflict with the proposed model.

Deletion of two thirds of the CP ORF (deleted region corresponding to nucleotides 5707-6062) resulted in viral RNA accumulation to about 10% relative to wild type in turnip protoplasts (Weiland and Dreher, 1993). A comparable result was obtained

in Chinese cabbage protoplasts inoculated with TYMV RNA transcripts unable to express CP because of mutation of the initiating AUG codon to UUG and introduction of a UAA termination codon 5 codons downstream (Bransom et al., 1995). The authors found that negative-strand genomic RNA accumulation appeared to be similar to that of wild type. These diminished accumulations of the plus sense RNAs are posively due to lack of protection of the viral RNAs in the absence of encapsidation, although involvement of CP in suppression of RNA interference or plus strand synthesis cannot be entirely excluded. Another role of CP was indicated by inoculation of the CP expression mutant RNA on Chinese cabbage plants (Bransom et al., 1995). These plants developed local lesions, but not systemic symptoms, indicating that CP is dispensable for cell-to cell movement, but required for long distance movement.

1.1.1.2 Symptomatic and cytological effects of TYMV infection

The natural hosts of TYMV are usually restricted to the *Cruciferae*. First isolated from turnip (*Brassica rapa*; Markham and Smith, 1946), TYMV has been studied in the experimental hosts Chinese cabbage (*Brassica pekinesis*), turnip and *Arabidopsis thaliana*. Symptom development upon TYMV infection on Chinese cabbage starts with vein clearing in young leaves, followed by an appearance of light green or whitish-yellow spots, resulting in a mosaic pattern of the leaves (Matthews, 1991). The chlorotic regions of leaves contain virus, whereas virus is absent in dark green areas (Hull, 2002).

TYMV infection is associated with an induction of cytological abnormalities that focus on the chloroplasts (Lesemann, 1977; Matthews, 1991), with the following changes occurring sequentially: formation of invaginations of both chloroplast membranes to form vesicles (50-100 nm in diameter) with narrow channels to the cytoplasm (Hatta et al., 1973), clumping and swelling of the chloroplasts followed by chloroplast vacuolation (Hatta and Matthews, 1974). The peripheral chloroplast vesicles were postulated to be the site of TYMV RNA synthesis based on experiments localizing the accumulation of [^{3}H] UTP-labeled RNA in the presence of actinomycin D (Bové and Bové, 1985) and by immunocytochemical methods detecting TYMV replicase (Garnier, 1986). Recently, p66

(containing the RdRp domain of p206) was demonstrated by immunogold labeling of TYMV-infected tissue to be localized near the peripheral vesicles (Prod'homme et al., 2001). In addition, the localization of p66 was shown to be dependent on the chloroplast localization of p141 (N-terminal portion of p206), which itself localized to the chloroplast membrane and induced chloroplast clumping (Prod'homme et al., 2003). It is not known whether p141 is solely responsible for peripheral vesicle formation on chloroplast membranes.

The dependence of RdRp membrane localization on a methyltransferase domain-containing replication protein has also been demonstrated with *Brome mosaic virus* (BMV) (Restrepo-Hartwig and Ahlquist, 1999) and *Semliki forest virus* (Peranen et al., 1995), suggesting that this process may be common to positive strand RNA viruses. Especially, the BMV1a protein (homologue of TYMV p141) is sufficient for vesicle formation on ER membranes, which are the site for BMV replication.

1.1.1.3 TYMV virions and RNA encapsidation

TYMV virions are about 30 nm in diameter and made up of 32 morphological subunits (20 hexamers and 12 pentamers), which total 180 CP molecules in the form of a T=3 icosahederon (Canady et al., 1996; Dreher, 2001). As well as encapsidating the TYMV genomic and subgenomic RNAs, empty shells are produced, indicating strong protein-protein interactions (Matthews, 1991). Encapsidation of the TYMV RNAs has been suggested to occur at the cytoplasmic side of the peripheral vesicles on the chloroplast membrane (Matthews, 1981) in a low pH environment (Hirth and Givord, 1985), which is postulated to be driven by the light-dependent proton pumping on the chloroplast membranes (Rohozinski and Hancock, 1996). However, TYMV appears to replicate and accumulate viral RNAs to a normal level in the dark in Chinese cabbage protoplasts (Boyer et al., 1993) and *Arabidopsis thaliana* protoplasts (Schirawski et al., 2000a). Thus, the proposed requirement for light-induced generation of a low-pH environment during TYMV infection may need to be re-investigated.

The TYMV genomic 5′-UTR has been proposed to serve in the initiation of RNA encapsidation. The genomic 5′-UTR has two hairpin structures of low stability (named HP1 and HP2), each with a symmetrical internal loop that can be stabilized by $C^+\bullet C$ and/or $C^+\bullet A$ base pairs optimally at pH 5.5 (Hellendoorn et al., 1996). Similar structures are found in the 5′-UTRs of other tymovirus genomic RNAs. Electrophoretic mobility shift assays showed that HP1 interacts with TYMV coat protein shells preferentially at pH 4.5 (Bink et al., 2002). Infection with genomic RNA with a deletion of both HP1 and HP2 (a deletion of 75% of the 5′-UTR) produced a lower ratio of filled virus particles to empty capsids compared to wild-type virus, consistent with the proposed role of the hairpins (Hellendoorn et al., 1997). On the other hand, Choi *et al.* (2002) reported that the *Brome mosaic virus* TLS mediates encapsidation of the genomic RNA in vitro, suggesting the possibility of the TYMV TLS serving a similar role.

1.1.2   PCV and related viruses

First reported in Senegal in 1967 (Bouhot, 1967), PCV is the type species of the genus *Pecluvirus*, to which *Indian peanut clump virus* (IPCV) also belongs. PCV and IPCV, whose appearances are concentrated in West Africa and southern Asia, are thought to be transmitted in peanut by seed (Thouvenel et al., 1978) and by *Polymyxa graminis* in the soil (Thouvenel and Fauquet, 1981). Experimental hosts are *Nicotiana* species. Early symptoms in peanut include mottling, mosaic, and chlorotic rings, followed by severe stunting and poor pod formation, resulting in up to 60% loss of crop yield (Reddy, 1983). Global economic loss annually from clump disease is estimated to be about $38 million (Sutic et al., 1999). The occurrence of PCV in the field may be readily prevented by the use of soil fumigants or crop rotation with a non-host of PCV (Sutic et al., 1999).

1.1.2.1   PCV genome organization

PCV has two plus sense genomic RNAs, both terminating with a valine-charging TLS. RNA 1 and 2 are 5897 nts and 4504 nts in length, respectively (Fig. 1.1B). RNA1

encodes two replication proteins, p131 and its readthrough product p191 (Herzog et al., 1994a). p15 is expressed from a subgenomic RNA, which is synthesized from RNA1. RNA1 can replicate by itself in protoplasts, although RNA accumulation is lower than when RNA2 is co-inoculated (Herzog et al., 1998). This may be due to lack of RNA protection by encapsidation with CP, which is expressed from RNA2.

p15 is a small cysteine-rich protein, which shows sequence homology with proteins from *Soil-borne wheat mosaic virus* (SBWMV) and *Barley stripe mosaic hordeivirus* (BSMV; Herzog et al., 1994a). p15 has been shown to be a replication enhancer since the abolition of full-length p15 expression resulted in about 10% accumulation of RNA1 relative to wild type in protoplasts; normal accumulation can be rescued by expression of p15 in trans (Herzog et al., 1998). Recently p15 was found to suppress the post-transcriptional gene silencing of a co-infiltrated GFP gene (Dunoyer et al., 2002). Interestingly, a C-terminal deletion mutation of ORF15 resulted in severely hindered local and systemic movement of the virus without affecting RNA accumulation in protoplasts and the silencing suppressor function (Dunoyer et al., 2002). This observation suggests that p15 has two separate domains, each responsible for virus movement and suppression of post-transcriptional gene silencing.

PCV RNA2 encodes five proteins: CP, p39 and the triple gene block (TGB) proteins. CP and p39 are directly expressed from PCV RNA2, with p39 being translated in rabbit reticulocyte lysate apparently by a leaky ribosomal scanning mechanism (Herzog et al., 1995). The function of p39 has not been elucidated, although an internal portion of the gene can be deleted without affecting viral replication and encapsidation (Manohar et al., 1993). Such variant viruses can be successfully propagated by mechanical inoculation, suggesting a role in fungus transmission of the virus. The PCV TGB consisting of p51, p14 and p17 is involved in cell-to-cell movement of the virus, and TGBp1 (p51) was found to be localized at the plasmadesmata (Erhardt et al., 1999). While TGBp1 is expressed from a subgenomic RNA, the mode of expression of p14 and p17 is still unknown.

1.1.2.2 PCV virions and encapsidation

PCV is a rod-shaped virus about 20 nm in diameter and 245 and 190 nm in length for capsids containing RNA1 and 2, respectively (Thouvenel et al., 1976). Cis-acting elements important for encapsidation of RNA1 were mapped to the N-terminal coding region of p15 by deletion analysis (Hemmer et al., 2003). Moreover chimeric fusion of the region to a non-encapsidatable portion of RNA2 rescued the ability for encapsidation. However, subgenomic RNA1, which encodes p15 was not detected as an encapsidated species, suggesting an involvement of another cis element for encapsidation. Two regions important for encapsidation were implicated on RNA2, located in the CP genes and in middle of the TGB (Hemmer et al., 2003). No sequence similarity among the regions specified for the encapsidation elements has been detected. The possibility of TLS-mediated encapsidation, which has been observed with BMV (Choi et al., 2002), cannot be entirely excluded for the PCV encapsidation mechanism.

1.2 tRNA-like structures

Remarkably resembling a canonical tRNA, the TYMV TLS can be considered to consist of the following five structural elements: the 3´-terminal ACCA that is included in the aminoacyl acceptor stem, T stem-loop, anticodon stem-loop and D stem-loop (Fig. 1.2B). These elements of the TLS are viewed as contributing to the overall 'L'-shaped configuration, just as observed for tRNA (see Fig. 1.2A and B). The three dimensional mimicry to tRNA is strongly supported by the ability of the TLS to interact with three cellular tRNA enzymes: [CTP, ATP]:tRNA nucleotidyltransferase (CCA-NTase), valyl-tRNA synthetase (ValRS) and translation elongation factor 1A (eEF1A, eukaryotic homolog of the bacterial EF-Tu).
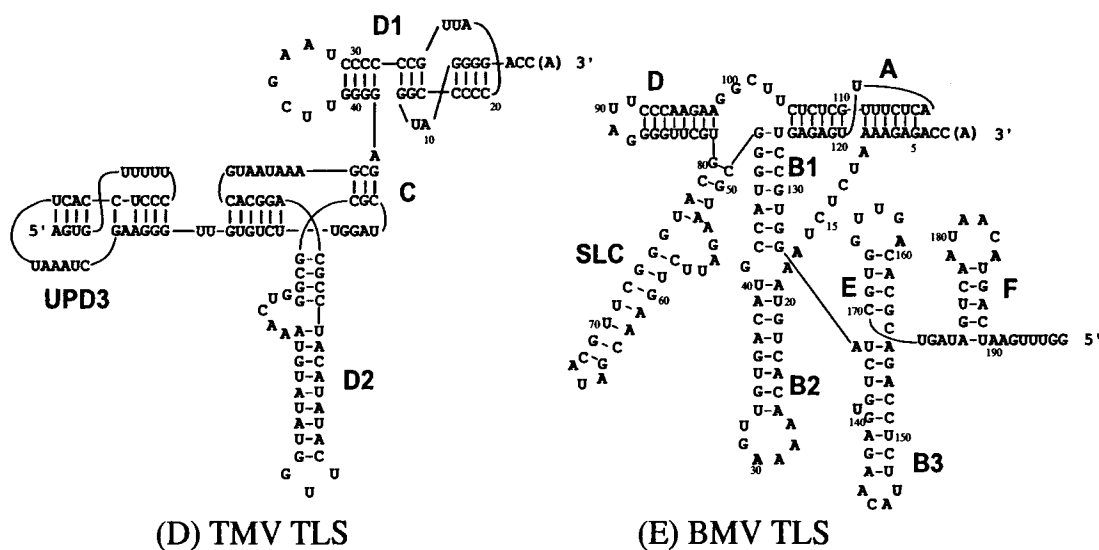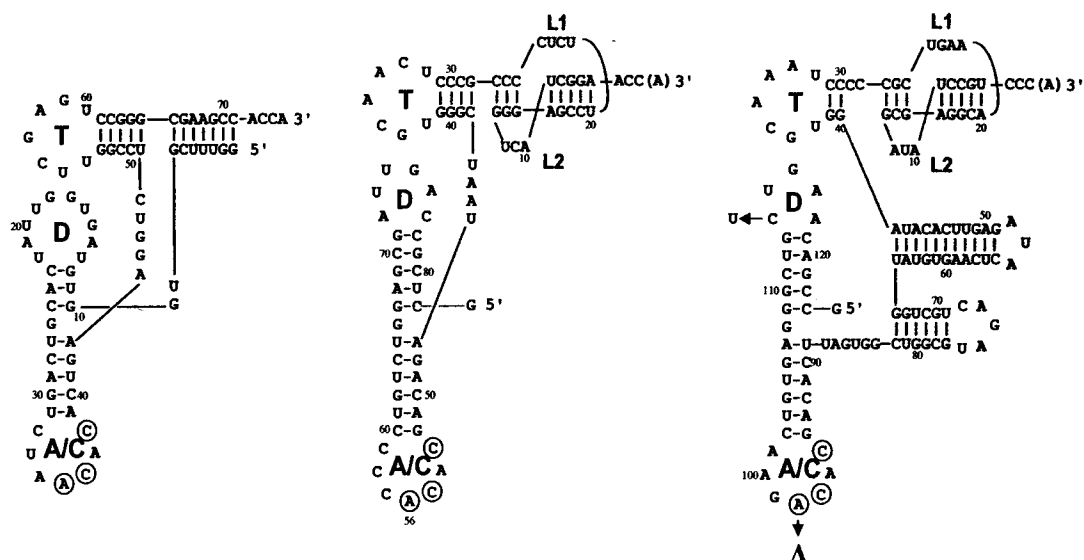
Fig. 1.2 tRNA^Val and plant viral tRNA-like structures

Fig. 1.2 tRNA^{Val} and plant viral tRNA-like structures
Proposed structures of plant (lupin) tRNA^{Val} shown without nucleotide modifications (**A**)
and TLSs of TYMV (**B**), PCV RNA1 (**C**), *Tobacco mosaic virus* (**D**) and *Brome mosaic
virus* (**E**) are presented. The nucleotides in tRNA^{Val} are numbered from the 5′-terminus,
while those in the plant viral TLSs are numbered from the 3′-terminus. The valine
identity nucleotides are circled, and the T, D and anticodon (A/C) loops are indicated in
tRNA^{Val}, the TYMV and the PCV TLSs. The acceptor stem pseudoknot in the TYMV
and PCV TLS has two internal loops, L1 and L2. In the PCV RNA2 TLS, the center
nucleotide of the anticodon is missing (indicated as Δ), and U is in the place of C114 of
RNA1. Domains indicated in the TMV and BMV TLSs are adapted from (Felden et al.,
1996; Dreher, 1999) and (Dreher and Hall, 1988a), respectively. The primary sequences
are taken from GenBank, accession number X05082 (lupin tRNA^{Val}), X16378 (the TLS
of TYMV, Corvallis isolate), NC_003668 (PCV, strain PCV2), AX040174 (the TLS
TMV, U1 strain) and J02042 (the TLS of BMV, Russian strain).

The 3´-terminal four nucleotides (5´-ACCA-3´) of both TLS and tRNA are single-stranded. Since most of the TYMV virion RNAs terminate at the 3´-end in CC (Briand et al., 1977), the terminal A of TYMV genomic RNA is considered to be added by host CCA-NTase upon entering the cell (Rao et al., 1989).

The acceptor stem of the TYMV TLS is represented by a pseudoknot with two internal loops (L1 and L2), which is made of the 3´-terminal 27 nts (see Fig. 1.2.B; Rietveld et al., 1982; Pleij et al., 1985). The solution structure of the pseudoknot has been determined by nuclear magnetic resonance spectroscopy (Kolk et al., 1998). This structural feature is amazingly similar to the differently built acceptor stem of canonical tRNA, which consists of the base paired duplex involving the 3´ and 5´-terminal regions of the molecule (Fig. 1.2A). Together with the T-stem on its upstream side, the TYMV pseudoknot forms a 12-bp acceptor/T stem, which is segmented with 4-3-5 bp stackings in the 5´ to 3´-direction (Fig. 1.2B). Some valine-charging TLSs (*Eggplant mosaic virus* and *Potato mop-top virus*, for example) have a 3-3-6 bp stacking configuration. The difference in the segmentation of the acceptor stem strongly correlates with efficiency for histidylation and eEF1A interaction (to be discussed in detail in 1.2.D and E, respectively).

As in the case of tRNA^{Val}, the anticodon loop of the TYMV TLS possesses valylation identity nucleotides, which are recognized by host ValRS (Dreher et al., 1992). The biological and biochemical significance of the valylation of the TYMV TLS will be discussed in sections 1.2.A and D. The importance of the interaction between the D-loop and T-loop in the TLS has been suggested by the conserved nucleotide pair at 36 and 75 and co-variation at 37 and 76, which is supported by recent reverse-generic experiments (see Fig. 1.2B; de Smit et al., 2002).

In addition to tymoviruses, the other positive-strand RNA plant viruses possessing a TLS at the 3´-termini of their genomic RNAs are furo-like viruses (the genera *Furovirus*, *Pecluvirus* and *Pomovirus*), tobamoviruses, bromoviruses, cucumoviruses, and hordeiviruses. Compared to the TLSs of tymoviruses and furo-like viruses, tRNA mimicries of other viral TLSs are structurally less obvious (compare Fig. 1.2B and C vs

D and E) because of the absence of a 7-nt anticodon loop and presence of additional structural elements as in the TMV and BMV TLSs. The TLSs of *Pecluviruses* are distinct from the typical tymo-like TLS due to the insertion of 42 nts between the two halves of the TLSs (Fig.1.2C), The position of this insertion is similar to that of tRNA variable loop.

Three amino acids have been shown to be esterified to the 3′-CCA terminus of the plant viral TLSs, generally in a genus-specific manner: valine for tymoviruses and furo-like viruses, histidine for tobamoviruses, and tyrosine for bromoviruses, cucumoviruses and hordeiviruses. Because of the efficient aminoacylation kinetics (discussed in 1.1.C), most viral TLSs that are aminoacylated in vitro, are thought to be charged in vivo. Indeed, TYMV RNA was reported to be valylated after inoculation on Chinese cabbage leaves (Joshi et al., 1982) and microinjection into *Xenopus* oocytes (Joshi et al., 1978). Likewise, [^{3}H]tyrosine was found associated with the BMV and *Barley stripe mosaic hordeivirus* genomic RNAs in barley protoplasts infected with the respective viruses (Loesch-Fries and Hall, 1982).

There are some deviations from the generally conserved aminoacylation identity of the TLS within a genus. It is intriguing that the genomic RNA of SHMV has a valine-charging TLS, unlike TMV (Meshi et al., 1981; Dreher and Goodwin, 1998), the type species of the genus *Tobamovirus*, whose TLS accepts histidine. The *Erysimum latent tymovirus* (ELV) 3′-UTR shows an interesting divergence from the TYMV TLS in having a poor tRNA mimicry that is restricted to partial activity with CCA-NTase (Dreher and Goodwin, 1998). Likewise, *Tomato aspermy cucumovirus* RNA failed to accept tyrosine, which is readily esterified to the closely related *Cucumber mosaic virus* RNA (Joshi and Haenni, 1986). There are further examples of vestigial tRNA mimicry as mentioned for ELV. In these cases, there is no aminoacylation, but the RNA can be adenylated by CCA-NTase. The 3′-terminal region of *Tobacco rattle virus* RNA2 has been suggested to fold like the acceptor stem pseudoknot like of the TYMV TLS, and has been shown to be adenylated by CCA-NTase (van Belkum et al., 1987). The 3′-UTR of *Alfalfa mosaic virus* can undergo a drastic conformational change between forms that

interact with CP and CCA-NTase (Olsthoorn et al., 1999). In the following section of the Introduction, the molecular nature and potential functions of plant virus TLSs will be discussed.

1.2.1   Aminoacylatability of the plant viral TLSs and its biological significance

Valylatability of the TYMV genomic RNA was shown to be essential for efficient virus replication in vivo; point mutation of A to G at position 56 (see Fig. 1.2.B; mutation of the central nucleotide of the anticodon, resulting in abolition of valylation) led to a near-background level of virus replication in Chinese cabbage protoplasts (Tsai and Dreher, 1991). In comparison, mutation of the wobble position (the 5´-nucleotide of the anticodon), retaining full valylation activity, did not significantly alter the replication ability.

As a means to further test the role of the TLS in TYMV RNA, the aminoacylation identity was converted from valine to methionine (Dreher et al., 1996). This required changing C53/A54/C55 to ACU, along with a shortening of pseudoknot loop L1. TYMV RNA with the methionine-accepting TLS was found to be infectious in Chinese cabbage plants. On the other hand, a variant with methionine identity but with the wild-type L1 showed low methionine charging ability and severely diminished replication in protoplasts. These results indicate that neither valylation in specific nor ValRS is required, but aminoacylation is important for efficient viral replication.

For multipartite genomes with TLSs, a significant effect of aminoacylatability in RNA amplification may be restricted to the RNA(s) that encode the essential replication proteins. This is the case with BMV, a tripartite virus whose replication proteins are encoded by RNA1 and 2. Mutations that specifically decrease aminoacylation but retain a wild-type capability for 3´-adenylation and initiation of minus strand synthesis (Dreher and Hall, 1988a) resulted in significantly diminished virus replication in barley protoplasts when the mutations were present in RNA1 (Duggal et al., 1994) or 2 (Rao and Hall, 1991). Conversely, when the mutation was present in RNA3 whose amplification is dependent on the presence of RNAs 1 and 2, virus and RNA3 replication were only

slightly decreased (Dreher et al., 1989). Therefore, the effect of an aminoacylation mutation on viral replication in protoplasts appears to be dependent on the coding context of the RNA in which the mutation resides.

Within TYMV genomic RNA, the TLS has been replaced with 3´-UTRs from TMV (partially modified), ELV and EMV resulting in infectious chimeric viruses (Goodwin et al., 1997). The RNA accumulations and infectivities of these viruses were about half those of wild-type TYMV in protoplasts (Filichkin et al., 2000). Despite being attenuated, the infectivities of these viruses indicate that these TLSs are compatible with the TYMV replication machinery, and that the entire TYMV TLS is not required for promotion of minus strand synthesis. Interestingly, the TYMV chimeras with the ELV and modified TMV TLSs were not chargeable with any amino acid under various in vitro conditions (Goodwin et al., 1997), indicating that the strict requirement for aminoacylation observed in wild-type TYMV (Tsai and Dreher, 1991; Dreher et al., 1996) can be circumvented in these particular chimeric variants.

1.2.2 TLSs harbor initiation sites of minus strand synthesis

Since the viral TLSs are located at the 3´-terminus of the plus sense RNA, they have been postulated to act as cis-acting elements, RdRp binding sites and/or promoter sequences controlling minus strand synthesis. BMV RNA, for example, possesses a feature controlling minus strand synthesis in stem-loop C (SLC) of the TLS (see Fig. 1.2E; Dreher and Hall, 1988b). Since the presence of this SLC upstream controlling region by itself (without the 3´-CCA terminus) was shown to inhibit RdRp activity, this region is thought to function as a preferential binding site for BMV RdRp (Chapman and Kao, 1999). The SLC conformation has been determined by nuclear magnetic resonance (Kim et al., 2000). The 5´-A of the triloop (5´-AUA-3´) of SLC is considered to be important for BMV RdRp recognition, because mutations of the 5´ A resulted in strongly diminished RNA synthesis in vitro (Dreher and Hall, 1988b; Chapman and Kao, 1999) and in vivo (Rao and Hall, 1993). Substitution of the 3´-terminal CA with AC or UU of the BMV TLS led to about 95% loss of minus strand template activity in vitro (Dreher

and Hall, 1988b). Likewise, the importance of the 3´-initiation sequence in a 41-nt RNA template carrying the bottom half of SLC (nt 58 to 74 in BMV TLS, numbered from the 3´-end) was demonstrated by mutation of the 3´-CCA to GGA, which resulted in near background levels of minus strand synthesis (Ranjith-Kumar et al., 2003). Together with the importance of the 5´-A of the SLC triloop, the authors have concluded that the RdRp-binding site and CCA initiation box comprise cis-acting features required for efficient BMV minus-strand synthesis.

Like in BMV, TMV RNA harboring the D2 region and central core (Fig. 1.2.D) can efficiently compete for RdRp against the 3´ terminal 194 nts, indicating that RdRp binds to these regions (Osman et al., 2000). In the same study, the TMV 3´-CCA initiation box was demonstrated to be important in an in vitro replication system. Either deletion or substitution of the terminal A and/or penultimate C residues resulted in the loss of detectable RNA synthesis, while substitution of C3 was found to be relatively less important, yielding about 60% of the minus strand level produced from the wild-type sequence.

In TYMV, on the other hand, two independent studies have confirmed that the 3´-CCA initiation box alone is sufficient to direct minus strand synthesis by partially purified TYMV RdRp (Deiman et al., 1998). Individual and stepwise deletions of the D, anticodon and T regions retained similar template activity to that of the full-length TLS (Singh and Dreher, 1997; Singh and Dreher, 1998). Stepwise deletion of nucleotides from the 3´-terminus of the TLS decreased the template activity with respect to the full-length TLS to about 51% after deletion of the 3´-terminal A, and 8% when the terminal CA was deleted (Singh and Dreher, 1997); similar results were obtained by Deiman et al. (1998). Furthermore, in vitro transcribed tRNAs whose 3´-CCA termini are the only sequence identity with the TYMV TLS were found to be efficient templates for the TYMV RdRp (Singh and Dreher, 1997; Deiman et al., 1998). Indeed, the TYMV RdRp can synthesize complementary strands of expected lengths by initiating from multiple CCA initiation boxes in an unstructured RNA (Singh and Dreher, 1998; Deiman et al., 2000; Yoshinari et al., 2000). Using an RNA template containing 5´-UGG-3´ able to

base pair to the 3´-terminal CCA, Singh and Dreher (1998) demonstrated that CCA must be single stranded for full function in initiation, and a similar conclusion was reported by Deiman et al. (2000). Although the TYMV replicase can initiate transcription from CCA located internally in the template, it has been hypothesized that the other CCA sequences scattered across the TYMV genome do not serve as initiation boxes because of secondary and tertiary structures that prevent RdRp access (Singh and Dreher, 1998; Dreher, 1999).

The importance of a 3´-CCA initiation box has been further extended to some viral RNAs whose 3´-termini do not fold into a TLS. Using bacteriophage Qβ replicase and *Turnip crinkle virus* RdRp, RNAs containing a 3´-CCA initiation box but lacking specific viral sequences could direct synthesis of complementary strands in vitro (Yoshinari et al., 2000). These observations indicate that the initiation box is a significant determinant directing minus strand synthesis in positive strand RNA viruses. With regard to TYMV and the role of tRNA mimicry, the finding that the CCA initiation box acts to promote minus strand initiation without relevance of the TLS means that promotion of minus strand synthesis is not a role of tRNA mimicry.

RdRps of positive strand RNA viruses catalyze three different RNA syntheses: minus sense genomic RNA, plus sense genomic RNA, and subgenomic RNA. In the regions close to the initiation site of TYMV plus strand and subgenomic RNA synthesis, no sequence or structural similarity to the TLS was observed. Especially, the subgenomic RNA initiates with an A residue, unlike the plus and minus sense genomic RNAs, which initiate with a G residue at their 5´-terminus. Although the synthesis of plus strand genomic and subgenomic RNA have not been studied in vitro, in vivo work on the control region for subgenomic RNA synthesis has been reported. Subgenomic RNA transcription initiates at nucleotide 5626 (Guilley and Briand, 1978) using minus-strand genomic RNA as a template (Gargouri et al., 1989). A recent study in mapping cis-elements involved the transfection of *Arabidopsis* protoplasts with full-length infectious TYMV transcripts carrying various duplicated forms of the subgenomic initiation region. Duplication of an 88-nt fragment (nucleotides 5578-5665), which spans the conserved 16 nt-long tymobox (conserved among the genus *Tymovirus*; Ding et al.,

1990), supports the synthesis of a novel subgenomic RNA of the expected length (Schirawski et al., 2000b). Mutation within the tymobox (G5611 to A) and of the subgenomic start site (A5626 to G) resulted in loss of subgenomic RNA synthsis. Therefore, TYMV subgenomic synthesis is thought to be controlled by the tymobox and initiation box (Ding et al., 1990; Schirawski et al., 2000b).

1.2.3   Role of CCA-NTase on viral TLS

The relative rate of adenylation of the 3′-CC of the TYMV TLS by wheat germ CCA-NTase is close to that to tRNA^{Val} (59%; Dreher and Goodwin, 1998). With BMV, CCA-NTase interaction was found to be important for maintenance of the 3′-CCA terminus. Substitution of C102/U103 with GG in the loop of the RNA3 TLS (numbered from the 3′-terminus) led to loss of 3′-adenylation by wheat germ CCA-NTase (2% of the wild-type TLS) while template activity for minus-strand synthesis was not greatly affected (about 40% of wild type; Dreher and Hall, 1988a). Co-inoculation of RNA3 bearing the adenylation mutation with wild-type RNAs 1 and 2 in barley protoplasts produced many progeny RNAs with one or two nucleotides missing from their 3′-termini (Dreher et al., 1989). RNA3 transcripts containing one or two nucleotide substitutions in the 3′-CCA terminal sequence were found to produce normal levels of progeny RNAs, which were found to have wild-type termini (Rao, et al., 1989). This result indicates that the mutant 3′-terminus went through rapid restoration to the wild-type 3′-CCA, which has most likely involved the CCA-NTase activity.

Since synthesis of minus strand RNA initiates opposite the 3′-most C (Miller et al., 1986; Kao and Sun, 1996), template-dependent synthesis of plus stand RNA terminates with the 3′-CC. Thus, the 3′-terminal A of the newly synthesized plus strand needs to be added by CCA-NTase or by the viral RdRp in a non-templated manner so that the CCA initiation box can fully function in the next round of minus strand synthesis. Therefore, these results suggest that the 3′-CCA terminus of the BMV TLSs function as a telomere in order to maintain an intact CCA initiation box. Interestingly, the 3′-terminus of AMV (Olsthoorn et al., 1999) and TAV (van Belkum et al., 1987) RNAs can be a

substrate for CCA-NTase, although the importance of the terminal nucleotides remains to be experimentally elucidated.

1.2.4 Aminoacylation of TLSs

Tymoviral and furo-like viral TLSs can be charged with valine because of the presence of valine identity nucleotides in the anticodon loop (5′-nnnACnC-3′; nucleotides C55, A56 and C53 in the TYMV TLS, see Fig 1.2B). Using valyl-tRNA synthetase (ValRS) partially purified from wheat germ, the valylation efficiency (rel. V_{max}/K_m) of the TYMV TLS was found to be 98% relative to that of plant tRNA^{Val} transcripts in a typical aminoacylation buffer (TM low salt buffer; Dreher and Goodwin, 1998). The TLSs from other tymoviruses (*Kennedya yellow mosaic virus* and EMV) and furo-like viruses (SBWMV, PMTV, *Beet soil-borne virus*, and *Indian peanut clump virus*) were also found to have about the same valylation efficiency as the tRNA^{Val} transcripts (Goodwin and Dreher, 1998). This was also true of the PCV RNA1 TLS, but the TLS of RNA2 (isolate PCV2) had more than 1000-fold lower efficiency for valine-charging than tRNA^{Val} (Goodwin and Dreher, 1998). This correlated with the absence of the central nucleotide in the anticodon of the RNA2 TLS (Fig. 1.2C). This non-valylatable TLS located on a trans-replicating RNA (i.e. RNA2) is an interesting deviation from the strict requirement for an aminoacylatable TLS for efficient replication of the monopartite TYMV. The effect of non-valylatable TLSs in PCV RNA1 (cis-replicating RNA) and/or RNA2 (trans-replicating RNA) is explored in Chapter 5.

In a buffer designed to approximate in vivo conditions (IV high salt buffer), all of the TLSs tested showed lower valylation efficiency (about 3 to 4-fold) relative to tRNA^{Val}, due either to elevated K_m or to reduced V_{max}. For SHMV TLS, the difference in valylation efficiency in the two buffer was even more pronounced: valylation kinetics of SHMV TLS were about 88% of tRNA^{Val} in TM buffer using wheat germ ValRS, but too low to be measured in IV buffers (Dreher and Goodwin, 1998). The exception is full-length TYMV RNA whose valylation remained very efficient in IV buffer. Versions of TLSs including further upstream sequences exhibited higher and faster valylation

profiles, especially with SBWMV RNA2 TLS being very similar to tRNA^{Val} (Goodwin and Dreher, 1998). Therefore, it appears that longer RNAs stabilize the folding of the TLSs in IV buffer, resulting in better substrates for ValRS.

The TLSs of TYMV, PCV, KYMV, SHMV, SBWMV and BSBV were also demonstrated to be substantially chargeable with histidine by a high concentration of purified yeast HisRS, while the EMV (Dreher and Goodwin, 1998) and PMTV TLSs (Goodwin and Dreher, 1998) were found to have a 6 to 11-fold lower plateau level than the above TLSs. Histidylation of plant viral TLSs is thought to result from the 3´-most nucleotide of loop L1 in the acceptor stem pseudoknot resembling residue –1 of tRNA^{His} (see Fig. 1.2B; Rudinger et al., 1994). The function of hystidylation in virus proliferation is not known, but is not as significant for virus replication as valylation because a TYMV variant with a non-valylatable TLS (such as the G56 mutation mentioned above) retained hystidylation (Dreher and Goodwin, 1998) but replicates very poorly in protoplasts (Tsai and Dreher, 1991).

Unlike the tymovirus TLSs, whose valine identity nucleotides are located in a clearly recognizable anticodon, the bromovirus TLSs have a less clear structural tRNA mimicry and no definite anticodon. Consequently, the tyrosine identity elements have not been identified. However, tyrosylation of the BMV TLS can be severely diminished by replacing U139/C140/U141 with AGA (numbered from the 3´-terminus) without significantly affecting other properties of the TLS, such as CCA-NTase catalysis (Dreher and Hall, 1988a). The TLS with this mutation was used to study the effect of tyrosylation in BMV RNA accumulation, which was discussed in section 1.2.A.

1.2.5 eEF1A interaction and its implicated roles in the virus life cycle

The finding that methionine charging TYMV variants are infectious (Dreher et al., 1996) strongly suggests that the subsequent eEF1A interaction, which is common to valine and methionine accepting TYMV RNA, is important for virus replication (Dreher et al., 1996). Supporting this hypothesis, a valylated 264-nt long 3´-fragment of TYMV RNA was found to interact as tightly with purified wheat germ eEF1A•GTP (dissociation

constant, K_d=1.9 nM) as valylated lupin tRNA^{Val} transcript (K_d=2.3 nM; Dreher et al., 1999). The K_d values of the valylated EMV and PMTV TLSs, whose acceptor/T stems have a 3-3-6 bp configuration (c.f. 4-3-5 for the TYMV-like TLS) were higher than 50 nM. Another group of TLSs with weak eEF1A binding are the PCV and IPCV TLSs, which have a 42-nt insertion between the two halves of the TLS (Fig. 1.2C; Goodwin and Dreher, 1998). However, it is not known whether these TLSs are truly incapable of interacting with eEF1A in vivo.

The excellent valylation kinetics of the TYMV TLS (Dreher et al., 1992) and subsequent tight interaction with eEF1A (Dreher et al., 1999) would be expected to hinder the access of the RdRp to the 3′-terminal CCA initiation box. These considerations make a previously postulated role of eEF1A in promoting minus strand synthesis (Hall, 1979) unlikely. In addition, the successful construction of infectious TYMV chimeric viruses with non-aminoacylatable TLSs (thus no eEF1A binding; Goodwin et al., 1997) is also inconsistent with eEF1A being a positive regulatory factor. Indeed, eEF1A was not detected in purified TYMV replicase fractions prepared from TYMV-infected leaves (Pulikowska et al., 1988). It thus seems that TYMV replicase is not modeled on Qβ replicase, which has EF-Tu (bacterial homologue of eEF1A) as a subunit (Blumenthal et al., 1972). Accordingly, Dreher (1999) has hypothesized that eEF1A binding to the TYMV TLS is likely to serve as a negative regulation, delaying the onset of replication while allowing continued translation and accumulation of viral proteins to a level sufficient for a successful virus infection. Because there is no indication of minus strand shut-off in later times of the TYMV replication cycle (Dr. B. Bradel and Dr. T. W Dreher, unpublished results), the involvement of eEF1A is likely to be early in the infection. Studies in Chapter 4 of this thesis provide in vitro evidence supporting the eEF1A repression of minus strand synthesis.

1.3 Eukaryotic elongation factor 1A, a multi-functional protein

eEF1A is a protein that has been highly conserved in the course of evolution. Amino acid alignment of eEF1A genes from *Arabidopsis*, carrot, barley, maize and

soybean shows more than 95% amino acid identity (Browning, 1996). Wheat eEF1A has 73% and 77% similarity to yeast and human eEF1A, respectively, and 55% weighted similarity to bacterial EF-Tu (Dreher et al., 1999). In this section, discussion is focused on the structural characteristics and on recently reported roles of eEF1A that may be involved in tRNA interaction and translation.

eEF1A has three structural domains, I, II and III. Domain I, alternatively called the G domain, is conserved among all G proteins, and is a binding site for GTP and GDP, which controls the activation status of eEF1A (reviewed in (Andersen et al., 2003). This nucleotide binding induces a drastic conformational change in part of domain I (termed the switch region), and in the relative position of domains I and II, the latter coming closer to domain I upon GTP activation (Andersen et al., 2003). The structure of the *Thermus aquaticus* EF-Tu•GDPNP•phe-yeast tRNA[Phe] ternary complex revealed that the T-stem and acceptor stem of tRNA make contact with domain III and the switch region of domain I, respectively (Nissen et al., 1995). The terminal A of the CCA-end is situated in a pocket of domain II, while the aminoacyl-ester bond is positioned in the linking region between domains I and II.

The classical role of eEF1A is to bring aminoacylated tRNAs to the A site of the translating ribosome (reviewed in (Browning, 1996). Upon activation by GTP binding, eEF1A has more than 10000-fold higher affinity for aminoacylated tRNAs compared to non-aminoacylated tRNAs (Dreher et al., 1999). Recently, rabbit eEF1A•GDP was reported to form a complex with non-aminoacylated tRNAs[Phe] with a dissociation constant (K_d) of 20 nM (Petrushenko et al., 2002), which decreased to 9 nM when PheRS was added in the reaction. The authors postulated that these complexes are involved in recycling tRNA off the ribosome.

Aminoacylated tRNAs (aa-tRNAs) were shown to be transported from nucleus to cytoplasm by an eEF1A-mediated pathway (Grosshans et al., 2000). More recently, tRNAs (regardless of aminoacylation status) were found to interact with exportin-5 and be transported in an eEF1A-independent manner (Calado et al., 2002). It has been proposed that eEF1A-mediated aa-tRNA export functions to suppress translation in the

nucleus by removing eEF1A from the nucleus (Bohnsack et al., 2002), rather than as an alternative pathway to exportin-t-mediated tRNA export, which occurs in the form of the ternary complex, tRNA•exportin-t•RanGTP (Arts et al., 1998).

Another important role for eEF1A is suggested by its association with the cytoskeleton. Overexpression of eEF1A has led to defective budding and enlarged cells in yeast (Munshi et al., 2001). As suggested by the actin binding/bundling property of eEF1A, this phenotype may arise from an abnormal actin cytoskeletal organization. In the normal cell, eEF1A association with actin has been proposed to play a role in organizing the translational apparatus within the cell (Condeelis, 1995).

Recently, eEF1A was identified as a protein cross-linked with a ribosome-nascent peptide complex (Hotokezaka et al., 2002). This interaction site on the ribosome appears to be different from the A site where aa-tRNA•eEF1A•GTP is usually positioned. As previously shown with EF-Tu (Kudlicki et al., 1997; Caldas et al., 1998), eEF1A was found to have chaperone-like function on denatured firefly luciferase in vitro. Together with the previous report of a ubiquitin-dependent degradation of N-acetylated proteins stimulated by eEF1A (Gonen et al., 1994), eEF1A may be involved in quality control of newly synthesized peptide chains.

Although eEF1A in many organisms from *Escherichia coli* (L'Italien and Laursen, 1979) to rabbit (Dever et al., 1989) is found to be heavily modified post-translationally with methyl and phosphoryl and other moieties, the link between these modifications and eEF1A function has not been elucidated (Browning, 1996). Recently, three eEF1A isoforms that are deposited in the maize endosperm at high levels were shown to differ in their binding to filamentous actin, but to bind aminoacylated tRNA with similar affinities (Lopez-Valenzuela et al., 2003). Using mass stectrometry, these purified isoforms appeared to have differences in their phosphorylation and methylation status. The relative amounts of the three isoforms appeared to be regulated during development, suggesting defined functions that have yet to be identified.

1.4 Translation of cellular and viral mRNAs

Following entry into a host cell and decapsidation, translation of the genomic RNA is the first event for positive strand RNA viruses initiating a replication cycle. The 5´-cap structure and 3´-poly(A) tail are standard features of cellular mRNAs and are required for efficient gene expression, while many viral mRNAs lack either or both. Thus, viruses have evolutionally developed a number of unique strategies to have their own mRNAs efficiently translated in competition with cellular mRNAs. In this section, the review focuses on the regulatory elements located in the 5´- and 3´-UTRs of the eukaryotic mRNAs, followed by discussion of strategies for enhanced gene expression employed by various viruses.

1.4.1   Translation of eukaryotic cellular mRNAs

Translation is typically controlled by structural features located in the UTRs of mRNAs. The most well-known controlling elements are the 5´-cap structure and the 3´-poly(A) tail, which cooperatively up-regulate translation when present in cis. The synergistic relationship between these elements present at both RNA termini reflects a higher than multiplicative combined effect of their individual contributions to translation (Gallie, 1991). The synergism is discussed in more detail in section 1.4.A.b.

1.4.1.1   Structural elements in the 5´-UTR

The overall efficiency of gene expression depends on many post-transcriptional events such as efficient translation steps (initiation, elongation, termination and perhaps recycling of ribosomes), half-lives of mRNA and synthesized protein, and intracellular localization. Translation initiation is usually the rate-limiting step in the course of translation (Kawaguchi and Bailey-Serres, 2002). The steps in translation initiation are described in many reviews (Browning, 1996; Sachs et al., 1997; Preiss and Hentze, 1999). In brief, the initiation of translation begins with the recognition of the 5´-^{m7}GpppN cap structure by eukaryotic initiation factor 4E (eIF4E; Sonenberg et al., 1978). Binding to eIF4E, eIF4G scaffolding protein also recruits eIF4A (ATP-dependent RNA

helicase), eIF4B (RNA binding protein), and the eIF3 complex, which itself is bound to the 40S ribosomal subunit. eIF4A-dependent unwinding of secondary structures in the 5′-UTR facilitates loading the 40S ribosomal subunit onto the 5′-proximal region of the UTR (Svitkin et al., 2001). Methionylated initiator tRNA^{Met} (in the form of the met-tRNA$_i^{Met}$•eIF2a•GTP ternary complex) also becomes associated with the small ribosomal subunit bound to the 5′-UTR. The small ribosome complex scans along the 5′-UTR in the 5′ to 3′-direction to look for the first AUG codon, followed by coupling with the 60S ribosomal subunit, after which translation elongation begins (Browning, 1996).

Translation initiation can be affected by the following properties of the 5′-UTR of an mRNA: the presence or absence of a 5′-cap, length of the leader sequence, secondary structure near the 5′-terminus and downstream of the initiation codon, and the initiation codon context. Although there can be other translation-controlling features in the 5′-UTR of cellular mRNAs, the discussion below is limited to features that are relevant to 5′-capped RNAs such as TYMV RNA. The cap structure at the 5′-terminus is known to enhance translation in comparison to uncapped RNAs because of the enhanced interaction with initiation factors. This stimulating effect by the 5′-cap structure in vivo has been measured to be 21.3 in tobacco protoplasts, 1.31 in CHO cells, 3.72 in yeast cells (Gallie, 1991), 12.0 to 36.4 in carrot cells (Leathers et al., 1993; Gallie, 2002), 1.11 in *Xenopus* oocytes (Gallie et al., 2000), about 4 in ST cells (Vende et al., 2000), about 11 in Vero cells, and about 38 in C6/36 cells (W-W Chiu, personal communication). In general the effect is estimated to be 2 to 100-fold depending on the source of the translation system, RNAs tested and specific conditions (Futterer and Hohn, 1996).

The strong dependency of translation initiation on the 5′-cap can be circumvented by the presence of an internal ribosome entry site (IRES), which was first identified in piocrnavirus mRNA (Pelletier and Sonenberg, 1988). Many of the IRESs that have been reported to date are from viral RNAs, although capped cellular mRNAs containing IRESs have also been reported (e.g., Hellen and Sarnow, 2001). eIF4E, eIF4A and the N-terminus of eIF4G were found to be dispensable for the IRES-dependent translation of poliovirus (Pause et al., 1994), while the C-terminus of eIF4G was reported to be

necessary from the IRES activity (Ohlmann et al., 1996). This C-terminal fragment of eIF4G is generated from proteolytic cleavage by polioviral protease during infection (Ehrenfeld, 1996). Detailed mechanisms of IRES-dependent translation initiation have yet to be elucidated.

The length of the 5´-UTR appears to affect translation efficiency. A 5´-UTR shorter than about 20 nts showed decreased gene expression compared to RNAs with longer 5´-UTR in the reticulocyte lysate system (Kozak, 1991b). In microinjected *Xenopus* oocytes, when the 5´-UTR was increased from 17 nts to 72 nts, the translation of a luciferase reporter gene was increased by about 2-fold for a capped, poly(A)-tailed RNA (Gallie et al., 2000), although this particular experimental system does not appear to support synergism between the 5´-cap and poly(A) tail, and thus needs further critical evaluation. Less efficient translation from short 5´-UTRs seems to be important for some bicistronic mRNAs where translation from the second AUG is dependent on relatively weak translation initiation from the first AUG (Johnston and Rochon, 1996).

Polysome analysis of a monocistronic CAT reporter RNA with an unstructured 22 nt long 5´-UTR in yeast revealed that the number of ribosomes on the RNA was about half that on RNA with a 77 nt-long UTR (Sagliocco et al., 1993). The decreased number of mRNA-associating ribosomes observed in the polysome analysis is possibly not due to to impaired loading of 40S ribosomal subunit at the 5´-terminus. If ribosome loading at the 5´-terminus were impeded because of the short 5´-UTR, translation at the second AUG as well as the first AUG in a bicistronic mRNA should be low. However, the amounts of translation products from the second AUG are comparable with those from RNAs without the first AUG (Slusher et al., 1991; Kozak, 1995). These observations indicate that sufficient number of ribosomal subunits can be loaded onto a short UTR. It is interesting that the lengths of the 5´-UTRs of many plant viral RNAs (usually subgenomic RNAs) are about 20 nts or even less (Guilley and Briand, 1978; Dasgupta and Kaesberg, 1982; Johnston and Rochon, 1996; Juszczuk et al., 2000), yet translation is very active. Translation of these RNAs may be compensated by other features present in

the RNAs, such as translation enhancer elements or lack of stable secondary structure in the 5´-UTRs.

The presence of secondary structure has been reported to impose opposite effects depending on its location in the mRNA. When a stable stem-loop structure (ΔG= -30 kcal/mol) is situated 12 nts away from the 5´-terminus, translation of the mRNA was found to be decreased in COS cells (Kozak, 1986b) and in reticulocyte lysate (Kozak, 1989). This perturbation is probably due to physical interference of ribosome loading and/or RNA interaction with initiation factors, especially eIF4A helicase, which is proposed to unwind the secondary structure to facilitate the loading of the ribosomal subunit (Rogers et al., 1999; Svitkin et al., 2001). This negative effect on translation was relieved as the secondary structure was moved away from the 5´-terminus (Kozak, 1989). When the stable secondary structure was located further away from the 5´-terminus, translation inhibition was only observed with more stable structures (ΔG= –60 kcal/mol; Kozak, 1986b), suggesting that the scanning ribosomal subunit can unwind more stable structures than those inhibiting subunit loading. A stem-loop with ΔG as small as -7.6 kcal/mol, placed 11 nt downstream of the 5´-terminus (Baim and Sherman, 1988) and one with ΔG= -15.6 kcal/mol, placed 18 nts downstream of the 5´-end, both resulted in about 10-fold decrease in gene expression (Wang and Wessler, 2001).

On the other hand, a stem-loop (ΔG=-19 kcal/mol) situated after an initiation codon in a suboptimal context (see below for discussion of initiation context) has led to improved start codon recognition by the scanning subunit (reviewed in (Kozak, 1991a). In the same study, the optimal position of the stem-loop was about 14 nts downstream of the AUG. Kozak hypothesized that the stem-loop in this position would slow down the scanning of the 40S ribosomal subunit to temporarily position it over the AUG and so facilitate initiation. In baby hamster kidney cells, a stable stem-loop structure in the coding region of the Sindbis virus subgenomic RNA encoding capsid protein was disrupted by point mutations without altering amino acid sequence (Frolov and Schlesinger, 1996). The mutations resulted in about 10-fold lower translation activity. However, this secondary structure is located 27 nts downstream of the initiation codon,

and its enhancing function was diminished as the structure was moved towards the initiation codon. Therefore, this structure is considered to enhance translation using a different mechanism from the secondary structure located at about 14 nts downstream of the AUG.

Finally, Kozak has characterized the importance of sequence context flanking an AUG initiation codon. In mammalian systems, by introducing one substitution mutation at a time in nucleotides around the initiation codon of preproinsulin, the most profound effect was observed for a purine at position –3 (Kozak, 1986a) and G at position +4, relative to A (+1) of the AUG initiation codon (Kozak, 1997). The optimal translation initiation context has been proposed to be GCC(A/G)CCAUGG (the initiation codon is underlined; Kozak, 1987). The mechanism by which context influences expression remains to be experimentally elucidated, although Kozak postulates the sequence upstream of the AUG slows down a scanning ribosomal subunit to improve the recognition of the initiation codon, similar to the proposed role of the secondary structure in the coding region (Kozak, 1999). In plants, the consensus sequences of initiation contexts for monocots and dicots are c(a/c)(A/G)(A/C)cAUGGCG and aaA(A/C)aAUGGCu, respectively (lower case nucleotides are less conserved; Joshi et al., 1997). In contrast to the animal system, the initiation context of plant system has some room for discussion because there have been conflicting results on the importance of the –3 and +4 positions (Lehto and Dawson, 1990; Johnston and Rochon, 1996). The point of the debate is whether both positions (as in animal systems) or either one is important in determining the strength of the initiation context. Since optimal contexts are often different from consensus sequences, the importance of initiation context needs to be evaluated experimentally on each RNA in each system.

1.4.1.2 Regulatory elements in the 3´-UTR

The 3´-poly(A) tail has been shown to increase mRNA stability and gene expression, although the latter effect overwhelms the former in significance. The translation enhancing effect is synergistically increased in the presence in cis of a 5´-cap.

This synergistic relationship is attributed to physical interactions through proteins that bind both termini, making the mRNA into a closed circle (Jacobson, 1996; Sachs et al., 1997). This closed circular model is based on the result that the poly(A) binding protein (PABP), which binds to the poly(A) tail, interacts with the eIF4G scaffolding protein (Tarun and Sachs, 1996), which in turn interacts with eIF4E bound to the 5′-cap of the mRNA (Wells et al., 1998b). Since mammalian PABP interacts with eRF3 translation termination factor, it has been proposed that this interaction promotes multiple rounds of translation by improved recycling of ribosomes (Uchida et al., 2002). In addition, PABP involvement in translation initiation is supported by the following two observations: 1) in wheat, a homodimer of eIF4B was shown to interact with PABP (Le et al., 2000) and to increase helicase activity of eIF4A (Bi and Goss, 2000); 2) wheat germ PABP was found to lower the dissociation rate of eIF4E from the 5′-cap (Luo and Goss, 2001).

The effect of the length of the 3′-UTR excluding the poly(A) tail was studied using capped luciferase reporter RNAs in CHO cells (Tanguay and Gallie, 1996b). The authors found that a step-wise 3′-UTR increase from 4 nts to 104 nts increased the translation efficiency in the absence of a poly(A) tail, while the translation efficiencies among poly(A)-tailed RNAs with different 3′-UTR length did not differ. This result indicates that the synergistic effect between poly(A) and the 5′-cap diminishes as the 3′-UTR length increases. Indeed, the synergy between 5′-cap and a long 3′-UTR (156 nts in length) was found to be 2.3 (Tanguay and Gallie, 1996b), a lower value than about 10, which was observed for the synergy between the 5′-cap and poly(A) in an RNA with a 19 nt-long 3′-UTR (Gallie, 1991). These results suggest that a long 3′-UTR and poly(A) tail partially overlap in function, at least in the CHO cells used for the study. The authors hypothesized that expression increases due to a poly(A) tail or a long 3′-UTR are due to increased local concentration of ribosome subunits that remain associated with the mRNA after the stop codon, and increased potential for ribosome recruitment by initiation factors bound to the 5′-terminus.

Other features in the 3′-UTRs are important for overall gene regulation, although they may be less relevant to the studies of this thesis. Briefly, the roles of features in the

3′-UTR include i) regulation of RNA stability, such as by AU-rich elements (Shaw and Kamen, 1986) or micro RNA binding sites (Lau et al., 2001; Lim et al., 2003); ii) intracellular localization as in *oskar* mRNA (Lie and Macdonald, 1999; Castagnetti et al., 2000); iii) presence of upstream ORF and ribosome re-initiation as in GCN4 mRNA (Dever, 2002); and iv) cytoplasmic polyadenylation (Mendez and Richter, 2001).

1.4.2   *Viral RNA translation*

1.4.2.1   Two translation enhancers of *Tobacco mosaic virus*

TMV genomic RNA has two translation enhancing elements, one each located in the 5′ and 3′-UTRs. The 5′ UTR, called Ω, is 68 nts in length, harboring a 25 nt-long poly(CAA) stretch where heat shock protein (HSP) 101 was found to interact (Wells et al., 1998a). HSP101 enhances translation through the active recruitment of eIF4G (Gallie, 2002). This competitive recruitment is consistent with the result that Ω-mediated translation enhancement calculated for uncapped non-poly(A) tailed RNA is about three times higher than the effect in the presence of the 5′-cap and 3′-poly(A) tail (Gallie, 2002), both of which are known to interact with eIF4G. The author considers that eIF4G directly competes for binding to Ω vs the 5′-cap and 3′-poly(A) tail, resulting in diminished Ω-dependent enhancement in capped poly(A) tailed RNA. Perhaps there is an advantage to possessing redundant translation enhancing features.

Extensive mutational analysis of reporter RNA constructs electroporated into carrot protoplasts mapped the 3′-translation enhancing element to the pseudoknot (UPSK3) immediately upstream of the TMV TLS (see Fig.1.1D; Leathers et al., 1993). In contrast with Ω, the mechanism of TMV 3′ translation enhancement is yet to be discovered, although three host proteins were found to interact with UPSK3, one of which (102 kDa protein) is likely to be HSP101 (Tanguay and Gallie, 1996a; Wells et al., 1998a). Recently, another group reported that eEF1A was UV cross-linked to the UPSK3, with nucleotides critical for the interaction (Zeenko et al., 2002) partially overlapping those for the 3′ translation enhancing activity (Leathers et al., 1993). Unlike Ω, the TMV 3′-translation enhancer functions synergistically with the 5′-cap (Leathers et

al., 1993). When the TMV 3´ UTR and Ω are present in the same RNA, their relationship is more or less multiplicative, suggesting independent mechanisms of enhancement (Gallie, 2002). The BMV 3´-most 105 nts, which harbors the entire TLS, has been demonstrated to enhance translation to similar levels to the TMV 3´-UTR (Gallie and Kobayashi, 1994), although its mode of action has not been elucidated.

Another interesting distinction between the TMV 5´- and 3´-translation enhancers is observed in the period 2 to 15 min after delivery of capped RNA transcripts into protoplasts. In this time period, the TMV 3´ UTR, like a poly(A) tail, does not seem to show translation enhancing activity. In contrast, significantly stimulated translation was observed in this time period from the Ω-containing RNA constructs (Gallie, 2002), suggesting that Ω is involved in the first round of translation. This observation fits nicely with the idea of ribosome-mediated directional disassembly of the virion particle by first exposing Ω to recruiting ribosomes, while the 3´ UTR is still protected by the coat protein (Wu et al., 1994).

1.4.2.2 Coat protein binding linked to translation enhancement in *Alfalfa mosaic virus*

Although AMV belongs to the family *Bromoviridae*, it is distinguished from BMV by its unique requirement for co-inoculation with CP or RNA4, the subgenomic RNA that expresses CP, in order to successfully initiate an infection (reviewed in (Jaspars, 1999). This unique phenomenon is termed genome activation. The CP has been demonstrated to bind to the AMV 3´-UTR, which has seven hairpins, each separated by an AUGC tetranucleotide (Reusken, et. al, 1994). This region may not, however, be the only region involved in encapsidation, since deletion of the 3´-UTR did not have a negative effect on encapsidation (Vlot et al., 2001).

The role of CP in genome activation appears to be functionally similar to that of PABP in terms of translation enhancement, because addition of poly(A) tails to the 3´-UTRs of AMV RNA1 and 2 partially circumvented the requirement for CP (Neeleman et al., 2001). However, inoculation with poly(A) tailed RNAs in protoplasts enhanced RNA amplification only about 50-fold in the absence of CP, while CP or RNA4 co-inoculation

allowed more than 1000-fold increase in RNA accumulation (Neeleman et al., 2001). This result suggests that CP binding may provide a stronger translation enhancing activity than PABP. Alternatively, CP may play additional roles in viral accumulation, such as regulating plus strand synthesis or protecting viral RNAs from nuclease attack. In in vitro transcription experiments, CP binding was found to have an inhibitory effect on minus strand synthesis (Houwing and Jaspars, 1986). A detailed mechanism of the CP-mediated translation enhancement of AMV RNA is yet to be elucidated.

The AMV RNA4 5′ UTR has been demonstrated as translation enhancer in tobacco mesophyll protoplasts (Gallie et al., 1987) and in vitro (Jobling and Gehrke, 1987; Jobling et al., 1988). This enhancing activity was not observed in polio-infected HeLa cells (Hann and Gehrke, 1995), suggesting that eIF4G may be involved in the translational enhancement mediated by the AMV RNA4 5′-UTR, since eIF4G is proteolytically cleaved in poliovirus-infected cells (Ehrenfeld, 1996).

1.4.2.3 RNA circularization as a mode of translation enhancement of Luteovirus RNA

Barley yellow dwarf luteovirus (BYDV) is a positive sense RNA virus whose genomic RNA lacks both a 5′-cap and a 3′-poly(A) (Allen et al., 1999). The efficient translation of BYDV RNA was found to depend on a 105 nt-long translation element (3′-TE) located in the 3′-UTR of the genomic RNA (Wang et al., 1997;1999). Its enhancing function has been observed both in the wheat germ vitro translation system and in oat protoplasts. For full translation enhancement in protoplasts, a longer sequence (869 nts) harboring the 3′-TE is required, resulting in more than 100-fold increase in gene expression relative to an uncapped RNA without the 3′-TE (Guo et al., 2000). Covariation mutation analysis in vivo and in vitro revealed that 3′-TE function requires 5′-3′ communication mediated through base-pairing between loop IV in the 5′-UTR and loop 3 in the 3′-UTR (Guo et al., 2001). Involvement of a protein to strengthen the interaction has not been excluded. Although the exact mechanism is still unknown, the mode of translation enhancement by the BYDV 3′-TE is essentially different from that controlled by an IRES because of its location in the 3′-UTR (Allen et al., 1999).

Furthermore, 3´-TE mediated translation was diminished by placement of a stable stem-loop structure (ΔG=-34.4 kcal/mol) at the 5´-terminus, suggesting 40S ribosomal subunit entry at the 5´-terminus of the RNA, and not internally as with IRES-mediated translation (Guo et al., 2001).

1.4.2.4   Translation enhancement by interaction of a rotavirus protein with eIF4G

The N-terminus of rotavirus NSP3 (36 kDa) was found to bind to the 3´-terminal conserved sequence, GACC, present in the 11 mRNAs present in rotaviral infections. No binding of NSP3 was observed to an RNA substrate whose 3´-terminal sequence is ACC (Deo et al., 2002), consistent with structural and binding studies emphasizing the importance of the entire GACC sequence (Poncet et al., 1994). The dissociation constant of the NSP3•RNA complex was reported to be 79 nM, and its half-life 8 hrs (Deo et al., 2002). In rotavirus-infected MA104 cells, the 3´-terminal GACC were found to enhance expression of a heterologous reporter gene inserted into the RNA bearing a generic 5´-UTR by about 4-fold, without significantly altering the physical stability of the RNA (Chizhikov and Patton, 2000). A more drastic effect of the 3´-translation enhancer was observed in NSP3-expressing swine testis cells, where the synergy value between the 5´-cap and the 3´-rotavirus sequence was found to be about 35 using luciferase reporter constructs (Vende et al., 2000). By co-immunoprecipitation analysis, the C-terminal domain of NSP3 was found to bind to human eIF4GI (Piron et al., 1998). This association was disrupted by PABP, suggesting that the same eIF4GI binding domain contacts rotavirus NSP3 and PABP. The NSP3•3´-UTR complex appears to functionally mimic the PABP•poly(A) tail complex in enhancing translation.

1.5   Transition from translation to minus strand synthesis

Following the expression of RdRp and other necessary viral proteins, the plus sense genomic RNA becomes a template for minus strand transcription. Since the ribosome and RdRp move along the plus strand RNA in opposite directions with respect to each other, some sort of traffic control is necessary in order to avoid collision by the two enzymes. It now seems that the following is generally true of the transition from initial translation to minus strand synthesis at early stages of positive strand RNA viral infections: 1) after a certain amount of viral gene expressions, a cessation of translation is organized so that ribosomes will not continue to associate with the RNA; 2) the RNA that serves as template for minus strand synthesis is physically separated from the translation machinery by sequestration to the membrane compartment where RNA replication occurs.

1.5.1   *Poliovirus 5´-cloverleaf structure serving as a switch influencing the transition from translation to replication*

A cloverleaf structure in the 5´-UTR of poliovirus genomic RNA was found to be crucial for plus strand accumulation because mutation of stem-loop b and d of the cloverleaf structure led to a 5 to 10-fold reduction of plus to minus strand accumulation ratio, with minus strand levels being less affected (Andino et al., 1990). The role of the cloverleaf in viral replication appears to be more than in promoting plus strand synthesis, as indicated by later studies. A cellular factor, poly(rC) binding protein (PCBP) was found to interact weakly with stem-loop b of the cloverleaf structure and strongly with stem-loop IV of the IRES, and to up-regulate viral translation (Gamarnik and Andino, 2000). Subsequently, the viral polymerase precursor 3CD, which emerges as a result of viral translation, binds to stem-loop d of the cloverleaf (Andino et al., 1990; Andino et al., 1993). This simultaneously represses translation and promotes minus strand RNA synthesis (Gamarnik and Andino, 1997; Gamarnik and Andino, 1998).

A key player in the switching from translation to minus strand synthesis is PCBP, whose binding to the cloverleaf was found to be greatly enhanced by the 3CD interaction

with stem-loop d (Gamarnik and Andino, 2000). Although not yet demonstrated in vivo, the 3CD-bound cloverleaf effectively competes against the IRES for PCBP binding, resulting in viral translation being shut down. Demonstrating that the RdRp is unable to amplify RNA undergoing active translation, Gamarnik and Andino proposed that the interaction of 3CD with the cloverleaf structure controls the transition from translation to RNA replication mode (Gamarnik and Andino, 1998).

Using an in vitro replication assay, deletion analysis showed that the 5'-cloverleaf structure was required in cis for minus strand initiation (Barton et al., 2001), which is thought to occur somewhere in the 3'-poly(A) tail. Both PCBP and 3CD have been demonstrated to interact with PABP, which binds to the poly(A) of poliovirus RNA in a poly(A) length-dependent manner (Herold and Andino, 2001). This finding led the authors to propose a 5'-3' terminal interaction (circularization of RNA) by means of a protein-protein bridge, bringing the RdRp (bound at the 5'-cloverleaf) within close proximity of the site of minus-strand initiation in the 3'-UTR.

1.5.2   *Repression of translation by bacteriophage Qβ replicase*

Qβ replicase binds to the S-site (nt position 1247 to 1346) and the M-site (nt position 2545 to 2867) of Qβ genomic RNA (Brown and Gold, 1995). These sites could be cross-linked to the subunits of the replicase, the ribosomal protein S1 and EF-Tu, respectively (Brown and Gold, 1996). The M-site was found to be necessary for Qβ replicase to start minus strand synthesis, despite being located about 1.5kb upstream of the 3'-terminus (Miranda et al., 1997). Covariation analysis led to the proposal that long distance base-pairing was important for the replicase bound at the M-site to access the 3'-terminus where minus strand synthesis initiates (Klovins et al., 1998). The importance of the terminal sequence has been reported recently (Yoshinari and Dreher, 2000; Tretheway et al., 2001).

Ribosome-associated Qβ RNA was demonstrated to have poor template activity for the replicase, and in turn, the replicase complexed with Qβ RNA inhibited translation initiation (Kolakofsky and Weissmann, 1971a). These results indicate that translation

and minus strand synthesis in bacteriophage Qβ, like poliovirus, are incompatible processes occurring on the same RNA molecule. Kolakofsky and Weissmann proposed a model for the switch from translation to replication, in which replicase binding to the ribosome binding site of the CP ORF (later verified to overlap the S-site; Senear and Steitz, 1976) prevents further ribosome loading and initiation of translation (Kolakofsky and Weissmann, 1971a, 1971b). As the last ribosome exits from the RNA, the replicase is free to initiate minus strand at the 3´-terminus of the template RNA.

1.5.3 *Common recognition sites shared by replicase and viral translation enhancer proteins (AMV and Rotavirus)*

As discussed in a previous section (1.4.B.b), AMV CP binds to the seven consecutive stem-loop structures in the 3´-terminal region of the genomic RNAs, enhancing gene expression (Neeleman et al., 2001). The 3´-terminal region can be folded into an alternative structure, a TLS formed through pseudoknot formation involving the loop and stem of the fourth and first stem-loop, respectively, from the 3´-terminus (Olsthoorn et al., 1999). Disruption of pseudoknot formation by mutation of the first stem sequence resulted in parallel loss of infectivity and of template activity for minus strand transcription in vitro, while a structure-restoring mutation in the fourth loop recovered both functions of the RNA (Olsthoorn et al., 1999). The alternative TLS conformation of the 3´-terminal region was found to be formed only when RdRp binds to the region (Olsthoorn et al., 1999). Consistent with these results, CP binding was found to have an inhibitory effect on minus strand synthesis (Houwing and Jaspars, 1986). Thus, this 3´-region has been proposed to control ribosome and replicase traffic, acting as a molecular switch between translation and replication (Bol, 2003). Furthermore, the accumulation of CP may be involved in shutting down minus strand synthesis later in the AMV life-cycle, achieving the common characteristics among plus strand RNA viruses of a very high plus to minus strand RNA ratio (Olsthoorn et al., 1999).

A similar molecular switch from translation to replication has been proposed for the rotavirus NSP3 protein, which is present in the virions of this double stranded RNA

virus (Deo et al., 2002). NSP3 was shown to bind the 3´-terminal sequence of the rotavirus mRNAs and enhance translation through interaction with the eIF4G scaffolding protein (Vende et al., 2000). The recognition sequence in the RNA corresponded in part to cis-acting elements required for minus strand synthesis (Wentz et al., 1996; Chen and Patton, 2000). Thus, the rather tight binding of NSP3 to the terminal sequence (K_d=79 nM) was proposed to have a negative effect on minus strand synthesis (Deo et al., 2002).

1.5.4 RNA conformational change exposing the 3´-terminal sequence for minus strand initiation in Luteovirus and Tombusvirus

The transition from translation to minus strand synthesis of the luteovirus *Barley yellow mosaic virus* RNA has been proposed to involve an RNA structural change. According to software prediction and structure probing, the 3´-terminal ACCC can be base-paired with GGGU located 56 nts upstream (Koev et al., 2002). Assuming viral replicase requires single-stranded termini for efficient minus strand initiation as observed with other positive stranded viruses, this embedded 3´-end was proposed to suppress minus strand synthesis. Consistent with this proposal, transfection of RNA with a deletion of a stem-loop structure (SL1) immediately upstream of the terminal ACCC, leading to predicted release of the 3´-end from base-pairing, resulted in high minus strand accumulation and background level of plus strand accumulation in oat protoplasts (Koev et al., 2002). This observation is consistent with the idea that the terminal structure is involved in regulating minus strand synthesis, which is eventually important for successful viral replication.

A similar inhibitory effect on minus strand synthesis in *Tomato bushy stunt virus* was demonstrated with an in vitro transcription system (Pogany et al., 2003). Covariant analysis revealed that a 5-nt long sequence in region IV of the 3´-UTR of the genomic RNA base-pairs with the minus strand promoter region consisting of the 3´-terminal 19 nts. The importance of this cis-acting replication silencer was also demonstrated in protoplasts. One of the possible roles postulated for the silencer region is to control the translation and minus-strand synthesis, because it shares a common nucleotide sequence

with a cap-independent translation enhancer, located in the 3´-UTR (regions III, 3.5 and IV; Wu and White, 1999). The mechanism of translation enhancement as well as the functional role of the replication silencer remain to be elucidated in the future.

1.5.5 *Role of RNA sequestration to membrane vesicles in the transition from translation to replication*

BMV 1a protein, containing the methyltransferase-like and helicase-like domain, has been shown to interact with recognition elements located in each of the three genomic RNAs (Diez et al., 2000; Chen et al., 2001b). In the absence of 2a protein (RdRp), the 1a interaction with BMV RNA3 increased the RNA stability without an elevation of CP (encoded by RNA3) accumulation, suggesting that the binding represses translation activity (Janda and Ahlquist, 1998). By the use of a yeast-based BMV replication system, it was shown that efficient replication of BMV RNA requires the yeast *LSM1* gene (Ishikawa et al., 1997), which was later found to be required for efficient translation of the BMV genomic RNAs and the RNA-1a protein interaction (Diez et al., 2000). Thus it appears that the RNA undergoing LSM1p-mediated translation is eventually recognized by the newly synthesized 1a protein, which in turn represses translation. Through 1a protein interaction, the BMV 2a RdRp protein is directed to ER membranes, to which the 1a protein is anchored (Chen et al., 2001b) and where RNAs are thought to be amplified in 1a-induced peripheral vesicles (reviewed in (Ahlquist et al., 2003). Thus, the physical segregation of the RNA template for minus strand synthesis from the translational machinery may further facilitate the transition from translation to replication.

Chapter 2 The tRNA-like structure of Turnip yellow mosaic virus RNA is a 3´-translational enhancer

Daiki Matsuda and Theo W. Dreher

2.1 Abstract

Many positive stand RNA viral genomes lack the poly(A) tail that is characteristic of cellular mRNAs and that promotes translation in cis. The 3′ untranslated regions (UTRs) of such genomes are expected to provide similar translation enhancing properties as a poly(A) tail, yet the great variety of 3′ sequences suggests that this is accomplished in a range of ways. We have identified a translational enhancer present in the 3′-UTR of *Turnip yellow mosaic virus* RNA, using luciferase reporter RNAs with generic 5′ sequences transfected into plant cells. The 3′-terminal 109 nucleotides comprising the tRNA-like structure (TLS) and an upstream pseudoknot (UPSK) act in synergy with a 5′-cap to enhance translation, with a minor contribution in stabilizing the RNA. Maximum enhancement requires that the RNA be capable of aminoacylation, but either the native valine or engineered methionine is acceptable. Mutations that decrease the affinity for translation elongation factor eEF1A (but also diminish aminoacylation efficiency) strongly decrease translational enhancement, suggesting that eEF1A is mechanistically involved. The UPSK seems to act as an important, though nonspecific, spacer element ensuring proper presentation of a functional TLS. Our studies have uncovered a novel type of translational enhancer and a new role for a plant viral TLS.

2.2 Introduction

The genomic RNAs of positive strand RNA viruses are used at the beginning of an infection as the mRNA from which the early viral genes are expressed. These RNAs must thus appear in a form that is efficiently utilized by ribosomes in competition with cellular mRNAs. Eukaryotic mRNAs almost universally have a $5′-^{m7}GpppN$ cap structure and a 3′ poly(A) tail, both of which promote translation. Small ribosome subunits are drawn to the 5′-terminus through interactions via the eIF3 initiation factor complex with the eIF4F complex that binds the cap (Pestova et al., 2001). The poly(A) tail promotes translation in part as a result of interactions between bound poly(A) binding protein and eIF4G, a subunit of eIF4F, thereby producing a circular RNA with termini in close proximity (Sachs et al., 1997; Gallis, 1998; Mangus et al., 2003). Many positive

strand viral RNAs deviate from the design of cellular mRNAs by lacking either a 5′-cap, 3′-poly(A) tail, or both. An appreciation of viral gene expression requires understanding how viral mRNAs overcome the disadvantage of lacking these features.

Turnip yellow mosaic virus (TYMV) is one of several plant viruses with a genomic RNA that has a 5′-cap but lacks a poly(A) tail. The 3′-noncoding region is a 109 nt sequence that comprises a tRNA-like structure (TLS) and an upstream pseudoknot (UPSK) (Fig. 2.1). The TLS is a highly efficient mimic of tRNA^{Val}, interacting with at least three tRNA-specific proteins as efficiently as tRNA^{Val}: CCA nucleotidyltransferase, which adds the 3′-terminal adenosine to complete the –CCA 3′-end (most virion RNAs lack the terminal A; Briand et al., 1977); valyl-tRNA synthetase, which covalently links valine to the 3′-end; and translation elongation factor eEF1A, which binds the valylated RNA to form a valyl-RNA•eEF1A•GTP ternary complex (Mans et al., 1991; Florentz and Giegé, 1995; Dreher and Goodwin, 1998). The UPSK and TLS comprise the entire 3′-UTR of the subgenomic RNA, from which the coat protein (CP) is translated (Fig. 2.2A). The genomic RNA has a considerably longer 3′-UTR that encompasses the entire CP ORF as well as the UPSK and TLS (Fig. 2.2A).

Translation enhancing elements have been mapped in the 3′-UTRs of the non-polyadenylated genomes of several positive strand RNA viruses (Gallie and Walbot, 1990; Gallie and Kobayashi, 1994; Hann et al., 1997; Wang et al., 1997; Meulewaeter et al., 1998; Wu and White, 1999; Qu and Morris, 2000; Neeleman et al., 2001; Koh et al., 2003). In this communication, we report our studies on the presence of translational enhancer activity in the 3′-UTR of TYMV RNA. While such activity has been observed in *Tobacco mosaic virus* (TMV) and *Brome mosaic virus* (BMV) RNAs, both of which possess a 3′-TLS, none was previously detected in TYMV RNA (Gallie and Kobayashi, 1994). We demonstrate that the 3′-terminal 109 nt of TYMV RNA does indeed provide strong translational enhancer activity. This activity is dependent on the ability of the RNA to be aminoacylated, and therefore assay RNAs must be produced with authentic 3′-termini, explaining the failure of the earlier study to detect translational enhancement.

L1

28

Xmn I

A C U
A   T   CCCG—CCC   /CUCU\   UCGGA┤ACC (A)3'
C G U |||| ||| / |||||
           GGGC GGG—/AGCCU┘
                  \
                   UCA

U G   U
U D A   A
A   C   A
      G-C U
      C-G
      G-C
      A-U   TLS
      G-C
      G
Dra I   G/
U   U-A
U   A   C-G
U   A   U-A
UPSK 96-/U A   G-C
        C   A U-A
        U-A   C-G
        A-U   C
        G-C   C A/C A
5' UAAGUUCUC-GUUAG   C
        | |
       107   83

The sequence drawing shows:
5' UAAGUUCUC-GUUAG—
107 ... 83

C (C)
C A/C A
C (A)(C)
56
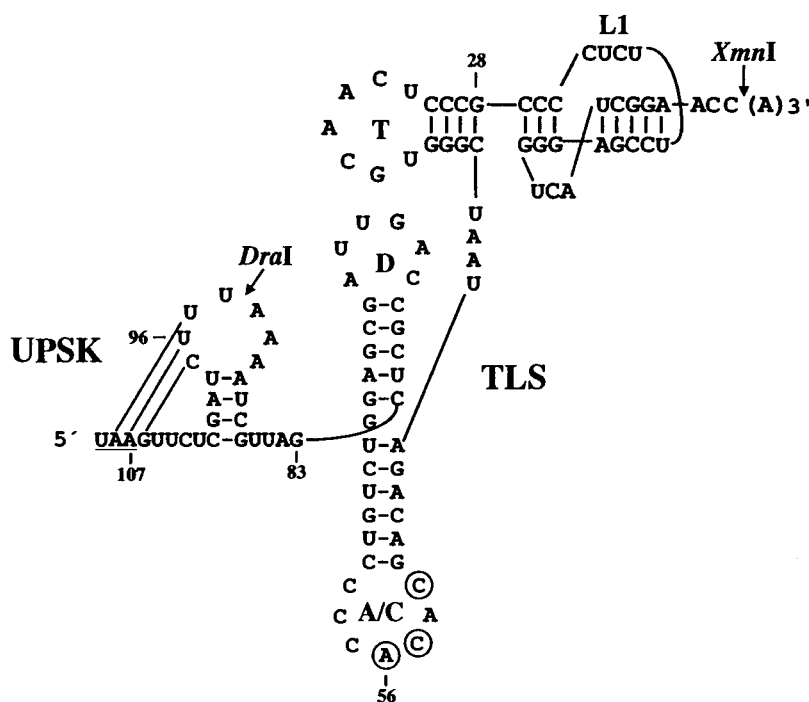
Fig. 2.1 The 3′-tRNA-like structure (TLS) and upstream pseudoknot (UPSK), distinctive features present at the 3′-end of TYMV RNA.

The sequence and secondary structure of the entire 3′-UTR of the coat protein (CP) subgenomic RNA are shown, with the CP stop codon underlined. The main structural features of the TLS are indicated as L1 loop (L1) in the acceptor/T arm, and the T-, D-, and anticodon (A/C) loops that are analogs of the same features in tRNAs. The major valine identity nucleotides in the anticodon loop are circled. The UPSK (nts 108 to 87) is shown with proposed tertiary base-pairing interactions marked as parallel lines. The endpoints of templates linearized by *Dra*I and *Xmn*I restriction enzymes (see Fig. 2.2) are shown. Nucleotides are numbered from the 3′-terminal A, which is shown in parentheses because it is not present on virion RNA but is thought to be added rapidly in the cytoplasm by host CCA nucleotidyltransferase.

2.3 Results

2.3.1 The TYMV 3′ noncoding region enhances translation synergistically with the 5′ cap

Two types of viral mRNAs are present during TYMV infections: the genomic RNA with overlapping ORFs from which p69 and p206 are translated, and the 3′-colinear subgenomic RNA from which the coat protein (CP) is translated (Fig. 2.2A). The genomic RNA has a long (684 nt) 3′-UTR, which we refer to as gUTR and which includes the silent CP ORF, the UPSK and the TLS. The subgenomic mRNA has a 109 nt long 3′-UTR, shown in Fig. 2.1, which we refer to as sgUTR and which contains the TLS and UPSK.

To assess the effect of the 3′ region of TYMV RNA on translation, the gUTR and sgUTR were placed downstream of a firefly luciferase (LUC) reporter gene and a short vector-derived 3′-UTR, using a BamHI site for cloning (Fig. 2.2B). A 17 nt-long vector-derived sequence served as the 5′-UTR. In vitro transcription with T7 RNA polymerase after linearization of plasmids with XmnI produced run-off transcripts L-TYg and L-TYsg (L for LUC), with CC 3′ termini that correspond to the termini of native encapsidated TYMV RNAs (Briand et al., 1977). A 3′-terminal A residue is thought to be added rapidly in the cytoplasm by the host tRNA-specific enzyme CCA nucleotidyltransferase, for which TYMV(3′-CC) RNA is an excellent substrate (Dreher and Goodwin, 1998). Transcripts were introduced into protoplasts by polyethylene glycol-mediated transfection, and messenger function was assayed as the activity of LUC present in extracts made from harvested cells. Typically, protoplasts made from cowpea mesophyll cells were used and harvested 8 hr after transfection, but similar results were obtained with Chinese cabbage mesophyll protoplasts and cultured carrot protoplasts. Although cowpea plants do not support systemic TYMV infections, cowpea protoplasts support TYMV replication (K. Gopinath and T.W.D., unpublished).

Addition of the genomic and subgenomic 3′-UTRs to the vector 3′-UTR (L-Bam RNA transcribed from BamHI-linearized plasmid) of 5′-^{m7}GpppG-capped RNAs increased LUC accumulation 11- and 25-fold, respectively (Fig. 2.2B). By comparison, the addition of a strong 3′-translational enhancer element from the 3′-UTR of TMV RNA

(Gallie and Kobayashi, 1994) increased expression 27-fold (Fig. 2.3C). These results show that the 3´-UTR of TYMV RNA contains sequences that strongly up-regulate gene expression. Indeed, LUC expression from capped RNA supported by the TYMV sgUTR is comparable to that supported by a LUC reporter RNA with a 3´ poly(A) tail (Fig. 2.3A, C).

	Truncation of 3´UTR (nts)	Relative LUC activity	RNA
	0	11.29 ± 1.86	L-TYg
	92	2.41 ± 0.63	L-TYg-Dra
	257	3.10 ± 0.46	L-TYg-Sma
	611	1.46 ± 0.11	L-TYg-Pvu
	0	24.64 ± 8.38	L-TYsg
	92	0.63 ± 0.11	L-TYsg-Dra
	684/109	1	L-Bam
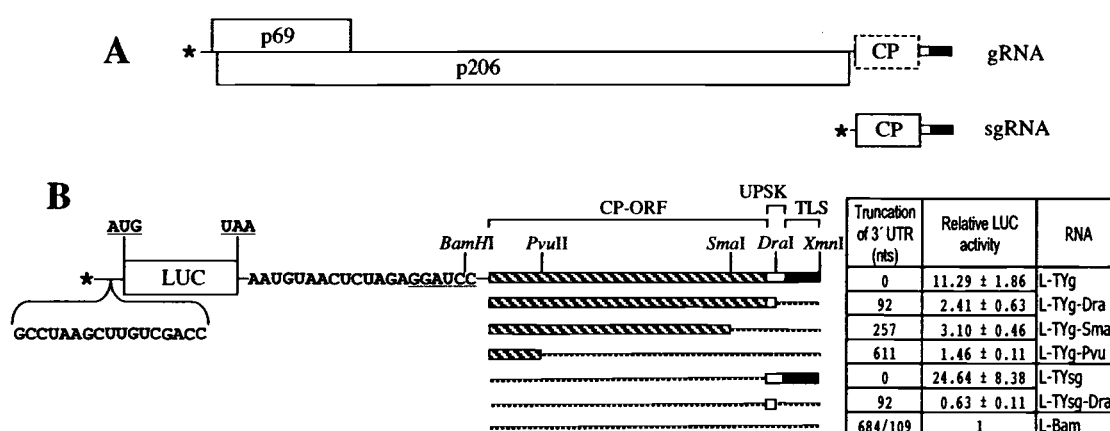
Fig. 2.2 Luciferase reporter RNAs demonstrating translational enhancement provided by the 3´-UTR of TYMV RNA.

(A) The TYMV genes are expressed from two 3´-colinear mRNAs, the genomic RNA (top) and the coat protein (CP) subgenomic RNA. The 3´-UTR of the genomic RNA includes the CP gene, which is translationally silent in the genomic RNA (indicated by a dashed box). The UPSK and TLS, common to the 3´-UTRs of both RNAs, are indicated as white and black bars, respectively. *, ^{m7}GpppG cap. (B) The reporter mRNA constructs used to assess gene expression in cells. The vector-derived 5´- and 3´-UTR sequences surrounding the luciferase-coding region (LUC) are shown. Two forms of TYMV 3´-UTR, represented by bars at right, have been analyzed. At the top is shown the 684 nt 3´-UTR of the genomic RNA (gUTR); this includes the silent coat protein ORF (cross-hatched) and the UPSK and TLS, indicated as in (A). Below is shown the 109 nt 3´-UTR of the CP subgenomic RNA (sgUTR), comprising only the UPSK and TLS. The TYMV UTRs were fused directly to the BamHI site (underlined) of the vector 3´-UTR to produce the L- family of RNAs (L for LUC). Restriction sites used to make RNAs with truncated 3´-ends are indicated, with dashed lines representing absent sequence; the missing length of RNA and the relative LUC expression levels of each capped RNA in cowpea protoplasts are tabulated at right. The data are derived from duplicate transcripts and at least two transfection experiments.

The domains within the 3´-UTR contributing to enhanced LUC expression were mapped by 3´-truncation of both L-TYg and L-TYsg RNAs. Truncated RNAs were produced by template linearization at upstream *Pvu*II, *Sma*I and *Dra*I restriction sites instead of the usual *Xmn*I (Fig. 2.2B). The *Dra*I site is positioned within the UPSK, upstream of the TLS, such that linearization at *Dra*I would produce RNAs lacking both the UPSK and TLS elements (Figs. 1 and 2B). Truncation of L-TYsg RNA at this site abolished all detectable enhancement of expression, while L-TYg-Dra and L-TYg-Sma RNAs supported LUC expression at levels 2 to 3-fold higher than L-Bam RNA (Fig. 2.2B). These results indicate that the strongest contribution to enhanced gene expression is found within the UPSK and TLS elements that comprise the sgUTR. Interestingly, these features have a weaker enhancing effect in the context of the longer gUTR, in which sequences further upstream (between the *Pvu*II and *Dra*I sites, 612 to 93 from the 3´-end) also contribute to expression. These observations seem analogous to the decreased influence of a poly(A) tail with longer 3´-UTRs and to the independent translation enhancing effect of long 3´-UTRs (Tanguay and Gallie, 1996a, b).

To distinguish whether increased LUC expression was a function of increased RNA stability or improved translation, we monitored LUC activity from L-TYsg RNA at 5 different time points up to 8 hr post transfection. In the experiment shown, LUC activity derived from capped L-TYsg RNA reached plateau between 6 and 8 hr post-transfection at a level 28.6-times higher than that reached after transfection with the L-Bam RNA (vector UTR; Fig. 2.3A, C). The functional half-life of L-TYsg RNA as an mRNA (time taken to reach half maximal LUC expression; Gallie, 1991) was 108 min, compared with 67 min for the L-Bam RNA (Fig. 2.3A, C). Improved RNA stability thus contributed 1.6-fold towards the increased LUC expression, leaving 17.6-fold increased LUC expression as the contribution of true translational enhancement. By comparison, addition of the 3´ UTR of TMV RNA (3´-terminal 191 nt) resulted in LUC expression 27.0 times higher than from L-Bam RNA (Fig. 2.3C). RNA functional half-life was increased by 1.5-fold, leaving an 18-fold enhancement of expression due to improved translational efficiency. The 3´ 109 nt of TYMV RNA thus provide RNA stabilization

and translational enhancement comparable to that provided by the TMV 3′ UTR (Gallie and Kobayashi, 1994).

LUC expression in cowpea cells was strongly dependent on the presence of a 5′-cap (^{m7}GpppG). Expression levels reached after transfection with uncapped RNA were up to a thousand-fold lower than those reached with capped RNA (Fig. 2.3B, C), and it was necessary to transfect with 4 times as much RNA to obtain LUC levels that were significantly above background. The poor expression from uncapped RNAs was not due to RNA instability, since the functional half-lives of uncapped RNAs were about 2 hr (Fig. 2.3C). Note that this half-life may be overestimated because low expression levels make accurate estimation difficult, but the uncapped RNAs are clearly quite stable. Similar results have previously been reported in plant cells with uncapped RNAs (Gallie and Kobayashi, 1994). Indeed, for RNAs in the cytoplasm, stability is considered to be the default status (Sachs, 1993), with rapid turnover resulting from the presence of specific destabilizing elements (Sachs, 1993; Jacobson and Peltz, 1996).

Direct comparison of LUC expression supported by capped and uncapped L-TYsg and L-Bam RNAs indicates that the 5′ cap and TYMV 3′-UTR act synergistically to enhance LUC expression. Thus, the independent effects (with reference to uncapped L-Bam RNA) of a 5′-cap and 3′-sgUTR are 162-fold and 2.93-fold, respectively (Fig. 2.3C), which predicts a 475-fold combined effect. However, expression from capped L-TYsg RNA was 4640-fold higher than from uncapped L-Bam RNA, indicating a 9.8-fold increase due to synergy (Fig. 2.3C). This type of synergy is considered to represent the advantage obtained from mechanistic interaction between 5′-cap and 3′-UTR (Tarun and Sachs, 1995; Mangus et al., 2003). Our results demonstrate the presence of a strong 3′ translational enhancer in the sgUTR of TYMV RNA.

A   Capped RNA

B   Uncapped RNA

C

Cap	RNA	RNA Functional Half-life (min)	LUC maximum activity (x10⁷)	Relative LUC (vs. capped L-Bam)	Relative LUC (vs. uncapped L-Bam)
+	L-TYsg	108.3 ± 1.5	11.6 ± 1.1	28.6	4640
	ELE-(A)₈₀	104.8 ± 16.5	19.8 ± 4.1	48.9	7920
	L-TMV	80.4 ± 2.4	11.1 ± 0.96	27.4	4440
	L-TY-CGC	58.5 ± 10.1	1.79 ± 0.16	4.42	716.0
	L-Bam	66.5 ± 7.8	0.405 ± 0.08	1	162.0
-	L-TYsg	127.8 ± 35.6	0.00732 ± 0.0013		2.928
	ELE-(A)₈₀	126.0 ± 22.1	0.0292 ± 0.0043		11.68
	L-Bam	122.8 ± 55.0	0.00250 ± 0.0062		1

Fig. 2.3 Synergistic stimulation of LUC expression by the TYMV 3′-UTR and a 5′-cap.

(**A, B**) Time courses of LUC expression in cowpea protoplasts are shown for the indicated capped and uncapped RNAs. (**C**) RNA half-life and LUC activities determined from experiments such as those in A and B, using data from duplicate transcripts and at least two transfection experiments. Functional half-life of each RNA was determined as time to half maximum LUC activity. All LUC activities are expressed as relative light units per min per mg total protein. ELE(A)₈₀ is a polyadenylated LUC RNA with human eEF1A 5′ and 3′-UTRs. Synergy between the 5′-cap and 3′-TYsg UTR is determined as the ratio of the 3′-UTR effect between capped and uncapped RNAs, using L-Bam as the unmodified reference RNA: 3′-TYsg effects are 28.6 (capped) and 2.93 (uncapped), with 9.8-fold enhancement due to synergy. L-TMV RNA has the 3′-190 nt from the genome of TMV (U1 strain), and is transcribed from DNA linearized with SmaI to produce RNAs with 3′-CC termini like those of the TYMV reporter RNAs.

2.3.2 Aminoacylatability correlates with TYMV 3′ translational enhancement activity

The importance of aminoacylation to infectivity (Tsai and Dreher, 1991; Dreher et al., 1996) and the localization of translational enhancement to little more than the TLS led us to investigate the role of aminoacylation. Mutations involving the major valine identity element in the anticodon (CGC and CCA replacing the CAC wild type anticodon) were introduced into L-TYsg RNA to produce L-TY-CGC and L-TY-CCA RNAs, respectively. Mutation of the wobble base C57 to produce anticodons GAC and AAC in L-TY-GAC and L-TY-AAC RNAs, respectively, was used as a control. The in vitro valylation activity of each of these LUC reporter RNAs was checked, confirming the abolition of valine charging upon mutation of nucleotide A56 and unchanged valylation upon mutation of the wobble base (Fig. 2.4A, B). RNAs defective in valylation expressed LUC at levels 13 to 14% relative to L-TYsg RNA (L-TY-CGC and -CCA RNAs), whereas wobble mutants (L-TY-GAC and -AAC RNAs) expressed LUC at relative levels of 61-62% (Fig. 2.4A). While the source of this minor decrease for the wobble mutations is unknown, these results indicate that the abolition of valylation has a strong effect on translational enhancement. Nevertheless, the LUC expression from L-TY-CGC and -CCA RNAs at a level about 3-fold higher than that from L-Bam RNA suggests that 3′ translational enhancement is not exclusively associated with valylation. The functional half-life of L-TY-CGC RNA was 59 min, similar to that of L-Bam RNA and shorter than that of L-TYsg RNA (Fig. 2.3C).

Mutations that convert the TLS identity from valine to methionine were introduced into L-TYsg RNA. As shown previously, a valine-to-methionine identity switch of the TYMV TLS requires changing both nucleotides in the anticodon loop and shortening the L1 loop of the acceptor stem pseudoknot (see Fig. 2.1) (Dreher et al., 1996). As a control with inefficient methionine charging (and no valine identity), we used a construct carrying a TLS with the methionine identity nucleotides in the anticodon but with wild-type L1 sequence (i.e., CUCU). L-TY-Met(L1=UU) RNA, which could be methionylated in vitro (Fig. 2.4A, C) and whose TLS corresponded to that of an infectious TYMV variant (Dreher et al., 1996), supported LUC expression to a level 48%

relative to L-TYsg RNA. L-TY-Met(L1=CUCU) RNA, which is poorly methionylated and whose TLS corresponds to that of a non-infectious TYMV variant (Dreher et al., 1996), supported 14% the LUC expression of L-TYsg RNA. As a control, mutation of only the L1 loop, retaining the wild type anticodon as well as the valylation and infectivity of genomic RNA (Dreher et al., 1996), resulted in LUC levels 67% relative to L-TYsg RNA [L-TY(L1=UU) RNA; Fig. 2.4A].

The results with paired RNAs that can and cannot be aminoacylated are the same regardless of the aminoacylation identity, valine or methionine. This involvement of tRNA properties in the translational enhancement provided by the 3´-UTR is essentially the same as in genome infectivity, and suggests an involvement of eEF1A, which is able to interact tightly with both valylated and methionylated TLSs. No discrete mutations in tRNAs or viral TLSs that selectively affect eEF1A interaction and not other tRNA properties have been described. Because eEF1A binding is prevented by bulky nucleotide modification in the T-stem (Dreher et al., 1999), we introduced one or two residues between TLS nucleotides 28 and 29 or between 29 and 30, hoping that these would be excluded from the helix and perturb eEF1A binding. Affinity for eEF1A•GTP is indeed decreased for L-TY-28A29 and –28U29 RNAs (Fig. 2.4A, D), although these RNAs also are partially defective in valylation. These RNAs were very inefficient mRNAs, supporting less LUC expression than L-TY-CGC and –CCA RNAs despite being considerably more active in valylation. Note that valylation assays performed on these LUC mRNAs made from XmnI-linearized templates are actually combined assays for 3´-A addition by CCA nucleotidyltransferase and valylation. Since L-TY-28A29 and –28U29 RNAs are at least partial substrates for adenylation and valylation, we conclude that their very low activity as mRNAs is a consequence of their reduced affinity for eEF1A.

A RNA	Relative LUC activity (%)	Relative valylation in vitro (%)	Relative methionylation in vitro (%)	eEF1A·GTP binding Kd (nM)
L-TYsg	100	100		1.80 ± 0.74
L-TY-CGC	13.7 ± 4.0	bkgd		
L-TY-CCA	13.0 ± 4.2	bkgd		
L-TY-GAC	60.9 ± 19.4	110.3 ± 3.4		
L-TY-AAC	61.6 ± 14.2	103.4 ± 1.0		
L-TY (L1=UU)	67.4 ± 11.7	91.7 ± 3.7		
L-TY-Met (L1=UU)	48.2 ± 8.6		37.0 ± 7.6	1.24 ± 0.81
L-TY-Met (L1=CUCU)	13.5 ± 1.7		bkgd	1.07 ± 0.19
L-TY-28A29	8.9 ± 3.2	16.2 ± 0.7		≥29.4
L-TY-28U29	7.0 ± 2.2	27.1 ± 0.9		≥66.9

B Valylation

C Methionylation
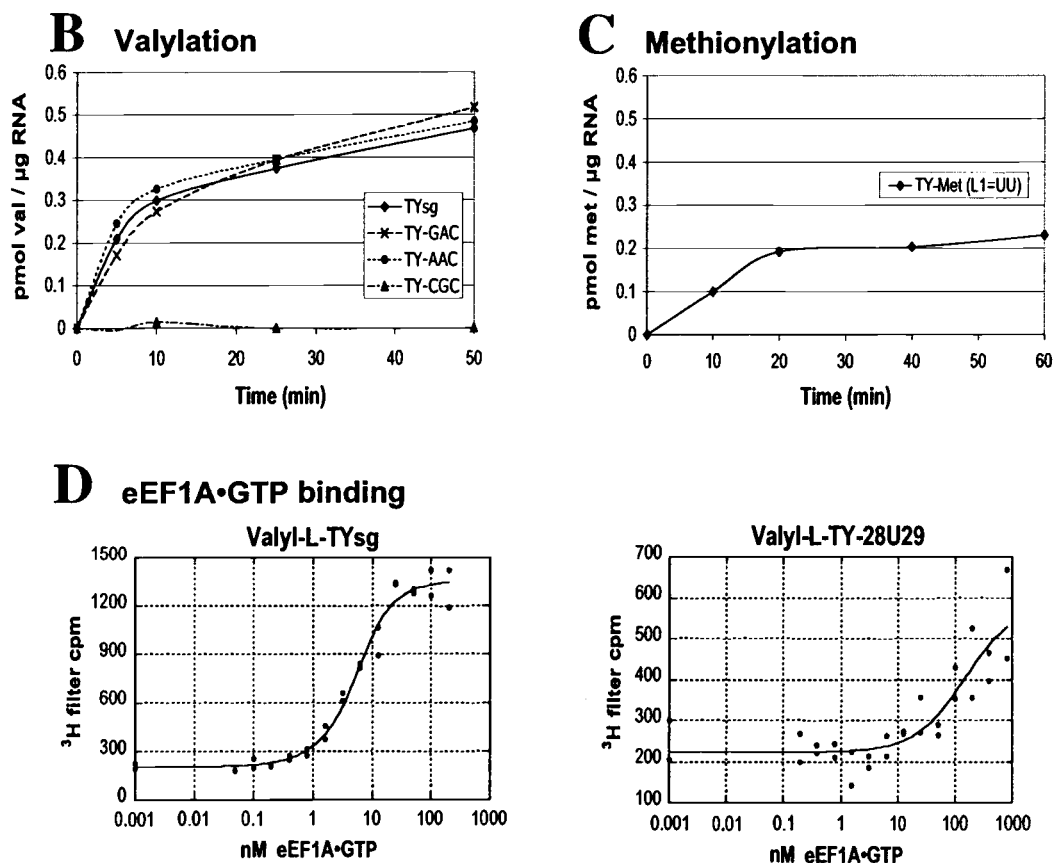
D eEF1A·GTP binding

Fig. 2.4 Close relationship between tRNA mimicry and translational enhancement.

Fig. 2.4 Close relationship between tRNA mimicry and translational enhancement.
(A) The in vitro aminoacylation and eEF1A•GTP binding properties for TLS mutant
variants of L-TY-sgUTR RNA are shown. Aminoacylation was tested in IV buffer using
a partially purified wheat germ aminoacyl-tRNA synthetase preparation. eEF1A•GTP
binding was studied with purified wheat germ eEF1A. Note that L-TY-28A29 and
–28U29 RNAs were more active in valylation in TM buffer, whereas L-TY-CGC RNA is
as inactive in this buffer as it is in IV buffer conditions (not shown). LUC expression (at
8 hr post-transfection) for each RNA construct is indicated. (B) and (C) show valylation
and methionylation profiles, respectively, for the indicated L-RNAs. (D) eEF1A•GTP
binding profiles recording protein-bound ^{3}H[valine]-labeled RNA recovered on filters.
Note the displacement of the valyl-L-TY-28U29 RNA binding curve to the right relative
to the valyl-L-TYsg curve and failure to reach binding saturation (plateau); valyl-L-TY-
28A29 RNA produced a similar binding curve (not shown).

2.3.3 The upstream pseudoknot plays a significant but non-specific role in 3′ translational enhancement

Alongside the TLS, the second distinctive feature present in the 3′ terminal 109 nt of the TYMV RNA is the UPSK. The translational enhancement provided by the TMV 3′-UTR has been mapped to a pseudoknot domain immediately upstream of the TLS (Gallie and Walbot, 1990; Leathers et al., 1993). We set out to test whether the UPSK contributes to the function of the TYMV 3′-UTR.

Deletion of the UPSK from the sgUTR resulted in an RNA (L-TYTLS RNA) that was poorly valylated and was not further tested as a LUC mRNA. We have previously observed an effect of the presence or absence of upstream sequence on the ability of the TLS to form a functional valylatable structure, and presumably in this case the TLS was predominantly mis-folded. For further experiments on the role of the UPSK, we substituted this element in L-TYsg RNA with generic spacers, A_9UA_9 and the stem/loop (SL) shown in Fig. 2.5A. As controls, these were also added upstream of the UPSK. The A_9UA_9 spacer was chosen because it has a weak potential for base pairing and interfering with overall RNA folding; the internal U residue was meant to preclude interaction with the poly(A) binding protein, which has been reported to require 11 or more consecutive A residues for high-affinity interaction (Sachs et al., 1987); a poly(A) tail shorter than about 30 residues was unable to promote translation (Preiss et al., 1998). The control constructs, L-A_9UA_9-TYsg and L-SL-TYsg RNAs, supported LUC expression at levels 116% and 126%, respectively, relative to L-TYsg RNA, indicating little or no independent effect of the spacers (Fig. 2.5C). L-A_9UA_9-TLS and L-SL-TLS RNA, in which the UPSK has been substituted with A_9UA_9 and SL, supported high levels of LUC expression, 135% and 81%, respectively (Fig. 2.5C). All RNAs were active substrates for valylation (Fig. 2.5C).

A

```
   A A
  G   A
   C-G
   G-C
   G-C
5'-G-C-3'

   SL
```

5'-AAAAAAAAAUAAAAAAAAA-3'

(A)₉U(A)₉

B

```
         U
      U    A
  96-U       A
      C        A
       \\   U-A
        \\  A-U
         \\ G-C
5'  UA G UUCUC-GUUAG
      |             |
     107           83

      wt UPSK
```

```
        U U  A
  96-G      A
       C      A
        // U-A   TY-96G
        // A-U
        // G-C
5'-UAAGUUCUC-GUUA-3'
```

```
       U U  A
      U      A
       C      A
       // U-A   TY-107C
       // A-U
       // G-C
5'-UA C GUUCUC-GUUA-3'
        |
       107
```

```
        U U  A
  96-G      A
       C      A
       // U-A   TY-96G/107C
       // A-U
       // G-C
5'-UA C GUUCUC-GUUA-3'
        |
       107
```

C RNA	Relative LUC activity (%)	Relative valylation in vitro (%)
L-TYsg	100	100
L-A9UA9-TYsg	116 ± 28.9	95.7 ± 3.3
L-A9UA9-TLS	135 ± 40.9	86.3 ± 7.4
L-SL-TYsg	126 ± 13.1	99.5 ± 1.2
L-SL-TLS	81.2 ± 14.9	64.5 ± 3.3
L-TY-96G	19.0 ± 4.0	55.8 ± 3.6
L-TY-107C	21.2 ± 3.8	61.4 ± 8.7
L-TY-96G/107C	36.5 ± 11.8	78.1 ± 5.9

Fig. 2.5 Involvement of the upstream pseudoknot in translational enhancement.
(A) The two spacer sequences inserted upstream of or replacing the UPSK are shown.
The SL element has a stable GNRA-type tetraloop. (B) The wt UPSK is shown, together
with the 96G and 107C sequence changes and their expected effects on pseudoknot
formation. The dashed lines for the single point mutants indicate base-pairings that are
destabilized by the central mismatches. (C) LUC activity (8 hr post-transfection) and in
vitro valylation levels (in IV buffer) of each RNA construct are tabulated.

In another test of UPSK function, we introduced point mutations (U96→G and
A107→C) that were designed to disrupt the tertiary interaction forming the UPSK (Fig.
2.5B). In genomic RNA, the U96→G mutation resulted in low infectivity that was
rescued by the A107→C mutation acting as a second site suppressor (Tsai and Dreher,

1992). RNAs L-TYsg-96G and L-TYsg-107C could be valylated in vitro to levels about 60% relative to L-TYsg RNA, and directed LUC expression to levels 19% and 21% relative to L-TYsg RNA (Fig. 2.5C). Combination of these mutations should rescue UPSK formation (Fig. 2.5B); such a construct (L-TYsg-96G/107C RNA) valylated to 78% the level of L-TYsg RNA and supported LUC expression at 37% relative to L-TYsg RNA (Fig. 2.5C).

These combined results suggest that the UPSK plays an important role in the 3′ translation enhancement function, but that this role is non-specific and is probably involved in encouraging the correct folding or presentation of the TLS so that it can be efficiently recognized by host valyl-tRNA synthetase.

2.4 Discussion

2.4.1 The TYMV 3′-UTR is a strong translational enhancer

Using a luciferase (LUC) reporter system with a generic (non-viral) 5′-UTR, we have shown that the 3′-UTR of TYMV RNA strongly enhances gene expression from 5′-capped mRNAs in plant cells. The addition of TYMV 3′-UTR sequences to a capped LUC mRNA increased LUC expression by 25-fold. Only a small part (1.6-fold) of this increase was due to RNA stabilization, with the bulk of the effect apparently due to increased translational efficiency. The TYMV 3′-UTR provided a modest 3-fold enhancement of LUC expression from uncapped mRNA, but its effect was almost 10-fold greater in the presence of a 5′-cap (Fig. 2.3), reflecting a synergistic interaction between these two features found at opposite ends of the mRNA. These properties in translational regulation are essentially identical to those of the 3′-UTRs of TMV and BMV, two other plant viruses whose genomes have a 5′-cap and a 3′ TLS (Leathers et al., 1993; Gallie and Kobayashi, 1994). The overall picture is similar to the contribution of the poly(A) tail to translation in plant cells (Gallie and Walbot, 1990; Gallie, 1991).

Maximal translational enhancement is provided by the 3′ 109 nt of TYMV RNA, which include the TLS and upstream pseudoknot (UPSK) (Fig. 2.1). This is the entire 3′-UTR of the subgenomic RNA, but only a fraction of the genomic 3′-UTR. In the latter

context, the 3´ 109 nt consistently provided 2 to 3-fold weaker translational enhancement. However, until mRNA constructs that include the viral 5´-UTR are studied, this does not necessarily mean that the genomic RNA is a weaker mRNA than the subgenomic RNA. In the genomic RNA, upstream 3´-UTR sequences contribute to translational expression (Fig. 2.2B), although we have not investigated whether this is due to specific sequences or is a non-specific property associated with the length (684 nt) of the 3´-UTR (Tanguay and Gallie, 1996a, b).

2.4.2   Transfer RNA mimicry is tightly associated with translational enhancement

Translational enhancement provided by the TYMV 3´-UTR was strongly associated with the intact tRNA mimicry of the TLS. Our reporter RNAs produced from *Xmn*I-linearized DNA templates were designed to provide a 3´-terminus (-CC) identical to that of the virion RNA, permitting the addition of a 3´ adenosine by host CCA nucleotidyltransferase and subsequent aminoacylation and interaction with eEF1A. Anticodon mutations controlling aminoacylation showed that aminoacylation is crucial for translational enhancement, although the identity of the amino acid (valine or methionine) is not crucial (Fig. 2.3). This relationship is identical to the relationship between aminoacylation and the infectivity of TYMV RNA (Table 1). Our results explain why previous studies, in which an inappropriate 3´-terminus was used, failed to detect translational enhancement by the TYMV 3´-UTR (Gallie and Kobayashi, 1994).

The requirement for aminoacylation, but not specifically with valine, suggests the involvement of eEF1A. Aminoacylated viral RNA is bound by eEF1A•GTP as tightly as aminoacylated tRNA (Dreher et al., 1999), and since eEF1A is abundant in the cell, aminoacylated viral RNA would be expected to become associated with eEF1A•GTP. We sought to obtain experimental evidence in support of a role for eEF1A using TLS mutants with specific defects in eEF1A binding. RNAs L-TY-28A29 and –28U29, with a single nucleotide insertion in the T-stem, had greatly decreased affinity for eEF1A•GTP, although their valylation activities were also partly compromised (Fig. 2.4). These RNAs supported less LUC expression than non-valylatable mutants (L-TY-CGC

and –CCA) despite their clearly superior aminoacylation activity (Fig. 2.4). We interpret this result to indicate that translational enhancement requires an interaction between the charged RNA and eEF1A•GTP, although this conclusion will need to be verified with additional experiments.

Our experiments also addressed the role of the UPSK in translational enhancement. The UPSK is certainly important, because upon its deletion from the L-TYsg reporter RNA, valylation was so poor that we did not test the RNA for translational activity. Since the TLS alone supports efficient valylation (Dreher and Goodwin, 1998), the effect of UPSK removal was likely via misfolding of the RNA. Further, point mutations disrupting the tertiary base-pairing that forms the pseudoknot (L-TY-96G and –107C) decreased translational enhancement significantly (Fig. 2.5), and LUC expression was partly rescued by the combination of these mutations to restore pseudoknot formation (Fig. 2.5; L-TY-96G/107C RNA). However, the UPSK could be entirely substituted with the generic spacers A_9UA_9 and SL (Fig. 2.5), and the UPSK is not a conserved feature of tymovirus 3´-UTRs (Hellendoorn et al., 1996). We favor the interpretation that the UPSK is an important feature that acts as a non-specific spacer to present the TLS in an optimal way, allowing it to fold into a conformation suitable for valylation.

2.4.3   Translational enhancement and the function of the TLS during TYMV infection

The initial event in a positive strand RNA virus infection is the translation of the viral genome to produce the proteins that will support genome replication. We have shown here that the 3´-UTR of TYMV RNA acts as a translational enhancer that synergistically supports the major role of the 5´-cap in directing translation by ribosomes. This function is similar to that of the poly(A) tail in cellular mRNAs, where translational enhancement is in large part due to the elaboration of molecular contacts between the 3´-poly(A) tail, poly(A) binding protein, and translation initiation factors that assemble around the 5´-cap (Sachs et al., 1997; Gallie, 1998; Mangus et al., 2003). These interactions that circularize the mRNA enhance translation at the initiation stage.

One model for the way in which the TYMV 3′-UTR promotes translation would be to recruit host factor(s), available at the outset of an infection, that recapitulate the RNA circularization of polyadenylated mRNAs through molecular contacts (direct or indirect) to the initiation factors that assemble at the 5′-cap. From our results, the translation elongation factor eEF1A would seem to be a prime candidate for participation in such a network, involving this *elongation* factor in an extraordinary role in regulating *initiation*. However, we are aware of no observations that link eEF1A to the translation initiation machinery. Another way in which the TYMV 3′-UTR promotes translation could be by influencing translation termination in such a way as to facilitate reinitiation, but without molecular bridging to the 5′-end, perhaps by retaining contact with the dissociated large ribosomal subunit. A precedent for such a mechanism is found in the communication between poly(A) binding protein and eRF3 translation termination factor (reviewed in Mangus et al., 2003). A further mechanism contributing to increased luciferase production might invoke the chaperone activity of eEF1A, conveniently sequestered in cis at the 3′-end, in promoting the productive folding of nascent polypeptides on the ribosome (Hotokezaka et al., 2002). Enhancement through increased translation elongation seems unlikely in view of the abundance of eEF1A and the fact that the elongation phase of translation is rarely rate limiting or the target of regulation (Macdonald, 2001).

Finally, the TYMV 3′-UTR might enhance translation through an interaction between the viral RNA and ribosomal A sites (Hall, 1979; Haenni et al., 1982). During the elongation phase of translation, aminocylated tRNA is delivered to the A site of the ribosome as aminoacyl-tRNA•eEF1A•GTP ternary complexes. It is not known whether aminoacylated TYMV RNA is capable of such an interaction, but if so, this could assist in the recruitment of ribosomes away from competing mRNAs. A ribosome sequestered in this way may dissociate to provide the small subunit that binds at the 5′-end for conventional initiation, although there would need to be a protective mechanism to prevent the same interference during TYMV RNA translation. A different scheme involving interaction between the TYMV 3′-UTR and a ribosome that circumvents the

standard steps of initiation has recently been suggested (Barends et al., 2003). That scheme is proposed to direct the initiation only of the p206 ORF and not the p69 ORF (see Fig. 2.2A) via a cap-independent process, and therefore must require guidance by some 5′ sequence. Because we have not used TYMV 5′-sequences in our experiments and do show 5′- cap/3′-UTR synergy, the scheme of Barends et al. does not seem to be applicable in explaining our observations.

An interesting question is whether the TLSs of other viral RNAs also function in translational enhancement with a similar reliance on aminoacylation and apparent reliance on eEF1A binding. The 3′-UTRs of both TMV and BMV RNA strongly enhanced translation in experiments in which the 3′-CCA termini were quasi-precise (CCAua; lower case representing additional nucleotides; Gallie and Kobayashi, 1994). The 3′-nucleotides of tRNAs are known to turn over in vivo (Deutscher, 1982), and exonuclease trimming in cells could have removed the two additional residues to produce TMV and BMV RNA termini capable of histidylation and tyrosylation (Mans et al., 1991), respectively. No experiments have directly addressed the relationship between tRNA mimicry and the translational enhancement of these 3′-UTRs. However, translational enhancement of the TMV UTR has been mapped to the upstream pseudoknot domain, with no activity detected for the TLS domain alone (Gallie and Walbot, 1990). Intriguingly, it has recently been deduced through UV cross-linking experiments that eEF1A binds to the upstream pseudoknot domain in addition to the aminoacylated TLS (Zeenko et al., 2002). TMV may have evolved two functionally redundant ways to recruit eEF1A for translational enhancement, and perhaps the upstream pseudoknot domain has become dominant in this role over the TLS. Given our experience with apparent misfolding of the TYMV TLS upon removal of upstream sequences, however, a reexamination of the role of the TMV TLS would be worthwhile.

As illustrated by the data summarized in Table 1, the tRNA-like properties of TYMV RNA are strongly correlated with 3′-translational enhancement and with the infectivity of the genomic RNA. Our observations indicate that an important role of tRNA mimicry is the provision of translational enhancement in support of optimal gene

expression. In the accompanying paper (Matsuda et al., 2004), we demonstrate that tRNA mimicry also allows regulation of minus strand transcription and is probably important in regulating the transition from the early phase of viral gene expression to the subsequent phase of genome replication.

Table 2.1   Correlation between infectivity, translational enhancement (TE) and aminoacylatability for 3′-UTR mutants

3′-UTR	Rel. TE[1]	Rel. Aminoacylation[2]	% Infectivity[3]
wt	1.00	1.00	100
CGC anticodon	0.14	0	0
CCA anticodon	0.13	0	0
AAC anticodon	0.62	1.03	100
GAC anticodon	0.61	1.10	100
CAC(L1=UU)	0.67	0.92	100
Met(L1=CUCU)	0.14	0	0
Met(L1=UU)	0.48	0.37	40

[1] Relative translational enhancement as reported in this paper
[2] Relative extent of aminoacylation as reported in this paper
[3] Infectivity (% of plants inoculated with variant genomic transcripts that become infected); data taken from Tsai and Dreher (1991, 1992); Dreher et al. (1996).

2.5 Materials and Methods

2.5.1 *Plasmid constructs and in vitro transcription*

The plasmid constructs used in this study were prepared by cloning PCR-amplified TYMV 3′ UTR derived from pTYMC (Weiland and Dreher, 1989)(GenBank accession X16378) into pLuc, a transcription plasmid that carries the firefly luciferase (LUC) ORF under the control of the T7 promoter (gift of D. Gallie, UC-Riverside). Upstream primers included a *Bam*HI site and downstream primers a *Sac*I site to permit easy directional insertion into pLuc. Amplification of the TMV 3′-UTR used pTMV004 (gift of Dr. W. O. Dawson) as template. PCR amplification used Vent DNA polymerase (New England Biolabs), and all plasmid constructs were verified by DNA sequencing. pELE(A)80 was a gift of W.-W. Chiu (Chiu and Dreher, unpublished).

RNAs were transcribed from appropriately linearized plasmid DNA with T7 RNA polymerase in the presence or absence of ^{m7}GpppG cap analog. Template DNA was removed by incubation with RNase-free DNase. RNA transcript quantity and quality were analyzed by native 1% agarose gel electrophoresis, using for calibration a dilution series of transcripts of known concentration. In some cases, [α-^{32}P]CTP was present in the transcription reaction, and TCA filter precipitation and liquid scintillation counting were used to quantify RNA.

2.5.2 *Protoplast transfection*

Mesophyll protoplasts were isolated from the first true leaves of cowpea (*Vigna unguiculata*) seedlings and transfected using polyethylene glycol as described previously for Chinese cabbage (Weiland and Dreher, 1989). Typically, 5 x 10^5 protoplasts were transfected with 2.5 μg of capped RNAs or up to 10 μg of uncapped RNAs. After washing, transfected protoplasts were resuspended in 1 ml growth medium [0.44 M D-mannitol, 3% sucrose, 0.01% inositol, 1 mg/l thiamine, 5 μM 2,4-D and 0.1 μM kinetin, adjusted to pH 5.6] and held for 8 hours under constant fluorescent illumination at room temperature (21°C) before harvesting. A linear relationship between transfected RNA and LUC light yield was maintained for up to 30 μg of RNA.

For each construct, RNAs transcribed in duplicate were each introduced at least twice into separately prepared protoplasts.

2.5.3 Analysis of luciferase activity

Harvested protoplasts were lysed in 50 μl Passive Lysis Buffer (Promega) for 5 min with constant shaking at room temperature. Typically, protoplasts were harvested 8 h post-transfection; LUC is a stable protein in plant cells, and time courses showed LUC activity reached a plateau 6-8 hr after transfection. Portions of each extract (10 μl) were loaded into the wells of clear-bottom black 96-well plates, and mixed with 50 μl Luciferase Assay Reagent (Promega) for luminometry in a 1450 MicroBeta TriLux counter (Wallac).

For normalization of LUC activity, the protein concentration of each sample was determined (Coomassie Plus protein assay, Pierce). The functional half-life of each RNA was determined as the time taken to reach half the maximum accumulation of LUC (Gallie, 1991).

2.5.4 Aminoacylation and eEF1A binding assays

Aminoacylation with valine or methionine used activities present in a partially purified wheat germ aminoacyl-tRNA synthetase preparation (Dreher et al., 1992). Valylation was carried out in TM buffer (25 mM Tris-HCl, pH 8.0, 2 mM $MgCl_2$, 1mM ATP, 0.1 mM spermine) or in IV buffer (30 mM HEPES, pH 7.5, 100 mM potassium acetate, 2.5 mM magnesium acetate, 1.5 mM ATP) with 10 μM [^{3}H]valine (24 Ci/mmol). Methionylation assays were conducted in IV buffer with 10 μM [^{35}S]methionine (500 Ci/mmol). Extents of aminoacylation were assayed by TCA precipitation as described (Dreher et al., 1992). Where applicable, aminoacylated RNAs were stored in 5 mM sodium acetate (pH 5.2) at –80°C (Dreher et al., 1999).

eEF1A binding assays were performed by ribonuclease protection assays as described (Dreher et al., 1999) using purified wheat germ eEF1A.

2.6   Acknowledgments

2.7   References

Barends, S., Bink, H. H., van den Worm, S. H., Pleij, C. W., and Kraal, B. (2003). Entrapping ribosomes for viral translation: tRNA mimicry as a molecular Trojan horse. *Cell* **112**, 123-9.

Briand, J. P., Jonard, G., Guilley, H., Richards, K., and Hirth, L. (1977). Nucleotide sequence (n=159) of the amino-acid-accepting 3'-OH extremity of turnip-yellow-mosaic-virus RNA and the last portion of its coat-protein cistron. *Eur J Biochem* **72**, 453-63.

Deutscher, M.P. (1982). tRNA nucleotidyltransferase. *The Enzymes* 15, 183-215.

Dreher, T. W., Tsai, C. H., Florentz, C., and Giegé, R. (1992). Specific valylation of turnip yellow mosaic virus RNA by wheat germ valyl-tRNA synthetase determined by three anticodon loop nucleotides. *Biochemistry* **31**, 9183-9.

Dreher, T. W., Tsai, C. H., and Skuzeski, J. M. (1996). Aminoacylation identity switch of turnip yellow mosaic virus RNA from valine to methionine results in an infectious virus. *Proc Natl Acad Sci U S A* **93**, 12212-6.

Dreher, T. W., and Goodwin, J. B. (1998). Transfer RNA mimicry among tymoviral genomic RNAs ranges from highly efficient to vestigial. *Nucleic Acids Res* **26**, 4356-64.

Dreher, T. W., Uhlenbeck, O. C., and Browning, K. (1999). Quantitative assessment of EF-1a-GTP binding to aminoacyl-tRNA, aminoacyl-viral RNA and tRNA shows close correspondence to the RNA binding properties of EF-Tu. *J. Biol. Chem.* **274**, 666-672.

Florentz, C., and Giegé, R. (1995). tRNA-like structures in plant viral RNAs. *In* "tRNA: Structure, Biosynthesis, and Function" (D. Söll, and U. L. RajBhandary, Eds.), pp. 141-163. ASM Press, Washington, D.C.

Gallie, D. R., and Walbot, V. (1990). RNA pseudoknot domain of tobacco mosaic virus can functionally substitute for a poly(A) tail in plant and animal cells. *Genes Dev* **4**, 1149-57.

Gallie, D. R. (1991). The cap and poly(A) tail function synergistically to regulate mRNA translational efficiency. *Genes Dev* **5**, 2108-16.

Gallie, D. R., and Kobayashi, M. (1994). The role of the 3'-untranslated region of non-polyadenylated plant viral mRNAs in regulating translational efficiency. *Gene* **142,** 159-65.

Gallie, D. R. (1998). A tale of two termini: a functional interaction between the termini of an mRNA is a prerequisite for efficient translation initiation. *Gene* **216,** 1-11.

Haenni, A. L., Joshi, S., and Chapeville, F. (1982). tRNA-like structures in the genomes of RNA viruses. *Prog Nucleic Acid Res Mol Biol* **27,** 85-104.

Hall, T. C. (1979). Transfer RNA-like structures in viral genomes. *Int Rev Cytol* **60,** 1-26.

Hann, L. E., Webb, A. C., Cai, J. M., and Gehrke, L. (1997). Identification of a competitive translation determinant in the 3' untranslated region of alfalfa mosaic virus coat protein mRNA. *Mol Cell Biol* **17,** 2005-13.

Hellendoorn, K., Mat, A.W., Gultyaev, A.P. and Pleij, C.W. (1996). Secondary structure model of the coat protein gene of turnip yellow mosaic virus RNA: long, C-rich, single-stranded regions. *Virology* **224,** 43-54.

Hotokezaka, Y., Többen, U., Hotokezaka, H., van Leyen, K., Beatrix, B., Smith, D.H., Nakamura, T. and Wiedmann, M. (2002). Interaction of the eukaryotic elongation factor 1A with newly synthesized polypeptides. *J Biol Chem* **277,** 18545-18551.

Jacobson, A., and Peltz, S. W. (1996). Interrelationships of the pathways of mRNA decay and translation in eukaryotic cells. *Annu Rev Biochem* **65,** 693-739.

Koh, D. C., Wong, S. M., and Liu, D. X. (2003). Synergism of the 3'-untranslated region and an internal ribosome entry site differentially enhances the translation of a plant virus coat protein. *J Biol Chem* **278,** 20565-73.

Leathers, V., Tanguay, R., Kobayashi, M., and Gallie, D. R. (1993). A phylogenetically conserved sequence within viral 3' untranslated RNA pseudoknots regulates translation. *Mol Cell Biol* **13,** 5331-47.

Macdonald, P. (2001). Diversity in translational regulation. *Curr Opin Cell Biol* **13,** 326-331.

Mangus, D.A., Evans, M.C. and Jacobson, A. (2003). Poly(A)-binding proteins: multifunctional scaffolds for the post-transcriptional control of gene expression. *Genome Biol* **4,** 223.

Mans, R. M., Pleij, C. W. and Bosch, L. (1991). tRNA-like structures. Structure, function and evolutionary significance. *Eur J Biochem* **201,** 303-324.

Matsuda, D., Yoshinari, S. and Dreher, T.W. (2004) eEF1A binding to aminoacylated viral RNA represses minus strand synthesis by TYMV RNA-dependent RNA polymerase. *Virology* **in press**.

Meulewaeter, F., Danthinne, X., Van Montagu, M., and Cornelissen, M. (1998). 5'- and 3'-sequences of satellite tobacco necrosis virus RNA promoting translation in tobacco. *Plant J* **14,** 169-76.

Neeleman, L., Olsthoorn, R.C., Linthorst, H.J. and Bol, J.F. (2001) Translation of a nonpolyadenylated viral RNA is enhanced by binding of viral coat protein or polyadenylation of the RNA. *Proc Natl Acad Sci U S A*, **98,** 14286-14291.

Pestova, T. V., Kolupaeva, V. G., Lomakin, I. B., Pilipenko, E. V., Shatsky, I. N., Agol, V. I., and Hellen, C. U. (2001). Molecular mechanisms of translation initiation in eukaryotes. *Proc Natl Acad Sci U S A* **98,** 7029-36.

Preiss, T., Muckenthaler, M. and Hentze, M.W. (1998). Poly(A)-tail-promoted translation in yeast: implications for translational control. *RNA* **4**, 1321-1331.

Qu, F., and Morris, T. J. (2000). Cap-independent translational enhancement of turnip crinkle virus genomic and subgenomic RNAs. *J Virol* **74**, 1085-93.

Sachs, A. B., Davis, R. W., and Kornberg, R. D. (1987). A single domain of yeast poly(A)-binding protein is necessary and sufficient for RNA binding and cell viability. *Mol Cell Biol* **7**, 3268-76.

Sachs, A. B. (1993). Messenger RNA degradation in eukaryotes. *Cell* **74**, 413-21.

Sachs, A. B., Sarnow, P., and Hentze, M. W. (1997). Starting at the beginning, middle, and end: translation initiation in eukaryotes. *Cell* **89**, 831-8.

Tanguay, R.L. and Gallie, D.R. (1996a). Translational efficiency is regulated by the length of the 3′ untranslated region. *Mol Cell Biol* **16**, 146-156.

Tanguay, R.L. and Gallie, D.R. (1996b). The effect of the length of the 3′-untranslated region on expression in plants. *FEBS Lett* **394**, 285-288.

Tarun, S. Z. and Sachs, A. B. (1995). A common function for mRNA 5′ and 3′ ends in translation initiation in yeast. *Genes Develop* **9**, 2997-3007.

Tsai, C. H., and Dreher, T. W. (1991). Turnip yellow mosaic virus RNAs with anticodon loop substitutions that result in decreased valylation fail to replicate efficiently. *J Virol* **65**, 3060-7.

Tsai, C. H., and Dreher, T. W. (1992). Second-site suppressor mutations assist in studying the function of the 3' noncoding region of turnip yellow mosaic virus RNA. *J Virol* **66**, 5190-9.

Wang, S., Browning, K., and Miller, W. (1997). A viral sequence in the 3'-untranslated region mimics a 5' cap in facilitating translation of uncapped mRNA. *EMBO Journal* **16**, 4107-4116.

Weiland, J. J., and Dreher, T. W. (1989). Infectious TYMV RNA from cloned cDNA: effects in vitro and in vivo of point substitutions in the initiation codons of two extensively overlapping ORFs. *Nucleic Acids Res* **17**, 4675-87.

Wu, B., and White, K. A. (1999). A primary determinant of cap-independent translation is located in the 3'-proximal region of the tomato bushy stunt virus genome. *J Virol* **73**, 8982-8.

Zeenko, V.V., Ryabova, L.A., Spirin, A.S., Rothnie, H.M., Hess, D., Browning, K.S. and Hohn, T. (2002). Eukaryotic elongation factor 1A interacts with the upstream pseudoknot domain in the 3′ untranslated region of tobacco mosaic virus RNA. *J Virol* **76**, 5678-5691.

Chapter 3 Expression of the two nested overlapping reading frames of TYMV RNA is enhanced by a 5´-cap and by 5´ and 3´ viral sequences.

Daiki Matsuda, Lisa Bauer, Kathryn Tinnesand, and Theo W. Dreher

3.1 ABSTRACT

The translation efficiency of an mRNA molecule is often determined by its 5'-and/or 3'-untranslated regions (UTR). Having previously found that the 3'-UTR of *Turnip yellow mosaic virus* (TYMV) RNA enhances translation synergistically with a 5'-cap, we investigated the role of 5' sequences from the genomic RNA on expression using a luciferase reporter system in cowpea protoplasts. The 5' 217 nucleotides from TYMV genomic RNA enhanced expression relative to a vector-derived 17 nucleotide-long 5'-UTR. Enhancement was greatest in RNAs with diminished 5'-cap/3'-UTR synergy, suggesting a functional overlap between the 5' TYMV sequences and the cap and/or TYMV 3'-UTR. In paired reporter constructs, the 5' 217 nucleotides harboring the UTR and the first 43 or 41 codons of the two overlapping TYMV ORFs, ORF-69 and ORF-206, respectively, were fused in frame with the luciferase gene. This allowed expression from the initiation codon of each ORF (AUG^{69} and AUG^{206}) to be monitored separately but from the normal sequence environment. Expression from both AUG codons was found to heavily depend on a 5'-cap, with three-fold higher expression occurring from AUG^{69} than from AUG^{206} in the presence of the genomic 3'-UTR. The ratio of expression originating from these AUG codons varied, with changes that interrupted the cap/3'-UTR synergy (i.e., removal of the cap or TYMV 3'-UTR) resulting in relatively stronger initiation from AUG^{206}. Mutation of the 3'-UTR to prevent aminoacylation, as well as deletion of 75% of the 5'-UTR, likewise resulted in a lower ratio of expression from AUG^{69} relative to AUG^{206}. Mutation of each AUG initiation codon increased initiation from the other. Taken together, these results only partially conform to the expectations of standard leaky ribosomal scanning as an explanation for the expression of the overlapping ORFs. However, our observations do not support a recent proposal based on in vitro studies in which the 3'-UTR is proposed to direct cap-independent initiation specifically at AUG^{206} and not at AUG^{69} [Barends et al., Cell **112**(2003):123-9].

3.2 INTRODUCTION

The 5′ and 3′ untranslated regions (UTRs) play major roles in controlling the translation of cellular and viral RNAs. The 5′ ^{m7}GpppN cap structure and 3′-poly(A) tail, both of which are characteristic features of eukaryotic mRNAs, are bound by the initiation factor eIF4E and poly(A) binding protein, respectively. Each of these proteins interacts with the scaffolding protein eIF4G, shaping the mRNA into a circularized closed loop that is considered to be the form of actively translated mRNAs (Sachs et al., 1997; Mangus et al., 2003). Through affinity to initiation factors bound to the above complex, ribosomal small subunits are loaded at the 5′-end of the RNA and then scan in the 3′ direction in search of an initiation codon, which is normally AUG (Pestova et al., 2001). The efficiency of initiation is modulated by the sequence context of the initiation codon, with a purine at −3 and G at +4 the most important contributors to an optimal context (Kozak, 1999; Lukaszewicz et al., 2000).

Among viral RNAs, alternative or additional elements enhancing translation have been identified. For instance, certain 3′-UTRs of non-polyadenylated viral RNAs enhance translation in a manner similar to that provided by a poly(A) tail, including a synergistic interaction with the 5′-cap. This has been demonstrated for rotavirus mRNAs (Vende et al., 2000), and for plant viral RNAs that terminate with a tRNA-like structure (TLS): *Tobacco mosaic virus* (TMV), *Brome mosaic virus* (Gallie and Kobayashi, 1994) and *Turnip yellow mosaic virus* (TYMV) (Matsuda and Dreher, 2004). Some 5′-UTRs of capped viral RNAs have been observed to enhance translational expression (Gallie et al., 1987a; Jobling and Gehrke, 1987; Tomashevskaya et al., 1993; Turner et al., 1999), adding additional control to the minimal elements normally present on mRNAs. The best-studied case is the 5′-UTR enhancer of TMV genomic RNA, the so-called Ω sequence. Through binding heat shock protein HSP101, Ω has been shown to enhance gene expression via elevated recruitment of the eIF4F complex (Wells et al., 1998; Gallie, 2002).

We have recently shown that the 3′-UTR of TYMV acts as a potent translational enhancer in plant cells. The TLS was the main feature responsible for translational

enhancement, which was maximal when aminoacylation and eEF1A binding properties were intact (Matsuda and Dreher, 2004). Those experiments utilized luciferase reporter constructs devoid of viral 5´ sequences. In the present study, we wished to investigate the translational role of the TYMV 5´-UTR and its relationship to the enhancing role of the 3´-UTR. This became of particular interest with the recent publication of a proposed scheme by which the 3´-UTR communicates specifically with one of two AUG initiation codons to promote translation by a novel cap-independent mechanism that avoids the quasi-ubiquitous involvement of initiator tRNA^{Met} (Barends et al., 2003).

The genome of TYMV is expressed from two RNAs, both of which possess a 5´-cap and the 3´-TLS. The genomic RNA is translated to express two extensively overlapping proteins, the movement protein (p69) initiating at nucleotide 88 (AUG^{69}, the 5´-most AUG triplet) and the replication polyprotein (p206) initiating at nucleotide 96 (AUG^{206}; Fig. 3.1A). The subgenomic RNA, which is collinear with the 3´-terminal 694 nts of the genomic RNA, is a dedicated mRNA for the translation of the coat protein. With the presence of a 5´-cap and absence of an extensive upstream untranslated region that could harbor an internal ribosome entry site (IRES) (Sarnow, 2003), normal cap-dependent translation of the genomic RNA would seem an adequate explanation for expression initiating from the two closely spaced 5´-proximal AUG triplets. Leaky scanning is a proven mechanism explaining expression from more than the first AUG (Kozak, 1999), although there is controversy concerning the rules governing ribosome selection of two closely spaced AUG triplets as found in TYMV RNA (Weiland and Dreher, 1989) and an influenza B virus mRNA (Williams and Lamb, 1989; Kozak, 1995).

With these considerations, the proposal based on in vitro studies that the TLS communicates directly to effect translation initiation of p206 at nucleotide 96 (and not of p69 at nucleotide 88) in a cap-independent manner (Barends et al., 2003) seemed unlikely and superfluous. Our experiments studying expression in cells do not support the proposed scheme. Translation from both AUG triplets is strongly cap-dependent, and there is no special functional interaction between the 3´-UTR and initiation at AUG^{206};

the 3´-UTR including the TLS is a general enhancer of translation. We further show that the 5´ sequences of TYMV genomic RNA enhance translation, with some of its enhancement properties being similar to those of the TMV Ω element.
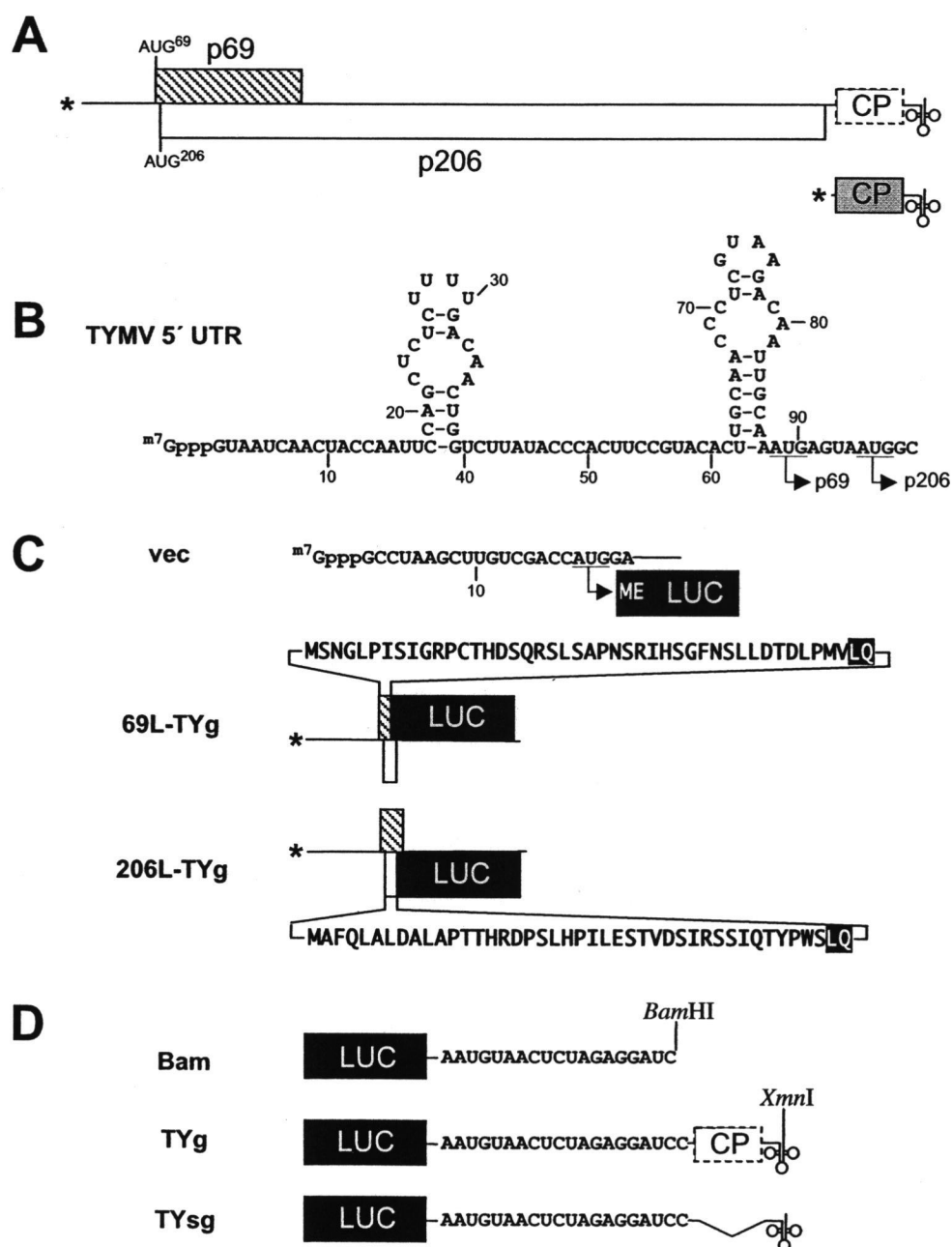
Fig. 3.1 Design of luciferase (LUC) reporter mRNAs investigating the translational regulation of TYMV RNA.

Fig. 3.1 Design of luciferase (LUC) reporter mRNAs investigating the translational regulation of TYMV RNA.

(A) Diagram of TYMV genomic RNA and subgenomic RNA with ORF expressing coat protein (CP, grey box). The genomic RNA is translated to produce p69 (hatched box) from initiation at AUG^{69} and p206 (open box) from initiation at AUG^{206}, but the CP ORF is silent (indicated by dashed outline). The $^{m7}GpppN$ cap of each RNA is indicated by an asterisk. The cruciform structure at the 3´ end represents the tRNA-like structure (TLS). (B) Sequences and proposed secondary structure (Hellendoorn et al., 1996) of the 5´ UTR of TYMV genomic RNA. The initiation codons at nucleotides 88 and 96 and corresponding translation products are marked. (C) Basic 5´-UTRs of LUC reporter RNA constructs. The sequence of the vector-derived (vec) 5´-UTR is shown, and the 5´ regions of paired constructs reporting initiation from each of the two TYMV AUG initiation codons are diagrammed. The wild type LUC protein produced from the vec 5´-UTR begins with the dipeptide ME (single letter amino acid code), as indicated. Constructs with 5´-TYMV sequences produce the LUC fusion proteins 69L or 206L, which have N-terminal fusions of 43 and 41 residues from the N-terminal portions of p69 and p206, respectively. The amino acid sequences derived from p69 and p206 are shown (single letter code), along with two bridging residues derived from a PstI site used for cloning (LQ, in reverse shading). (D) Basic 3´-UTRs of LUC reporter RNA constructs. The sequence of the vector-derived 19 nt-long 3´-UTR referred to as Bam is shown. This 3´-UTR is produced from DNA templates linearized with BamHI. The two types of TYMV 3´-UTR used are shown: TYg and TYsg, which include the 684 nt-long UTR of the genomic RNA and the 109 nt-long UTR of the subgenomic RNA, respectively. Both UTRs are fused as indicated to the generic Bam 3´-UTR sequence. Transcription from plasmid linearized with XmnI produces RNAs with the same 3´ termini as virion RNA.

3.3 MATERIALS AND METHODS

3.3.1 *Plasmid constructs and in vitro transcription.*

To permit ready replacement of 5′-sequences, the firefly luciferase (LUC) reporter plasmid pDCLD (a kind gift of W. W. Chiu) was adapted by replacing the 3′-UTR with the TYMV genomic (g) 3′ UTR from pL-TYg (Matsuda and Dreher, 2004) to generate pDCL-TYg. This involved subcloning a fragment spanning the SphI site within the LUC ORF and the polylinker SacI site downstream of the XmnI site used to linearize pL-TYg prior to transcription. TYMV 5′ fragments containing a T7 promoter, 5′-UTR and the beginning of a LUC fusion ORF were generated with appropriate primers by PCR amplification, followed by insertion into the NotI and PstI sites of pDCL-TYg. This created p69L-TYg, p206L-TYg and related plasmid constructs. To make p69L-TYsg and p206L-TYsg, the genomic (g) 3′ UTR was replaced by the TYMV subgenomic (sg) 3′ UTR from pL-TYsg (Matsuda and Dreher, 2004) (BamHI to SacI fragment). Tables 3.1 and 3.2 list the sequences of the PCR primers and descriptions of the plasmid constructs, respectively. The cloned portions of all plasmid constructs were confirmed by DNA sequencing.

RNA transcripts, in capped (with ^{m7}GpppG; Epicentre) or uncapped form as appropriate, were prepared as described previously (Matsuda and Dreher, 2004) in the presence of $[\alpha\text{-}^{32}\text{P}]$CTP (0.2 μCi per 20 μl reaction) to facilitate assessment of the quality and quantity of the transcripts. TCA filter precipitation and liquid scintillation counting were used to quantify the transcripts. For examination of RNA quality, transcripts were analyzed by electrophoresis on 1% agarose gels and phosphorimagery.

3.3.2 *Protoplast transfection.*

Mesophyll protoplasts were prepared from the first leaves of cowpea plants as described (Matsuda and Dreher, 2004). The washed protoplasts were resuspended in cold EB buffer (0.6 M D-mannitol, 5 mM MES, 5 mM $CaCl_2$, and 40 mM KCl, adjusted to pH 5.7 with KOH) at 2 x 10^6 cells/ml. Aliquots (0.6 x10^6 protoplasts) were mixed with RNA

transcripts (5-10 μg /pmol capped RNA and 30 pmol uncapped RNA for a time course experiment) in pre-chilled electroporation cells (2 mm gap, BioRad) and placed on ice for 10 min. Electroporation was then performed with a GenePulser Xcell device (BioRad) set at 450 V/cm and with time constant of 50 ms, delivering a capacitance of about 900±50 μF. After electroporation, the protoplasts were transferred to a microfuge tube containing 1.13 ml of growth medium (0.44 M D-mannitol, 3% sucrose, 0.01% inositol, 1 mg/l thiamine, 5 μM 2,4-D and 0.1 μM kinetin, adjusted to pH 5.7 with NaOH) and held under constant fluorescent illumination at room temperature (21°C).

Table 3.1   Sequences and descriptions of PCR primers

Name	Length (nts)	Sequence (5'-3')	UP/LP Primer[1]	Short description[2]
AG2	23	CGACGCGGCCGCTAATACGACTC	UP	universal 5' NotI-T7 promoter
TY4	53	CGACGCGGCCGCTAATACGACTCACTATAGTAATCAACTACCAATTGCAAATG	UP	5' NotI-T7 promoter- 5'Δ (TYMC seq)
TY1	32	ACCATCCTGCAGGGACCATGGGTAGGTCTGTAT	LP	3' PstI-NcoI-p69LUC fusion (LUC in frame with p69)
TY2	33	ACCATCCTGCAGGGACCATGGGTAGGTCTGTAT	LP	3' PstI-NcoI-p206LUC fusion (LUC in frame with p206)

[1] Upper (UP) and lower primer (LP) are indicated for each PCR primer.
[2] The features of each primer are described.

Table 3.2   Descriptions and sources of transcriptional templates

Name	5' UTR	LUC fusion	3' UTR	Backbone plasmid	Insert	UP (5')[1]	LP (3')[1]	PCR template
pL-TYg[2]	vector	no	TY gUTR					
pL-TYsg[2]	vector	no	TY sgUTR (WT)					
pDCL-TYg	Dengue	Den CP	TY gUTR	pDCLD(SphI-SacI)	pL-TYg (SphI-SacI)	n/a	n/a	n/a
p69L-TYg	WT	69	TY gUTR	pDCL-TYg (NotI-PstI)	PCR (NotI-PstI)	AG2	TY1	pTYMC/EcoRI[3]
p206L-TYg	WT	206	TY gUTR	pDCL-TYg (NotI-PstI)	PCR (NotI-PstI)	AG2	TY2	pTYMC/EcoRI[3]
p69L-TYsg	WT	69	TY sgUTR (WT)	p69L-TYg (BamHI-SacI)	pL-TYsg (BamHI-SacI)	n/a	n/a	n/a
p206L-TYsg	WT	206	TY sgUTR (WT)	p206L-TYg (BamHI-SacI)	pL-TYsg (BamHI-SacI)	n/a	n/a	n/a
p69L-TYsg(CGC)	WT	69	TY sgUTR (G56)	p69L-TYg (BamHI-SacI)	pL-TYsg(CGC)(BamHI-SacI)	n/a	n/a	n/a
p206L-TYsg(CGC)	WT	206	TY sgUTR (G56)	p206L-TYg (BamHI-SacI)	pL-TYsg(CGC)(BamHI-SacI)	n/a	n/a	n/a
p5'Δ 69L-TYg	TYMC 5'Δ	69	TY gUTR	pDCL-TYg (NotI-PstI)	PCR (NotI-PstI)	TY4	TY1	pTYMC/EcoRI[3]
p5'Δ 206L-TYg	TYMC 5'Δ	206	TY gUTR	pDCL-TYg (NotI-PstI)	PCR (NotI-PstI)	TY4	TY2	pTYMC/EcoRI[3]
p69L(p206/ACG)-TYg	p206(ACG)	69	TY gUTR	pDCL-TYg (NotI-PstI)	PCR (NotI-PstI)	AG2	TY1	pTY206ACG/HindIII[3]
p206L(p69/AAG)-TYg	p69(AAG)	206	TY gUTR	pDCL-TYg (NotI-PstI)	PCR (NotI-PstI)	AG2	TY2	pTY69AAC/HindIII[3]

[1] Upper (UP) and lower primer (LP) used for each PCR reactions are shown (see Table 3.1 for primer descriptions). The plasmids with n/a in these sections were constructed without PCR step.
[2] These plasmids were described in (Matsuda and Dreher, 2004).
[3] These plasmids were described in (Weiland and Dreher, 1989).

3.3.3   Analysis of luciferase activity.

Protoplasts were collected by pelleting in a microfuge at 3000 rpm, and lysed in Passive Lysis Buffer (Promega; 20 μl per 7.5 $\times 10^4$ cells) for 5 min with constant shaking at room temperature. Portions of each extract (10 μl) were loaded into the wells of black, clear-bottom 96-well plates, mixed with 50 μl Luciferase Assay Reagent (Promega) before luciferase activity was read in a 1450 MicroBeta TriLux counter (Wallac). To enable analysis of LUC expression at early times post-transfection, we delivered RNAs into cowpea protoplasts by electroporation rather than PEG-mediated transfection as used previously (Matsuda and Dreher, 2004). Expression from capped and uncapped gen-L-TYsg and gen-L-Bam RNAs revealed a 10-fold synergy between the enhancing effect of the 5´-cap and 3´-sg UTR [calculated from the ratio of 3´-sg effect in the capped (33.5; Fig. 3.3A) versus uncapped (3.4; Fig. 3.3B) state]. The identical synergy value was found previously in our PEG-mediated transfection studies (Matsuda and Dreher, 2004), showing that expression patterns are not influenced by the RNA delivery methodology.

3.3.4   Analysis of RNA survival in protoplasts.

At appropriate time points, total RNA was extracted from protoplasts with TRIzol reagent (GibcoBRL) according to the manufacturer's directions. The resulting RNAs were glyoxalated and analyzed by 1% agarose gel electrophoresis as described (Weiland and Dreher, 1989).

3.4   RESULTS

3.4.1   Relative expression of ORF-69 and ORF-206 in protoplasts.

Building on our previous studies describing the translational control provided by the 3´-UTR, we constructed luciferase (LUC) reporter RNAs that also had 5´ sequences from the genomic TYMV RNA, including the entire 5´-UTR. Because the genomic RNA expresses both the p69 and p206 proteins by initiation from the two closely placed out-of-

frame AUG codons, AUG[69] at nucleotide 88 and AUG[206] at nucleotide 96 (Fig. 3.1A, B), paired constructs were needed to monitor expression from each initiation site one at a time. To preserve the native initiation environment of AUG[69] and AUG[206], these paired constructs had in common 217 nts from the 5′-end of the TYMV genomic RNA, considerably more than the 5′-UTR. Consequently, ORF-69 expression was monitored by the production of a p69/LUC fusion protein (69L) made up of the first 43 amino acids of p69 fused to the dipeptide Leu-Gln and then to LUC (Fig. 3.1C). The sister construct monitoring ORF-206 expression encoded a p206/LUC fusion protein (206L) made up of the first 41 amino acids of p206 fused through Leu-Gln to LUC (Fig. 3.1C).

TYMV UTR function was studied by comparing expression from RNAs with the above TYMV 5′-sequences with expression from RNAs with a 17 nt-long generic, vector-derived 5′-UTR (referred to as vec in the names of constructs) that directed the synthesis of wild type LUC (Fig. 3.1C). To check how the fusion with p69 and p206 sequences affected LUC specific activity (relative light units per mole), we produced wild type LUC (made from RNAs with 5′-vec sequences), 69L and 206L in [^{35}S]methionine-labeled form by translation in reticulocyte lysates. Bands from SDS-PAGE corresponding to each form of LUC were counted to determine the moles of LUC protein made, while the LUC activities (RLU) made in those lysates were measured in parallel. No significant differences in specific activity were found (not shown), permitting direct comparisons of LUC activity when measuring translational expression.

Interactions between the 5′ and 3′ UTRs were studied with RNAs bearing either the 684 nt-long 3′-UTR of genomic TYMV RNA (TYg), the 109 nt-long 3′-UTR of the subgenomic RNA (TYsg), or a basal vector-derived 19 nt-long 3′-UTR (Bam)(Fig. 3.1D). These same 3′-UTRs were used in our previous study in reporter RNAs with the 5′-vec sequences (Matsuda and Dreher, 2004). As in that study, we monitored translation by transfection of cowpea protoplasts with LUC reporter RNAs, followed by measurement of LUC activities from the protoplast extracts.

The 5′-capped reporter RNAs 69L-TYg and 206L-TYg (Fig. 3.2A) contain the 5′ and 3′ UTRs of the TYMV genomic RNA, and thus best reflect the translational behavior

of that RNA. The LUC expression from capped 69L-TYg RNA, based on maximum RLU levels reached in time courses following electroporation, was 5.1 times that from capped 206L-TYg RNA (Fig. 3.2A; 3.5/0.7). We noticed from the time-courses, however, that while the levels of the 69L protein remained fairly steady after plateau, the levels of the 206L protein reached maximum earlier than 69L and subsequently declined (Fig. 3.2A). This pattern, also evident in Figs. 3.3 and 3.5, indicates a faster turnover of either the 206L protein or the RNA encoding it, or both. Since 69L-TYg and 206L-TYg RNAs differ only by the presence or absence of a residue 217 nucleotides from the 5´-end that places the LUC ORF to be in-frame with ORF-69 or ORF-206, differences in RNA stability are highly unlikely. There was no indication of protoplast death induced by 206L expression (not shown) to explain the decrease in 206L levels. We thus conclude that the 206L protein is less stable in the protoplasts than 69L or wild type LUC. To minimize the resultant underestimation of 206L expression, we have also estimated relative expression from reporter RNAs in terms of the maximum rate of LUC accumulation (RLU/hr; Fig. 3.2). On this basis, 69L-TYg RNA supported 3.1 times the expression from 206L-TYg RNA (Fig. 3.2A). This would correspond to 3-fold higher translation of p69 than p206 from the genomic RNA.

3.4.2 *Translational enhancement by 5´ TYMV sequences.*

Expression from capped 69L-TYg RNA was 3.8 times that from capped vec-L-TYg RNA (Fig. 3.2A), suggesting that the 5´ 217 nts of TYMV RNA enhance expression. Because the profiles of LUC expression from these RNAs were very similar (similar LUC expression half-life; Fig. 3.2A), the expression difference is not complicated by different protein or RNA stabilities, and seems to reflect different translational efficiencies. These are directly measured, with a similar result (3.8), by the initial linear rate of LUC increase (Fig. 3.2A). The enhanced expression from the 5´-most AUG (AUG^{69}) occurred despite its weaker context (-3C/+4A) compared to the strong context of the AUG codon following the vec UTR (-3A/+4G)(Fig. 3.1). The 5´-TYMV sequences thus appear to direct substantial translational enhancement.
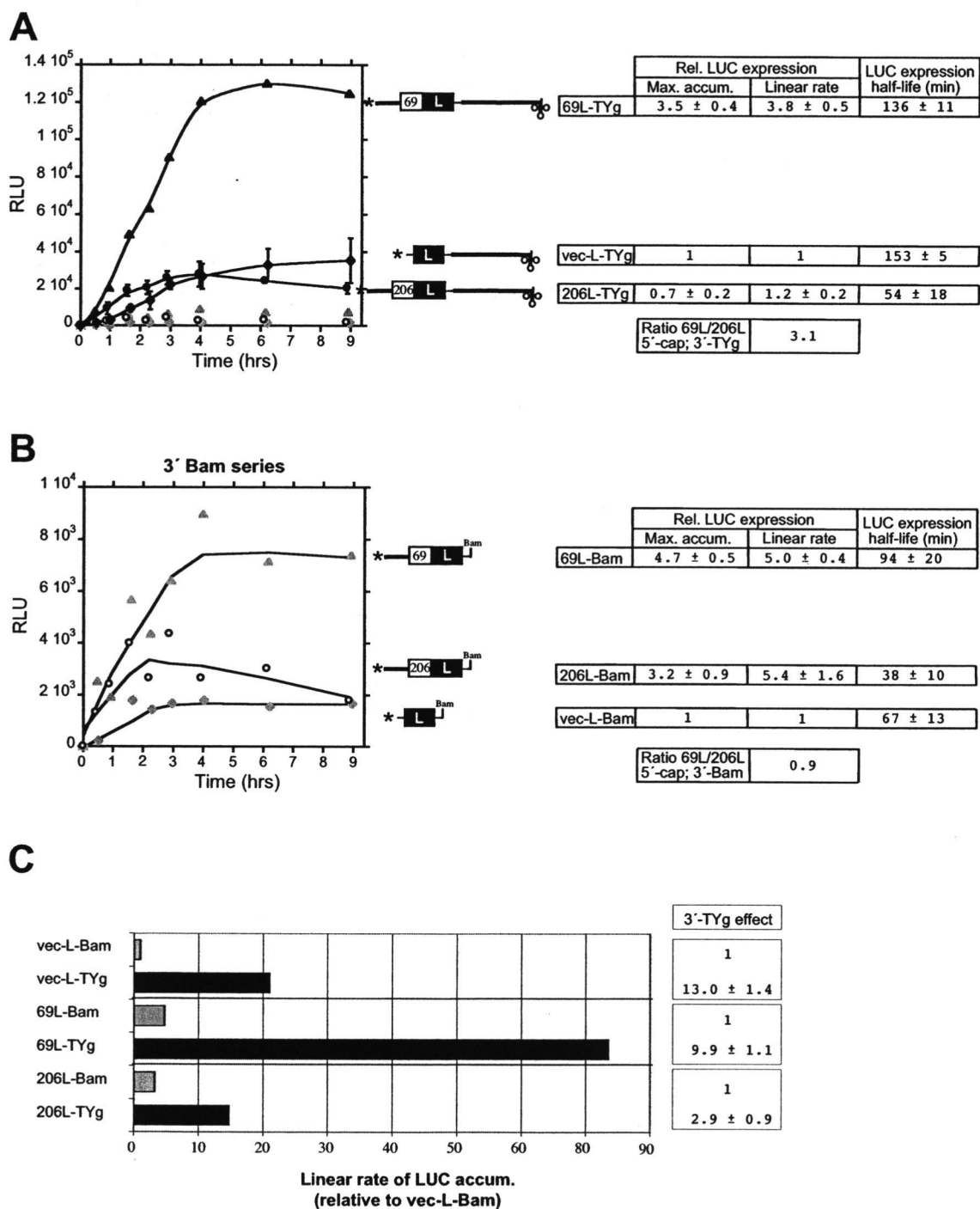
Fig. 3.2 Relative expression of ORF-69 and ORF-206 in protoplasts.

Fig. 3.2 Relative expression of ORF-69 and ORF-206 in protoplasts.
Luciferase expression directed by the indicated capped reporter mRNAs with the TYg 3´-UTR (A) and Bam 3´-UTR (B) is presented. In the reporter mRNA diagrams, the asterisk represents a 5´-cap, thick lines represent TYMV 5´ or 3´ terminal sequences, and the cruciform represents the 3´-TLS. Bam indicates the 3´-terminus of the generic Bam3´-UTR. The graph shows time courses of the accumulation of LUC activity (relative light units, RLU) produced from the indicated RNAs after electroporation into cowpea protoplasts. LUC expression is expressed in tabular form based on maximum levels reached and on the maximal linear rate of accumulation. The latter parameter is less sensitive to differences in RNA or protein turnover, which is expressed as LUC expression half-life, determined as the time taken to reach half the maximum LUC accumulation. For RNAs encoding the same form of LUC, or equally stable forms of LUC, this parameter equates to RNA functional half-life. Because the half-life of 206L protein expression is shorter than for other forms of LUC, comparisons involving expression of 206L and other forms of LUC (e.g., determination of 69L/206L expression ratio) are best done using the linear rate data. All data were derived by pooling two independent transfection experiments with duplicate transcripts per experiment (4 data points). Error bars represent standard deviation. (C) Comparison of the response to adding the TYg 3´-UTR to reporter RNAs with different 5´ sequences (data derived from linear rate data from A and B).

To determine whether this enhancement depended on the presence of 3′ TYMV sequences, we compared expression from capped 69L-Bam and vec-L-Bam RNAs (Fig. 3.2B). The 5′-TYMV sequences increased expression 5-fold (Fig. 3.2B). Expression from capped 206L-Bam RNA was also 5-fold higher than from vec-L-Bam RNA on the basis of initial rates of LUC accumulation (Fig. 3.2B), indicating similar initiation at AUG^{69} and AUG^{206} in the presence of the 3′-Bam UTR. Surprisingly, the 3′-UTR appears to influence the behavior of ribosomes on the TYMV 5′-UTR and the relative initiation at the AUG codons at nts 88 and 96. Barends et al. (Barends et al., 2003) have postulated a communication between the 3′-UTR and the 5′-end that selectively enhances initiation from AUG^{206}. Our results indicate that stimulated expression derived from the TYMV 3′-UTR in fact benefits initiation from both AUG codons, but more so from AUG^{69} (Fig. 3.2C).

3.4.3   Translation of both ORF-69 and ORF-206 is cap-dependent.

To better understand the contribution of the TYMV 5′ sequences, we compared expression from capped and uncapped RNAs with and without 5′ TYMV sequences. In these experiments, we also wished to assess the role of the cap in TYMV gene expression. Based on the fact that TYMV RNA is naturally capped and lacks an extended 5′-UTR with upstream AUG codons, it seems most reasonable to expect the RNA to be translated by the standard cap-dependent initiation mechanism, with leaky scanning (Kozak, 1999) or random selection (Williams and Lamb, 1989) explaining the choice between initiation at the closely spaced starts at AUG^{69} and AUG^{206}. On the other hand, the recent proposal based on in vitro studies (Barends et al., 2003) calls for ORF-206, though not ORF-69, to be translated by a cap-independent mechanism. Experiments with capped and uncapped RNAs were designed to test between these proposals. Because expression from uncapped RNAs was low, we utilized RNAs with the TYsg 3′-UTR, which is a roughly 2-fold stronger translational enhancer than TYg (Matsuda and Dreher, 2004).

The enhancing effect of the 5′-cap on expression from vec-L-Bam, an RNA lacking a 3′-translational enhancer capable of interacting synergistically with the cap, was 43-fold (Fig. 3.3A). The cap effect for vec-L-TYsg RNA (Fig. 3.3A) was 10-fold higher because of synergy between the cap and 3′-TYsg enhancer (Matsuda and Dreher, 2004). With TYMV 5′ sequences additionally present, the cap effect was 197-fold and 56-fold (Fig. 3.3A) when monitoring 69L or 206L protein synthesis, respectively. Clearly, expression from all RNAs tested was strongly cap-dependent, especially so for each of the RNAs with 3′ TYMV sequences, from which there was additional expression due to synergistic effects with the cap. The cap-dependency observed means that expression from uncapped 69L-TYsg and 206L-TYsg RNAs was only 0.5% or 2% that from capped forms of the same RNA (see RLU data, Fig. 3.3). Indeed, gene expression from uncapped RNAs was so low that even though three times the amount of capped RNAs was transfected (followed by appropriate corrections), LUC signals from some RNAs were close to background (RLU for vec-L-Bam; Fig. 3.3B).

3.4.4 Joint contribution of 5′ and 3′ TYMV sequences to enhanced expression.
As previously observed with capped RNAs (Matsuda and Dreher, 2004), enhancement by the TYsg 3′-UTR (33.5-fold; Fig. 3.3A) was about twice (1.6 times) that from TYg (21.0-fold; from data of Fig. 3.2 experiment). In comparison with 3′-TYg, 3′-TYsg displayed a similar relationship with the capped TYMV 5′ sequences: similar ratios of 69L to 206L expression and relationship to the levels of LUC produced from the vec 5′-UTR and strong translation from the combined effects of 5′ and 3′ TYMV sequences (compare time courses of Figs. 3.2A and 3.3A).

Comparing expression from 69L-TYsg and vec-L-TYsg RNAs showed that the TYMV 5′ sequences enhanced expression from AUG[69] in both the capped (Fig. 3.3A) and uncapped (Fig. 3.3B) states. This occurred despite a minor decrease in RNA stability (shorter LUC expression half-life; Fig. 3.3A, B). Note also that functional RNA half-lives [time to half-maximal LUC when comparing RNAs making the same protein;

(Gallie, 1991)] of uncapped RNAs are no less than 50% relative to the capped form of the same RNA, as previously observed (Matsuda and Dreher, 2004).
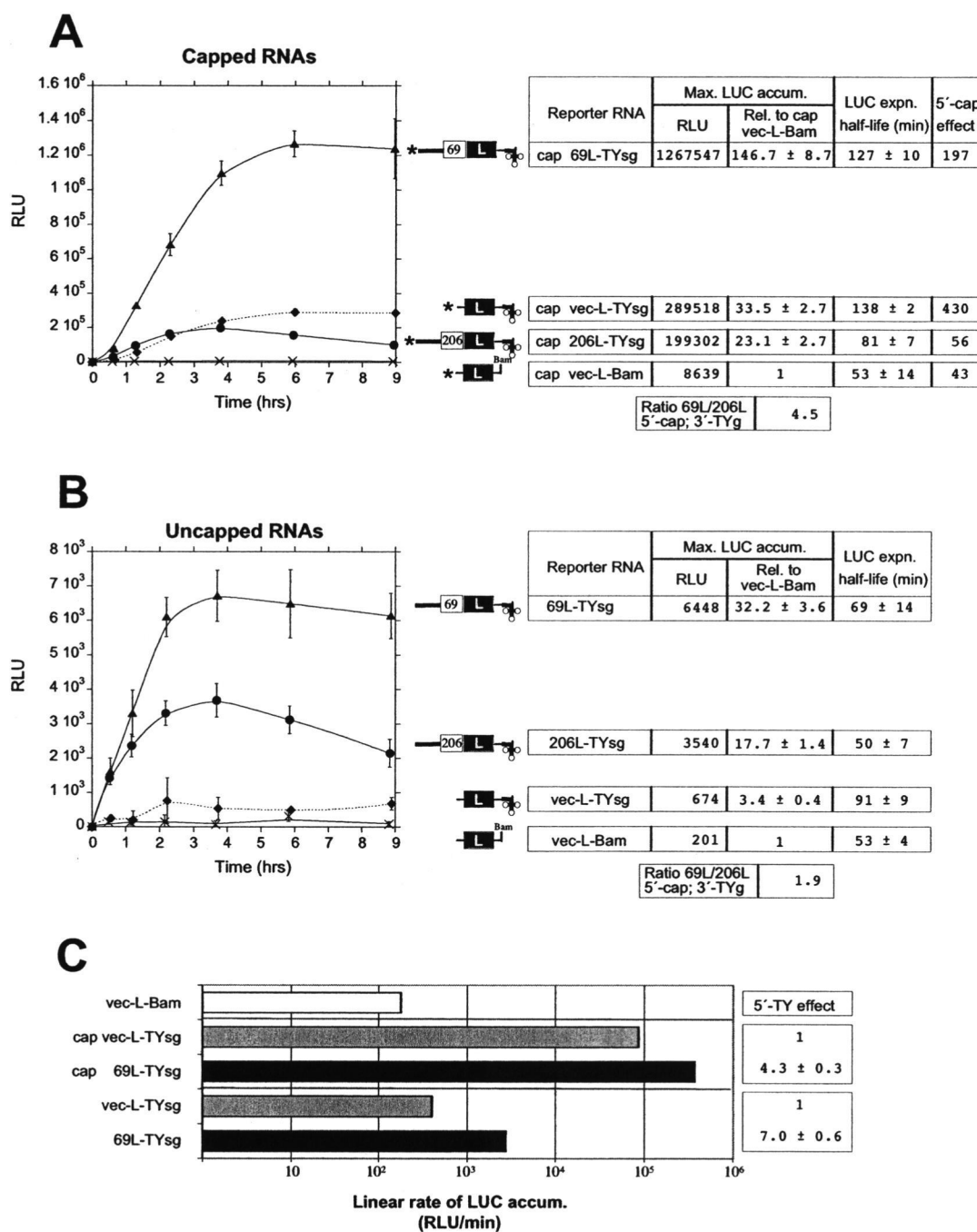
Fig. 3.3 Combined influences of a 5´-cap and the TYMV 5´ and 3´ terminal sequences.

Fig. 3.3 Combined influences of a 5´-cap and the TYMV 5´ and 3´ terminal sequences.

Expression in cowpea protoplasts directed by the indicated capped (**A**) and uncapped (**B**) RNAs is presented as in Fig. 3.2. The 5´-cap effect represents the ratio of maximum LUC expression directed by capped and uncapped forms of the same RNA, with data taken from the time courses in (A) and (B). Raw RLU data (after background subtraction) are reported in the tables at right, with the background for these assays being 642 RLU. To improve signals from uncapped RNAs, three times more uncapped than capped RNAs were transfected; expression is linearly dependent on the amount of RNA transfected (up to at least 30 pmol), and all data in this figure are normalized to permit direct comparison to expression data from capped RNAs. The time course plots shown are derived from a single experiment with duplicates (error bars represent standard deviation), while the tabulated data are derived from two such experiments (4 data points). (**C**) Comparison of the response to adding 5´ TYMV sequences to reporter RNAs with a TYsg 3´-UTR (data derived from linear rate data from A and B); note logarithmic scale.

The 5´ TYMV sequences also enhanced expression initiating from AUG^{206} of uncapped 206L-TYsg RNA relative to that from vec-L-TYsg (Fig. 3.3B), but LUC activities derived from the capped forms of the two RNAs were similar (Fig. 3.3A). Likewise, a lower TYMV 5´-UTR-dependent enhancement from capped than from uncapped RNAs was evident with 69L-TYsg RNA (Fig. 3.3C). Interestingly, the response of 69L and 206L expression to the addition of 5´ TYMV sequences is different, so that the ratio of initiation from AUG^{69} relative to AUG^{206} was 1.9 from the uncapped 3´-sg RNAs (Fig. 3.3B), but 4.5 from the capped RNAs (Fig. 3.3A). This is reminiscent of a ratio of 0.9 from capped RNAs with 3´-Bam UTR (Fig. 3.2B) but 3.1 for capped RNAs with the TYg 3´-UTR (Fig. 3.2A). In both cases, the presence of two terminal translation enhancers (5´-cap and TYMV 3´-UTR) resulted in a more skewed initiation profile in favor of ORF-69. Also in both cases, this resulted from a greater stimulation of ORF-69 than ORF-206 expression when comparing to related reporter constructs lacking one of the terminal enhancers. In Fig. 3.2C, this is seen by comparing the response from adding a TYg 3´-UTR to the basal 3´-Bam in the presence of 5´-69L (9.9-fold increase) compared to 5´-206L sequences (2.9-fold increase). Interestingly, the greatest stimulation due to 3´-TYg occurred in the presence of the vec 5´-UTR (13-fold increase). The parallel trend is evident in Fig. 3.3A in the gradation of cap effects for RNA with 3´-TYsg and differing 5´-UTRs (5´-vec > 69L > 206L). Note, however, that while the response to the addition of a 5´-cap or TYMV 3´-UTR is smaller in the presence of 5´-TYMV sequences, absolute expression levels are highest for RNAs with all enhancing elements, cap and 5´ and 3´ TYMV sequences (Fig. 3.3C).

Another way to view these results is in terms of the combined response of adding a capped 5´-UTR and TYsg 3´-UTR to the basal reporter vec-L-Bam RNA. For RNAs with the vec 5´-UTR, we observed 10-fold higher response to the addition of both 5´-cap and 3´-TYsg than expected from the individual effects of these enhancers (derived from data in Fig. 3.3). This corresponds to previous estimates of 5´-cap/3´-TYsg synergy (Matsuda and Dreher, 2004). When the TYMV 5´-UTR was added together with the cap, the "excess" response was 4.6-fold when adding 5´-69L and 1.3-fold when adding 206L

sequences. These results suggest some functional overlap between the TYMV 5′-UTR and the other enhancers, and an influence of the terminal enhancers on the ratio of 69L and 206L expression (see also later).

3.4.5 Role of valylation in 3′-UTR translational enhancement.

In previous studies, we have shown that maximal translational enhancement by the TYsg 3′-UTR requires aminoacylation (Matsuda and Dreher, 2004). The valylation of TYsg can be completely destroyed by a point mutation that changes the anticodon from CAC to CGC, a mutation whose effect we studied in the TYsg(CGC) 3′-UTR against different capped 5′-UTRs (Fig. 3.4). Because comparisons between 206L, 69L and wild type LUC expression (from vec-L RNAs) are best made on the basis of rates of LUC accumulation, we focused in these experiments on early times post-electroporation.

	Linear rate of LUC accum.			
D	Rel. RLU / min	Ratio WT / CGC	Effect of 5′ TY	
			3′ TYsg series	3′ TYsg (CGC) series
	(a)	(b)	(c)	(d)
vec-L-Bam	1			
vec-L-TYsg	25.8 ± 0.4	5.2 ± 0.1	1	
vec-L-TYsg(CGC)	5.0 ± 0.5	1		1
69L-TYsg	95.9 ± 4.7	2.8 ± 0.1	3.7 ± 0.2	
69L-TYsg(CGC)	34.4 ± 2.4	1		6.9 ± 0.5
206L-TYsg	26.6 ± 1.2	1.7 ± 0.1	1.0 ± 0.1	
206L-TYsg(CGC)	15.6 ± 3.3	1		3.1 ± 0.7
	Ratio 69L/206L	3.6	2.2	
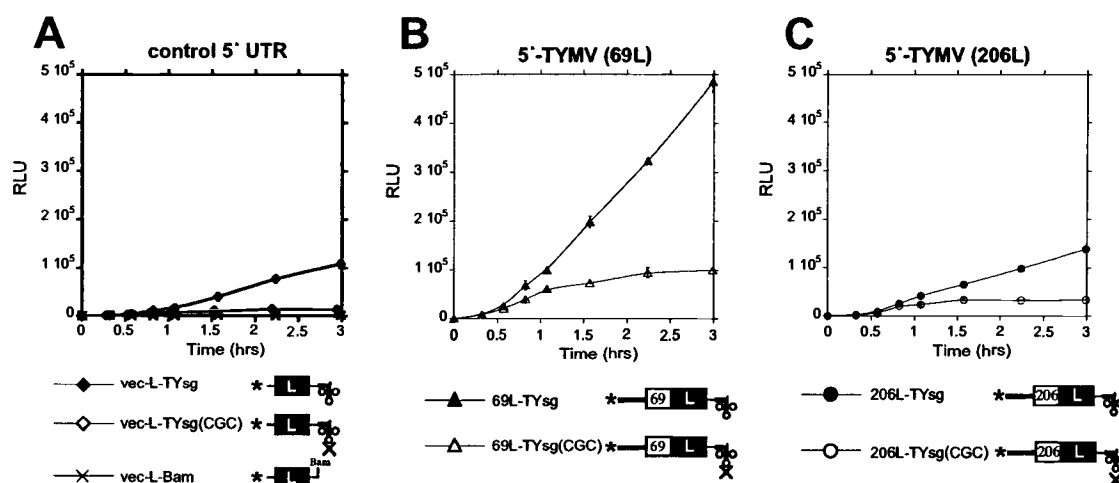
Fig. 3.4 Influence of 3′-aminoacylation on expression of 69L and 206L.

Fig. 3.4 Influence of 3′-aminoacylation on expression of 69L and 206L.

Time courses of LUC accumulation in cowpea protoplasts directed by the indicated capped RNAs with 5′-vec **(A)**, 5′-69L **(B)** and 5′-206L **(C)** sequences are shown. The CGC mutation refers to mutation of the CAC anticodon of the 3′-TLS to CGC, resulting in abolition of valylation. The time course plots shown are derived from the same single experiment reported in Fig. 3.3 with duplicates (error bars represent standard deviation), while the tabulated data are derived from two experiments (4 data points). **(D)** Tabulation of results from the time courses.

With a vec 5´-UTR, the CGC mutation decreased LUC expression by a factor of 5.2 (Fig. 3.4D, column b). 69L and 206L expression were decreased by factors of 2.8 and 1.7, respectively, in response to the anticodon mutation (Fig. 3.4D, column b). This means that the ratio of expression from AUG^{69} and AUG^{206} was 3.6 from RNA with the wild type sg 3´-UTR (Fig. 3.4D, column c) and 2.2 in the presence of the CGC mutation (Fig. 3.4D, column d). These results once again echo the observation above on the influence of the 5´ TYMV sequences in tempering the stimulatory effects of the terminal translational enhancers. Thus, the enhancement derived from the 5´ TYMV sequences was stronger in RNAs with the weakened 3´-enhancer TYsg(CGC) than with the wild type TYsg (Fig. 3.4D, column d vs. column c). Another expression of these relationships is that for capped RNAs with the 5´ TYMV sequences, 206L expression benefits less from the 3´-translation enhancement effect than 69L (Fig. 3.4D, column b: 1.7 vs. 2.8-fold). This is opposite to the proposed influence of the 3´-UTR specifically on ORF-206 expression (Barends et al., 2003).

3.4.6 Differential effect on ORF-69 and ORF-206 translation after internal deletion of the 5´-UTR.

In order to gain more insight into coordination of ORF-69 and ORF-206 translation by the TYMV genomic 5´-and 3´-UTRs, we tested expression from RNAs with three-quarters of the 5´-UTR missing due to deletion of nucleotides 13 through 79. This deletion leaves a 21 nt-long UTR with unchanged context around the initiation codons. TYMV RNA with this mutation was viable and genetically stable in plants, though somewhat defective for systemic spread (Hellendoorn et al., 1997).

Introduction of the 5´-UTR deletion (5´Δ) into the 5´ TYMV sequences of capped RNAs decreased the rate of 69L accumulation 2-fold (Fig. 3.5A), while increasing 206L accumulation 3.5-fold (Fig. 3.5B). Consequently, in the presence of the 5´Δ UTR, the rate of 206L expression was higher than 69L (also observed for RNAs with 3´-Bam; Fig. 3.5C), meaning that many ribosomes were bypassing the first AUG without initiating.

These changes in 69L and 206L expression were made without significantly altering the functional stability of the RNA (Fig. 3.5A, B).

Another reason the $5'\Delta$ mutation was of interest to us was in relation to the $5'$-UTR function in the scheme proposed by (Barends et al., 2003). If the $3'$-TLS were to direct translation specifically of ORF-206 as proposed, there should be some collaborative cis-elements near the AUG, perhaps in the $5'$-UTR. If removed by the $5'\Delta$ deletion, this should result in specific negative effects in the relationship between ORF-206 expression and the $3'$-UTR. We observed that replacement of the Bam with the TYg $3'$-UTR had the same effect (5.4-fold increase; Fig. 3.5C) on the rate of expression of both 69L and 206L. By contrast, with the wild type $5'$ TYMV sequences, this same $3'$ replacement increased expression of 69L 9.9-fold and of 206L 2.9-fold (Fig. 3.2C). Thus, the initiation behavior at AUG^{69} and AUG^{206} was changed by the $5'\Delta$ mutation, with ORF-206 expression favored. This suggests that the deleted portion of the TYMV $5'$-UTR does not collaborate with the $3'$-UTR in promoting initiation of ORF-206.

3.4.7 Knockout of either start codon increases gene expression from the reciprocal start codon.

The previously discussed experiments indicated an influence of the terminal enhancer elements (the $5'$-cap and $3'$-UTR) on the selection by ribosomes between initiation at AUG^{69} and AUG^{206}. An understanding of this surprising effect necessitates knowledge of the normal selection mechanisms between these AUGs. We have previously used rabbit reticulocyte lysates to study this issue, using mutations to inactivate each initiation codon (Weiland and Dreher, 1989). Mutation of the AUG^{69} to AAG eliminated in vitro expression of ORF-69, while slightly increasing ORF-206 expression. The reciprocal mutation of AUG^{206} to ACG, while retaining the native coding sequence of ORF-69, substantially increased the expression of ORF-69 (Weiland and Dreher, 1989), behavior that is not expected of simple leaky scanning (Kozak, 1995). To examine the situation in vivo, we revisited this issue with the appropriate LUC reporter RNAs.
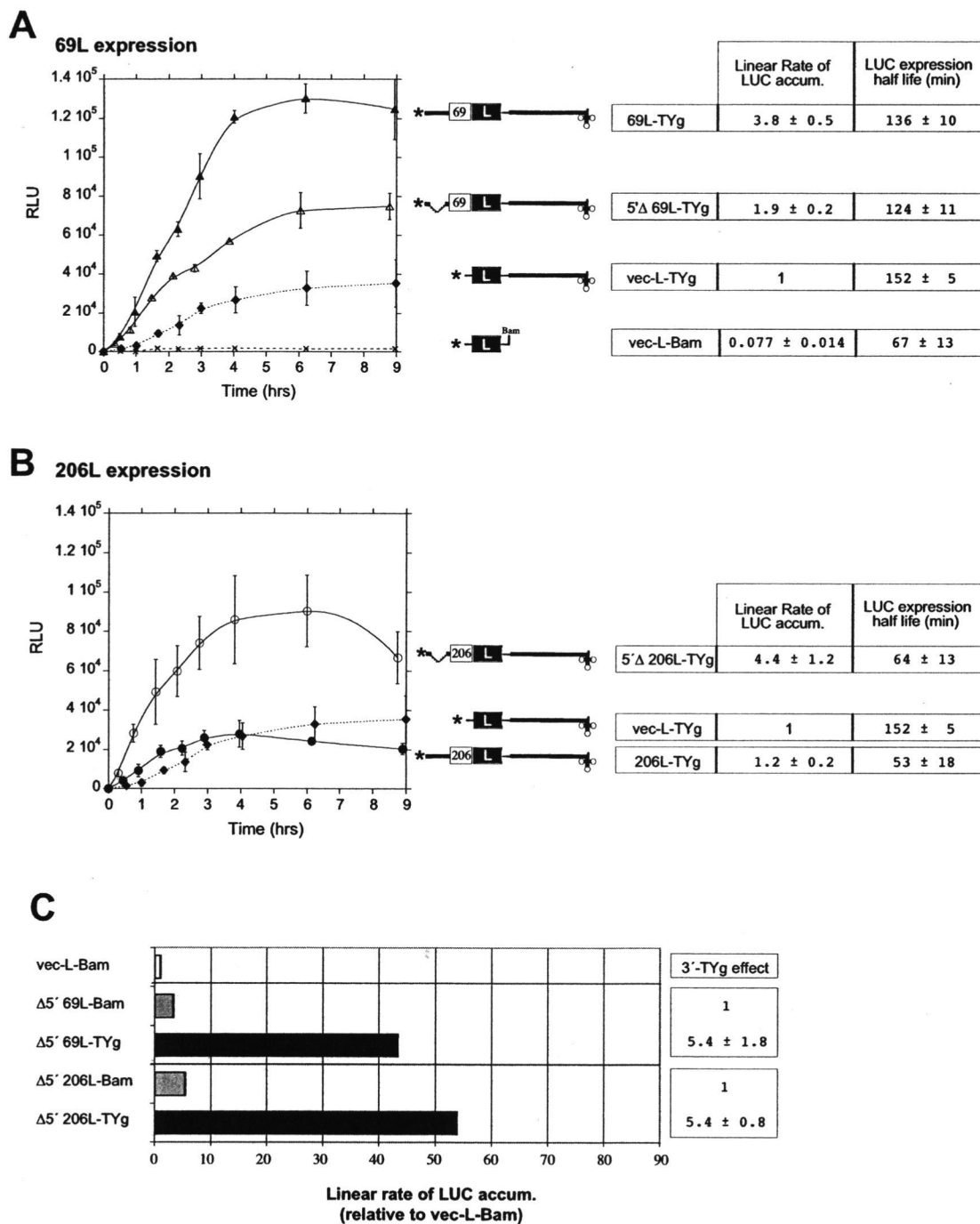
Fig. 3.5 Differential effect on 69L and 206L expression of a large internal deletion in the TYMV 5´ UTR.

Fig. 3.5 Differential effect on 69L and 206L expression of a large internal deletion in the TYMV 5′ UTR.

Expression in cowpea protoplasts directed by the indicated capped reporter RNAs expressing 69L (**A**) and 206L (**B**) is presented as in Fig. 3.2. The deletion of nts 13 through 79 of the 5′ UTR was adapted from an infectious TYMV variant reported by Hellendoorn *et al.* (Hellendoorn et al., 1997). The linear rates of LUC accumulation are expressed relative to expression from vec-L-TYg, which is shown in both (A) and (B). The time course plots shown are derived from the same single experiment reported in Figs. 3.3 and 3.4 with duplicates (error bars represent standard deviation), while the tabulated data are derived from two experiments (4 data points). (**C**) Comparison of the response to adding the TYg 3′-UTR to reporter RNAs with different 5′ sequences (data derived from linear rate data from A and B).

Knockout of AUG[69] increased expression from AUG[206] (downstream) by 3.9-fold [206L(p69/AAG)-TYg RNA; Fig. 3.6B], while knockout of AUG[206] increased expression from AUG[69] (upstream) by 2.5-fold [69L(p206/ACG)-TYg RNA; Fig. 3.6A]. The functional stabilities of the RNAs were only slightly increased by the mutations (Fig. 3.6), indicating substantial differences in translational behavior. The effect of the p206/ACG mutation in increasing expression from the upstream AUG[69] is similar to that observed in vitro (Weiland and Dreher, 1989), and is abnormal behavior for leaky scanning. On the other hand, we observed a greater increase of ORF-206 expression upon removal of the upstream AUG in these results than in reticulocyte lysates. These results are more compatible than the in vitro studies with ribosomes accessing the ORF-206 AUG by leaky scanning.
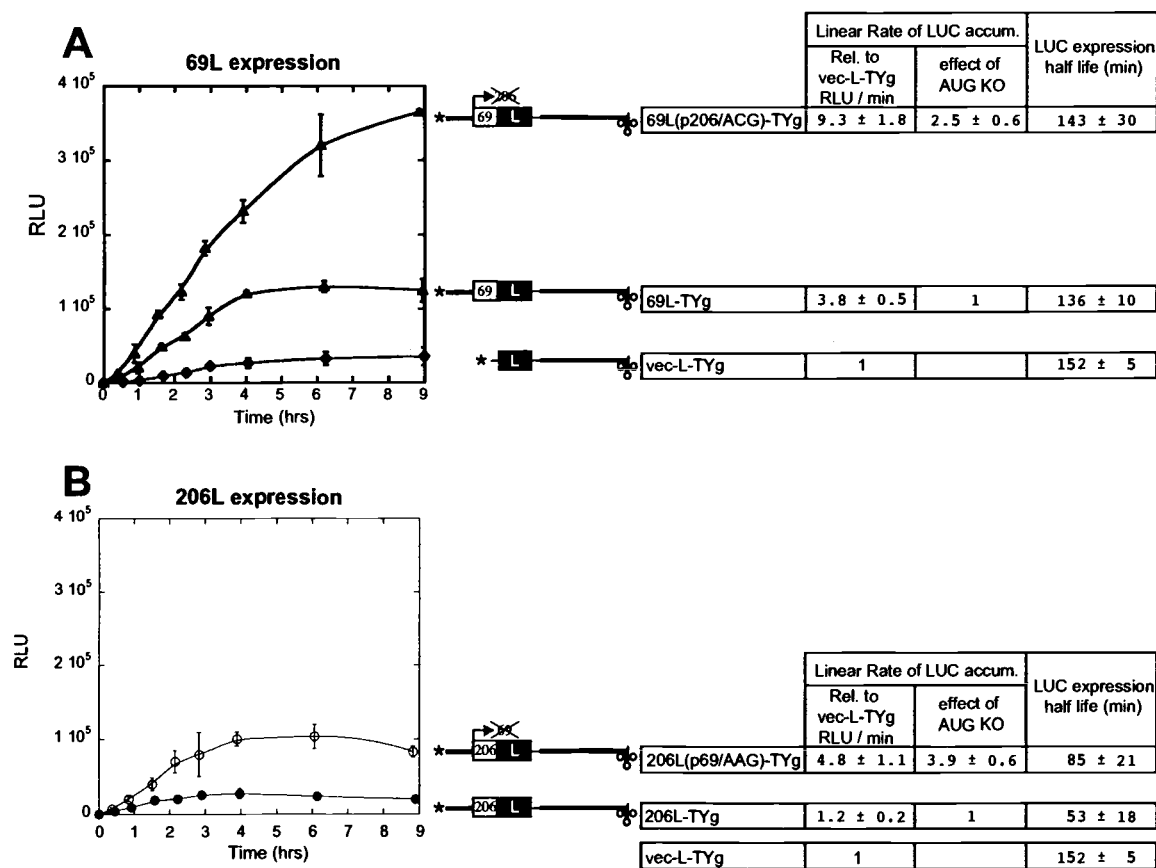
	Linear Rate of LUC accum.		LUC expression half life (min)
	Rel. to vec-L-TYg RLU / min	effect of AUG KO	
69L(p206/ACG)-TYg	9.3 ± 1.8	2.5 ± 0.6	143 ± 30
69L-TYg	3.8 ± 0.5	1	136 ± 10
vec-L-TYg	1		152 ± 5

	Linear Rate of LUC accum.		LUC expression half life (min)
	Rel. to vec-L-TYg RLU / min	effect of AUG KO	
206L(p69/AAG)-TYg	4.8 ± 1.1	3.9 ± 0.6	85 ± 21
206L-TYg	1.2 ± 0.2	1	53 ± 18
vec-L-TYg	1		152 ± 5

Fig. 3.6 Mutation of either AUG[69] or AUG[206] increases expression from the remaining AUG initiation codon.

Fig. 3.6 Mutation of either AUG^{69} or AUG^{206} increases expression from the remaining AUG initiation codon.

Time courses of LUC accumulation in cowpea protoplasts directed by the indicated capped RNAs expressing 69L (**A**) and 206L (**B**) is presented as in Fig. 3.2. In 69L(p206/ACG)-TYg RNA (**A**), the ORF-206 initiation codon has been mutated to ACG, and in 206L(p69/AAG)-TYg RNA (**B**), the ORF-69 initiation codon has been mutated to AAG. No mutations alter the encoded amino acid sequence. Both AUG mutations resulted in abolished expression of the respective gene in vitro (Weiland and Dreher, 1989).

3.5 DISCUSSION

3.5.1 5´ TYMV sequences enhance translation.

By comparison to a 17 nt-long generic (vec) 5´-UTR, 5´ genomic TYMV sequences increased expression from the 5´-most AUG without stabilizing the RNA (Figs. 3.2 and 3.3). In transfected protoplasts, the expression was enhanced 4.3-fold from capped RNAs and 7.0-fold in the absence of a cap (Fig. 3.3C). Future studies will need to refine the properties of this enhancement, since the mRNAs used in this study varied in 5´-UTR length and in the context surrounding the initiation codons (Fig. 3.1B). Since the context of the TYMV AUG[69] codon is considerably weaker than that of the AUG codon in the vec 5´-UTR (-3C/+4A vs. –3A/+4G), we may well have underestimated the enhancement. Even with three-quarters of the TYMV 5´-UTR deleted, producing a UTR similar in length to the vec UTR, expression from AUG[69] (the 5´-most AUG) was stronger than from the vec UTR (Fig. 3.5A). This supports the conclusion that the TYMV 5´-UTR does include translation enhancing sequences.

A previous study failed to detect translational enhancement by the TYMV 5´-UTR in tobacco protoplasts using β-glucuronidase reporter genes (Gallie et al., 1987b). This was evidently due to the design of the reporter constructs used, with the β-glucuronidase initiation codon placed downstream of the AUG[69] codon. With a similar reporter, we observed no significant enhancement in expression from the downstream AUG[206] codon upon addition of 5´ TYMV sequences (Fig. 3.2A, 206L-TYg vs. vec-L-TYg; Fig. 3.3A, 206L-TYsg vs. vec-L-TYsg).

3.5.2 The 5´ TYMV sequences diminish the enhancing effects of the cap and 3´-UTR.

The highest expression observed in these studies came from RNAs containing all three enhancing elements: the 5´ cap, the 5´ TYMV sequences, and the TYMV 3´-UTR (Fig. 3.3, capped 69L-TYsg RNA). These elements are clearly important in optimizing expression from TYMV RNA. However, in characterizing the function of the TYMV 5´ sequences, we noticed that the stimulatory effects (enhancement ratios) provided by the

cap (Fig. 3.3A) and the TYMV 3′-UTR (Fig. 3.2C) were lower when the 5′-TYMV sequences were present. Vice versa, the enhancing effects of the 5′ TYMV sequences in capped RNAs were greater when the TYMV 3′-UTR was absent or weakened by mutation of the anticodon (Fig. 3.4D, column c vs. column d).

The behavior of the 5′ TYMV sequences shares similarities with that of the TMV Ω enhancer. The presence of the Ω element in an RNA decreases the stimulatory effect of a cap, particularly in the presence of a poly(A) tail (with which it can synergistically interact) and vice versa (Gallie, 2002). Among capped RNAs, enhancement by Ω was greatest in the absence of a poly(A) tail. It was concluded from those studies that Ω and the cap provide overlapping or partially redundant functions that can be in competition, which can also affect the ability of the cap to interact synergistically with the poly(A) tail. Thus, while the presence of both cap and Ω provides the highest levels of translation, the enhancing potential of each of these elements is blunted in the presence of the other, perhaps because of overlapping action such as the recruitment of eIF4F, which is typically limiting (Gallie, 2002).

A further similarity between the TYMV and TMV systems is in the influence of the viral 5′ sequences on the earliest stages of translation. Inspection of the earliest parts of the LUC expression time courses revealed a longer lag before reaching a maximal linear rate of LUC accumulation for RNAs lacking 5′ TYMV sequences (Figs. 3.2A, 3.3A, 3.4). This suggests that, as hypothesized for the TMV Ω element (Gallie, 2002), the TYMV 5′ sequences facilitate the earliest rounds of translation in a way that the cap is not capable of.

3.5.3   Expression of the overlapping ORFs of TYMV RNA.

Using capped reporter RNAs with the same 5′ and 3′ terminal sequences as genomic TYMV RNA (69L-TYg and 206L-TYg RNAs), we have estimated the ratio of ORF-69 to ORF-206 expression in cowpea protoplasts to be about 3 (Table 3.3). This estimate relied on the comparison of the maximum rates of LUC accumulation early in the expression profile (Fig. 3.2A), in order to avoid bias due to a short half-life of 206L

expression compared to 69L. Neither protoplast death induced by 206L expression nor RNA lability (RNAs with 5′ 69L and 206L sequences differ only by the presence or absence of one nucleotide that matches LUC to ORF-69 or ORF-206) appear to be responsible for the faster turnover of 206L expression. We therefore deduce that 206L is a less stable protein, and it will be interesting to see in the future whether this is true of the native TYMV proteins with the same N-terminal sequence, p206 and its proteolytically processed daughter, p141. Ironically, accelerated turnover of p69, not p206, has been reported, though residues implicated in ubiquitin-dependent degradation (Drugeon and Jupin, 2002) were not present in our 69L constructs.

Table 3.3 Ratio of the rate of expression of 69L to 206L proteins

Translation enhancer elements	Ratio 69L/206L
5′TY – 3′TYsg	1.9
cap - 5′TY – 3′TYsg	3.7, 4.5[1]
cap - 5′TY – 3′TYsg(CGC)	2.2
cap - 5′TY – 3′Bam	0.9
cap - 5′TY – 3′TYg	3.1, 3.1[1]
cap - 5′ΔTY – 3′TYg	0.44
cap - 5′ΔTY – 3′Bam	0.48

Data derived from Figs. 3.1-3.5, based on linear rates of LUC expression.
[1]Independent estimates from different experiments

The likeliest expression strategy for ORFs 69 and 206 involves leaky scanning. The upstream AUG^{69} context is rather weak, and should permit sufficient ribosomes to continue scanning for initiation at AUG^{206}. We observed that initiation at both AUGs was strongly dependent on a 5′-cap (Fig. 3.3A), consistent with expression by ribosomes that were initially recruited to the 5′-terminus by the cap. Mutation of the upstream AUG^{69} increased the expression rate from AUG^{206} 3.9-fold (Fig. 3.6B), an observation

that is further consistent with leaky scanning. However, contrary to the behavior expected of leaky scanning, mutation of AUG^{206} led to an increase (2.5-fold; Fig. 3.6A) of expression from AUG^{69}, which lies upstream. This response might be explained by the release of a restriction on ORF-69 expression at the elongation phase of translation by relatively slow progress of ribosomes translating the overlapping ORF-206. Slow elongation on ORF-206 might occur because of slow decoding at certain codons, and ribosomes translating ORF-69 would be limited to the same elongation rate because ribosomes are unable to pass on an mRNA. Expression limitation of this sort has been suggested for reovirus S1 RNA, which also has overlapping ORFs (Fajardo and Shatkin, 1990). Perhaps ORF-206 expression is normally limited by both slow elongation and limited initiation due to interference by the upstream AUG^{69}.

A proposal by (Williams and Lamb, 1989) provides another model for ribosome behavior on TYMV RNA. These authors studied the synthesis of Influenza B virus NB and NA proteins from overlapping ORFs that are separated by 4 nucleotides as in TYMV RNA. Based on a mutagenic study and expression in cells, they suggested that ribosomes reach the paired AUG initiation codons by conventional scanning, but then select between the closely spaced AUGs by random choice. This scheme has been disputed by (Kozak, 1995) based on studies with the same closely spaced initiation codons. However, those studies were performed in vitro and with non-influenza sequences flanking the initiation sites, and so may not have studied the same phenomenon as (Williams and Lamb, 1989).

Future studies will test the applicability of the random choice model to TYMV gene expression. Those studies will need to take into account the surprising observations summarized in Table 3.3. We observed the expression from AUG^{69} relative to AUG^{206} to vary depending on the presence or absence of translational enhancers at the 5´ and 3´ termini, i.e., the cap and TYg or TYsg 3´-UTRs. The expression ratio was also different after deletion of much of the 5´-UTR (5´Δ). The presence of translational enhancers — cap, 5´ TYMV sequences or TYMV 3´-UTR — favored ORF-69 over ORF-206 expression. The effect of the 5´-UTR deletion may be explained by the positioning of

AUG^{69} close enough to the 5´-end to promote ribosome bypassing, a phenomenon described by (Kozak, 1991). The other observations suggest a mechanism whereby translation that is occurring on an RNA for which there is synergy between 5´ and 3´ enhancers is carried out principally by ribosomes that are recycled from the 3´-end and that carry with them some attribute that favors initiation at the first AUG codon.

3.5.4 Is ORF-206 translation facilitated by "tRNA mimicry as a molecular Trojan horse?"

Our studies have provided a test of some aspects of the TYMV gene expression model recently proposed by (Barends et al., 2003) and described in terms of a molecular Trojan horse. Unlike those studies, which were conducted in wheat germ extracts, our experiments used protoplasts capable of supporting a TYMV infection. Although we used LUC reporter RNAs, gene expression was assayed in the same milieu as that of a natural infection, and the reporter RNAs had considerable TYMV sequence at both ends. The tested aspects of the proposed scheme were: [1] is ORF-206 translation cap-independent?; [2] does the TYMV 3´-UTR containing the tRNA-like structure (TLS) enhance, perhaps in an obligatory way, expression of ORF-206 but not of ORF-69?; [3] is there a sequence in the 5´-UTR that collaborates with the TLS to direct expression of ORF-206?

Our experiments make it clear that translation from both AUG^{69} and AUG^{206} is strongly cap-dependent. We have also observed that the TYMV 3´-UTR is a general enhancer, with a principal mode of action being synergy with the cap (Matsuda and Dreher, 2004). The 3´-UTR enhanced translation from RNAs with 5´-vec or 5´-TYMV sequences, and from AUG^{69} as well as from AUG^{206} (Fig. 3.2C). We did observe a difference in the influence of the 3´-UTR on initiation at AUG^{69} compared to AUG^{206}, but ORF-206 expression was less dependent on the 3´-UTR than expression of ORF-69 (Fig. 3.2C). This is opposite to the proposal of (Barends et al., 2003).

We performed only one test for 5´ sequences that might interact with the TLS as suggested by the scheme of Barends *et al.* (Barends et al., 2003), involving deletion of

three-quarters of the 5´-UTR. The UTR is the most likely site for such a collaborating sequence: this is the location of internal ribosome entry sites, the elements capable of directing cap-independent translation (Sarnow, 2003), and the sequence constraints of the overlapping reading frames would make the coding regions an unlikely location. The 5´Δ mutation resulted in higher expression of ORF-206 relative to ORF-69 (Table 3.3). Removal of a feature that functions together with the 3´-TLS to direct ORF-206 translation would have had the opposite effect.

Our experiments thus do not support the Barends *et al.* (Barends et al., 2003) model, and in fact contradict it. That model may describe an in vitro phenomenon or be the result of studies that attempted to identify TYMV proteins without immunological verification.

3.6 ACKNOWLEDGMENTS

3.7 REFERENCES

Barends, S., Bink, H. H., van den Worm, S. H., Pleij, C. W., and Kraal, B. (2003). Entrapping ribosomes for viral translation: tRNA mimicry as a molecular Trojan horse. *Cell* **112,** 123-9.

Drugeon, G., and Jupin, I. (2002). Stability in vitro of the 69K movement protein of Turnip yellow mosaic virus is regulated by the ubiquitin-mediated proteasome pathway. *J Gen Virol* **83,** 3187-97.

Fajardo, J. E., and Shatkin, A. J. (1990). Translation of bicistronic viral mRNA in transfected cells: regulation at the level of elongation. *Proc Natl Acad Sci U S A* **87,** 328-32.

Gallie, D. R., Sleat, D. E., Watts, J. W., Turner, P. C., and Wilson, T. M. (1987a). The 5'-leader sequence of tobacco mosaic virus RNA enhances the expression of foreign gene transcripts in vitro and in vivo. *Nucleic Acids Res* **15,** 3257-73.

Gallie, D. R., Sleat, D. E., Watts, J. W., Turner, P. C., and Wilson, T. M. (1987b). A comparison of eukaryotic viral 5'-leader sequences as enhancers of mRNA expression in vivo. *Nucleic Acids Res* **15,** 8693-711.

Gallie, D. R. (1991). The cap and poly(A) tail function synergistically to regulate mRNA translational efficiency. *Genes Dev* **5**, 2108-16.

Gallie, D. R., and Kobayashi, M. (1994). The role of the 3'-untranslated region of non-polyadenylated plant viral mRNAs in regulating translational efficiency. *Gene* **142**, 159-65.

Gallie, D. R. (2002). The 5'-leader of tobacco mosaic virus promotes translation through enhanced recruitment of eIF4F. *Nucleic Acids Res* **30**, 3401-11.

Hellendoorn, K., Michiels, P. J., Buitenhuis, R., and Pleij, C. W. (1996). Protonatable hairpins are conserved in the 5'-untranslated region of tymovirus RNAs. *Nucleic Acids Res* **24**, 4910-7.

Hellendoorn, K., Verlaan, P. W., and Pleij, C. W. (1997). A functional role for the conserved protonatable hairpins in the 5' untranslated region of turnip yellow mosaic virus RNA. *J Virol* **71**, 8774-9.

Jobling, S. A., and Gehrke, L. (1987). Enhanced translation of chimaeric messenger RNAs containing a plant viral untranslated leader sequence. *Nature* **325**, 622-5.

Kozak, M. (1991). A short leader sequence impairs the fidelity of initiation by eukaryotic ribosomes. *Gene Expr* **1**, 111-5.

Kozak, M. (1995). Adherence to the first-AUG rule when a second AUG codon follows closely upon the first. *Proc Natl Acad Sci U S A* **92**, 2662-6.

Kozak, M. (1999). Initiation of translation in prokaryotes and eukaryotes. *Gene* **234**, 187-208.

Lukaszewicz, M., Feuermann, M., Jerouville, B., Stas, A., and Boutry, M. (2000). In vivo evaluation of the context sequence of the translation initiation codon in plants. *Plant Science* **154**, 89-98.

Mangus, D. A., Evans, M. C., and Jacobson, A. (2003). Poly(A)-binding proteins: multifunctional scaffolds for the post-transcriptional control of gene expression. *Genome Biol* **4**, 223.

Matsuda, D., and Dreher, T. W. (2004). The tRNA-like structure of Turnip yellow mosaic virus RNA in a 3´-translational enhancer. *Virology* **in press**.

Pestova, T. V., Kolupaeva, V. G., Lomakin, I. B., Pilipenko, E. V., Shatsky, I. N., Agol, V. I., and Hellen, C. U. (2001). Molecular mechanisms of translation initiation in eukaryotes. *Proc Natl Acad Sci U S A* **98**, 7029-36.

Sachs, A. B., Sarnow, P., and Hentze, M. W. (1997). Starting at the beginning, middle, and end: translation initiation in eukaryotes. *Cell* **89**, 831-8.

Sarnow, P. (2003). Viral internal ribosome entry site elements: novel ribosome-RNA complexes and roles in viral pathogenesis. *J Virol* **77**, 2801-6.

Tomashevskaya, O., Solovyev, A., Karpova, O., Fedorkin, O., Rodionova, N., Morozov, S., and Atabekov, J. (1993). Effects of sequence elements in the potato virus X RNA 5' non-translated alpha beta-leader on its translation enhancing activity. *J Gen Virol* **74**, 2717-2724.

Turner, R. L., Glynn, M., Taylor, S. C., Cheung, M. K., Spurr, C., Twell, D., and Foster, G. D. (1999). Analysis of a translational enhancer present within the 5'-terminal sequence of the genomic RNA of potato virus S. *Arch Virol* **144**, 1451-61.

Vende, P., Piron, M., Castagne, N., and Poncet, D. (2000). Efficient translation of rotavirus mRNA requires simultaneous interaction of NSP3 with the eukaryotic translation initiation factor eIF4G and the mRNA 3' end. *J Virol* **74,** 7064-71.

Weiland, J. J., and Dreher, T. W. (1989). Infectious TYMV RNA from cloned cDNA: effects in vitro and in vivo of point substitutions in the initiation codons of two extensively overlapping ORFs. *Nucleic Acids Res* **17,** 4675-87.

Wells, D. R., Tanguay, R. L., Le, H., and Gallie, D. R. (1998). HSP101 functions as a specific translational regulatory protein whose activity is regulated by nutrient status. *Genes Dev* **12,** 3236-51.

Williams, M. A., and Lamb, R. A. (1989). Effect of mutations and deletions in a bicistronic mRNA on the synthesis of influenza B virus NB and NA glycoproteins. *J Virol* **63,** 28-35.

Chapter 4 eEF1A binding to aminoacylated viral RNA represses minus strand synthesis by TYMV RNA-dependent RNA polymerase

Daiki Matsuda, Shigeo Yoshinari and Theo W. Dreher

4.1 Abstract

The genomic RNA of *Turnip yellow mosaic virus* (TYMV) has an 82 nucleotide-long tRNA-like structure at its 3´ end that can be valylated and then form a stable complex with translation elongation factor eEF1A•GTP. Transcription of this RNA by TYMV RNA-dependent RNA polymerase (RdRp) to yield minus strands has previously been shown to initiate within the 3´-CCA sequence. We have now demonstrated that minus strand synthesis is strongly repressed upon the binding of eEF1A•GTP to the valylated viral RNA. eEF1A•GTP had no effect on RNA synthesis templated by non-aminoacylated RNA. Higher eEF1A•GTP levels were needed to repress minus strand synthesis templated by valyl-EMV TLS RNA, which binds eEF1A•GTP with lower affinity than does valyl-TYMV RNA. Repression by eEF1A•GTP was also observed with a methionylated variant of TYMV RNA and with aminoacylated tRNA[His], tRNA[Ala] and tRNA[Phe] transcripts. It is proposed that minus strand repression by eEF1A•GTP binding occurs early during infection to help coordinate the competing translation and replication functions of the genomic RNA.

4.2 Introduction

Positive strand RNA viruses are unique in that their genomes serve both as messenger RNAs directing viral gene expression and as templates for genome amplification. In the former process, ribosomes traffic from 5´ to 3´, while in the latter, RNA-dependent RNA polymerase (RdRp) complexes move in the opposite direction on the same strand. Evidence from two systems to date suggests that genomic RNA usage is highly regulated so that each strand participates in only one of the above processes at a given time. In both prokaryotic (Qβ bacteriophage: Kolakofsky and Weissmann, 1971a, 1971b) and eukaryotic (poliovirus: Gamarnik and Andino, 1998; Barton et al., 1999) systems, it has been observed that ribosomes translating an RNA prevent full-length transcription by viral RdRp. Ribosomes thus must be cleared from genomic RNA before productive replication can commence. Coordination between translation and replication

may also help to minimize the production of partial-length double-stranded RNA fragments that in eukaryotic cells can act as potent inducers of antiviral defenses (Jacobs and Langland, 1996; Ahlquist, 2002).

The Qβ and poliovirus systems both regulate the messenger and template usage of their genomic RNA in a mutually antagonistic fashion. Ribosomes and Qβ replicase compete for a common binding site at the initiation site for coat protein synthesis (Kolakofsky and Weissmann, 1971a, 1971b), the major ribosome entry point on Qβ RNA (van Duin, 1988). In the case of poliovirus RNA, binding by the 3CD protease-polymerase precursor protein to the 5′ cloverleaf structure simultaneously represses translation and enhances minus strand synthesis (Gamarnik and Andino, 1998; Barton et al., 2001). A further mechanism for separation of translation and replication that is probably general to eukaryotic positive strand viruses is the physical sequestration of templates into membrane vesicles that are the sites of active RNA replication (Chen et al., 2001b; Schwartz et al., 2002).

Turnip yellow mosaic virus (TYMV) possesses a positive-strand genomic RNA that terminates at the 3′-end with a tRNA-like structure (TLS, Fig. 4.1). The TLS mimics tRNA^{Val} both structurally and functionally (Rietveld et al., 1982; Dreher and Goodwin, 1998) through the presence of features such as a –CCA 3′-terminus, a valine-specific anticodon that directs interaction with host valyl-tRNA synthetase (Dreher et al., 1992), and interacting D- and T-loops (de Smit et al., 2002). The valylation efficiencies of TYMV RNA and the TLS with wheat germ valyl-tRNA synthetase (ValRS) are similar to that of plant tRNA^{Val}, and valylated TYMV RNA and tRNA^{Val} also have similar high affinities for translation elongation factor 1A (eEF1A•GTP) (Dreher and Goodwin, 1998). As might be expected from this remarkable degree of tRNA mimicry, mutations that prevent aminoacylation destroy the infectivity of viral RNA in plants (Tsai and Dreher, 1991), although the wild type TLS can be replaced by certain non-aminoacylatable termini (Goodwin et al., 1997; Filichkin et al., 2000).

By virtue of its location at the 3′-end, the TLS plays a role in genome amplification by serving as the origin of replication. Using in vitro assays with TYMV RdRp, it has been

shown that minus strand synthesis initiates opposite the penultimate C (Singh and Dreher, 1997) within the –CCA 3′-terminal sequence that serves as a major element controlling minus strand initiation (Deiman et al., 1998; Singh and Dreher, 1998). No other specific features within the TLS have been identified as promoter elements directing minus strand synthesis (Deiman et al., 1998; Singh and Dreher, 1998), leading to speculation that the tRNA mimicry serves to permit interactions that negatively regulate minus strand synthesis (Dreher, 1999; Filichkin et al., 2000). The sensitivity of minus strand synthesis to inhibition by the inclusion of the initiation site in secondary structure (Singh and Dreher, 1998) suggested that the binding of eEF1A•GTP could repress initiation. Valylated TYMV RNA forms a tight complex with eEF1A•GTP (K_d = 2 nM) (Dreher and Goodwin, 1998) in which the bound protein contacts the aminoacyl-CCA terminus and the remainder of the aminoacyl-acceptor arm (Joshi et al., 1986; Dreher et al., 1999). Such a repressor function would be regulated by the aminoacylation of the viral RNA, since the difference in eEF1A•GTP affinity for charged and uncharged tRNA is about 10^4 (Dreher et al., 1999).

In this study, we provide direct evidence using an in vitro transcription system that eEF1A•GTP can act negatively on minus strand initiation by TYMV RdRp, and that it does so only when the template is aminoacylated. This negative regulation is most likely to occur at the earliest stages of an infection before viral RdRp complexes appear and begin to compete for interaction with the 3′-terminus to initiate minus strand synthesis. We propose that this regulation serves to differentiate the translation and replication functions of the viral RNA. In the accompanying paper, we show that the TYMV TLS acts as a translational enhancer element, and that the enhancement of messenger function is dependent on the capacity of the RNA to be aminoacylated and to bind eEF1A•GTP (Matsuda and Dreher, 2004). Thus, as observed in the Qβ and poliovirus systems, TYMV appears to employ an interaction that simultaneously switches between the translation and replication functions of the genomic RNA to influence the transition between these two functions of the same RNA.

```
                              /CUCU
          C    30      /        \
    A       U  CCCG—CCC  /UCGGA┤A CCA  3'
    A   T      ||||   |||/  |||||
    C      U  GGGC   GGG/-AGCCU
       G      40  |     \ /      20
                        UCA
    U  G      U          |
  U   D  A    A          10
    A   C     A
       G-C    U
   70-C-G    /
      G-C-80/
      A-U   /
      G-C/——G 5'
      G  /
      U-A/
      C-G
      U-A
      G-C-50
      U-A
   60-C-G
      C    ©
    c A/C A
      C  Ⓐ©
      56
```
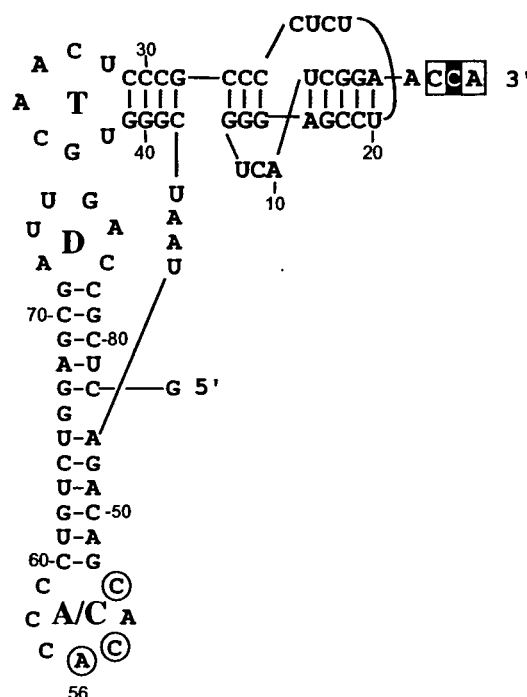
Fig. 4.1. The TYMV tRNA-like structure (TY83 RNA).

The secondary structure model emphasizes similarities to canonical tRNA: CCA 3´-terminus, 12 base-pair acceptor/T arm, interacting D- and T-loops, and an anticodon loop (A/C) with a valine-specific anticodon (CAC). Unlike canonical tRNAs, however, the acceptor stem consists of a pseudoknot. The 3´ CCA (boxed) serves as an initiation box controlling minus strand synthesis directed by TYMV RdRp, which initiates opposite the 3´-most C residue (reverse shading; Singh and Dreher, 1997). The circled nucleotides in the anticodon loop constitute the valine identity elements that direct specific valylation of the 3´-end of the RNA by plant valyl-tRNA synthetase (Dreher et al., 1992). Nucleotides are numbered from the 3´-end.

4.3 Results

4.3.1 Preparation of aminoacylated RNAs to be used as templates for TYMV RdRp

In order to test the ability of eEF1A•GTP to repress minus strand synthesis by TYMV RdRp, it was a priority to generate as uniform a population of aminoacylated templates as possible. Contaminating uncharged RNAs, unable to bind eEF1A•GTP,

would be resistant to any repression and would result in a background level of minus strand synthesis. First, in order to maximize the proportion of RNAs with correct -CCA 3′-ends, templates were made by transcription with T7 RNA polymerase from PCR-generated DNAs that incorporated 2′-O-methyl modifications of the two 5′-most nucleotides of the template strand read by T7 RNA polymerase (see Materials and methods). Such modifications suppress the addition of untemplated 3′ nucleotides (Kao et al., 1999). Preparative aminoacylation of a range of template RNAs achieved best charging levels of 60-95%, as judged by acid-urea PAGE (Fig. 4.2). Residual uncharged molecules may have incorrect 3′-ends or be incorrectly folded (Uhlenbeck, 1995).
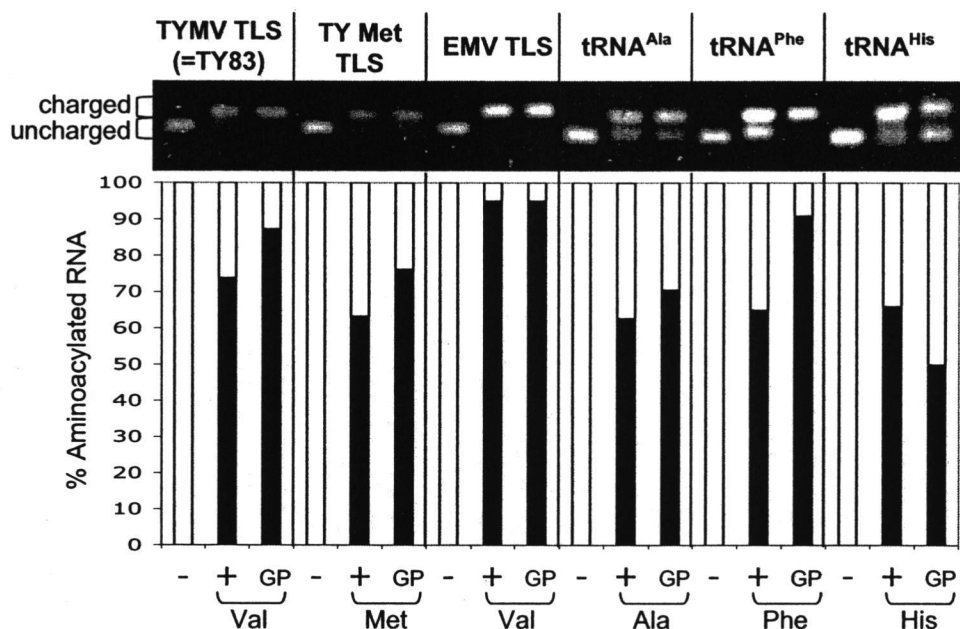
Fig. 4.2. Preparation of aminoacyl-RNAs to be used as templates for TYMV RdRp. The indicated RNAs were analyzed before (-) and after (+) preparative aminoacylation with the amino acid indicated below each lane, as well as after purification of aminoacyl-RNAs by elution after acid-urea PAGE (GP, gel-purified). The top panel shows the migration of RNAs in analytical acid-urea PAGE (6.5%) stained with ethidium bromide. The upper and lower bands represent aminoacyl and free RNAs, respectively, identified as charged and uncharged species at left. The lower panel plots the result of quantitative scans of acid-urea gels, reporting the proportion (%) of aminoacylated RNA (black bars).

Purification of aminoacyl-RNAs by elution after separation by acidified denaturing PAGE (Varshney et al., 1991) was found to be superior to several other strategies for enriching charged over uncharged RNAs. Improved levels of purity were obtained in this way for all aminoacyl-RNAs except histidyl-tRNA^{His}, achieving final charging levels of 70-95% (Fig. 4.2). These levels may be somewhat underestimated because a small amount of deacylation could occur during the lengthy electrophoresis analysis, especially with histidyl-tRNA^{His}. The ester linkages of all aminoacyl-RNAs are subject to spontaneous hydrolysis in aqueous conditions. To suppress deacylation during preparation and storage, aminoacyl-RNAs were kept at low pH and low temperature (see Materials and methods). Because the histidyl linkage is least stabilized under these conditions (Hentzen et al., 1972), exposure to lengthy purification was avoided and histidyl-tRNA^{His} was used as a template without gel purification.

Assessment of repression by eEF1A•GTP also relied upon minimal deacylation of aminoacyl-RNAs during the course of the RdRp assay, and on the maintenance of preformed ternary complexes (aminoacyl-RNA•eEF1A•GTP) under assay conditions. Tests with [^{3}H]valyl-TY83 RNA incubated at 14°C in complete RdRp reactions lacking only nucleoside triphosphates showed that at most 10% of molecules lost their bound [^{3}H]valine during a 20 min incubation (not shown). To minimize the effects of template deacylation during minus strand synthesis reactions, single-round transcription assays were employed in which product was initiated during a 3 min incubation at 14°C in reactions lacking ATP, and then completed during a 12 min incubation at 30°C following the addition of ATP and polyethylene sulfonate (PES). PES is a polymerase scavenger that binds free RdRp to prevent re-initiation (Barrera et al., 1993).

The maintenance of valyl-TY83•eEF1A•GTP ternary complexes under TYMV RdRp reaction conditions was estimated by standard RNase protection assay (Dreher et al., 1999). A constant proportion (70%) of valyl-TY83 RNA was found to be bound to eEF1A•GTP during a 20 min incubation at 14°C (not shown). With the conditions of excess eEF1A•GTP used (0.5 pmol valyl-RNA and 6 pmol eEF1A•GTP) a level of at least 90% complex formation was expected. It is not known why this level was not

reached, although we measured consistently lower ternary complex levels under the RdRp conditions than in our standard assay conditions that incorporate higher ionic strength (100 mM NH_4Cl; Dreher et al., 1999). Based on assay for eEF1A activity in RdRp preparations by RNase protection using [^3H]valyl-TY83 RNA, no significant amounts of eEF1A are present in our RdRp fractions, confirming previous reports based on Western detection (Joshi et al., 1986; Pulikowska et al., 1988).

4.3.2 *Aminoacylation and eEF1A•GTP interaction inhibit template activity for minus strand synthesis*

RNA corresponding to the TYMV TLS (TY83 RNA; Fig. 4.1) is an active template for minus strand synthesis by TYMV RdRp (Singh and Dreher, 1997)(Fig. 4.3A, lane 2). This activity was not significantly changed when the RNA was preincubated with eEF1A•GTP (lane 3), indicating that eEF1A•GTP does not influence the activity of TYMV RdRp, as previously reported (Pulikowska et al., 1988). Intriguingly, the template activity of valyl-TY83 RNA (lane 4) was less than half (45%) that of uncharged TY83 RNA. Minus strand synthesis was further reduced to 17% when valyl-TY83 RNA (2 pmol) preincubated with excess eEF1A•GTP (10 pmol) was used as template (lane 5). As indicated in Fig. 4.3A, this level is close to the background level of product (13%) expected from the uncharged RNA present in our valyl-TY83 RNA preparations (lane 6). Given that 13% of the product in lanes 4 and 5 of Fig. 4.3A originated from uncharged templates (open column), the estimated template activities of valyl-TY83 RNA in the presence and absence of eEF1A•GTP were 37% and 5%, respectively, that of uncharged TY83 RNA. The template activity of valyl-TY83 RNA was entirely restored when the RNA was intentionally deacylated by incubating at 37°C for 10 hours (not shown).

A

eEF1A•GTP	-	-	10	-	10
Val-TY83	-	-	-	2	2
TY83	-	2	2	-	-

		1	2	3	4	5
☐	Before bkgd corr.	1	0.95	0.45	0.17	0.13
■	After bkgd corr.	1	0.94	0.37	0.05	

B

eEF1A•GTP	-	-	10	-	10
MetI-TY83	-	-	-	2	2
TY83	-	2	2	-	-

		1	2	3	4	5
☐	Before bkgd corr.	1	1.02	0.49	0.26	0.24
■	After bkgd corr.	1	1.03	0.32	0.02	
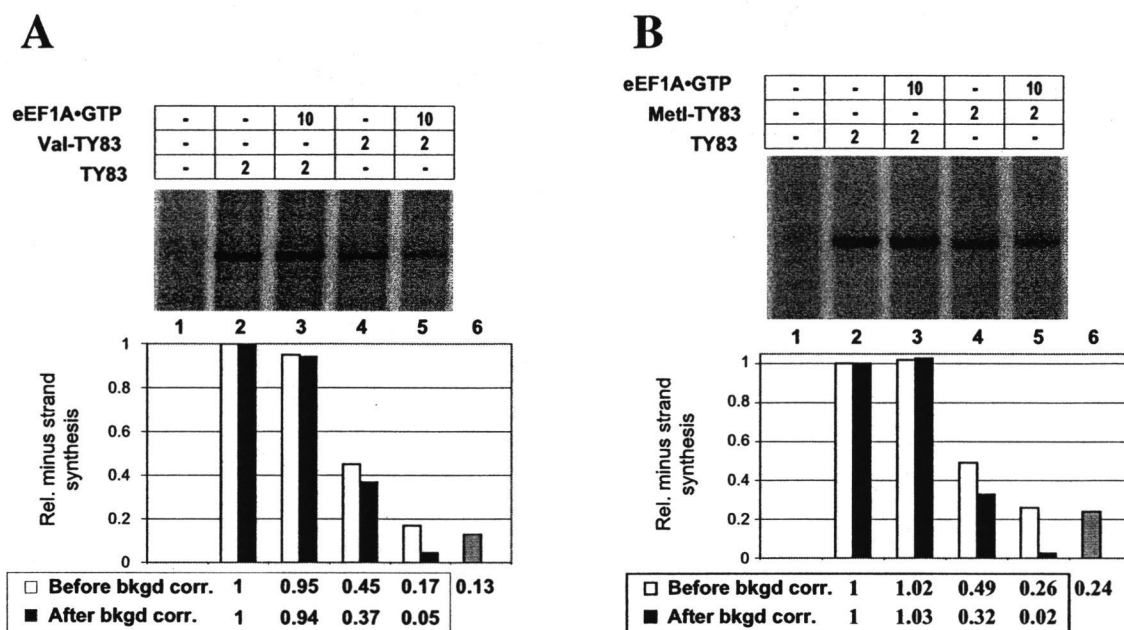
Fig. 4.3. Repression of minus strand synthesis from TYMV RNA by aminoacylation and eEF1A•GTP binding.

TY83 RNA (**A**) and a methionylatable derivative, TY-Met-TLS RNA (**B**), were used as templates for minus strand synthesis by TYMV RdRp. Where indicated, the aminoacylated forms of these RNAs were used, or RNAs were preincubated with an excess of eEF1A•GTP. The additions of 2 pmol of RNA and 10 pmol of eEF1A•GTP are indicated. The ^{32}P-labeled products of single-round transcription reactions were separated by 12% native PAGE and visualized by phosphorimagery. The yields of minus strand product are graphed below each gel lane (averages of duplicate experiments). The product derived from residual uncharged template RNA present in each assay of aminoacylated templates is represented as the gray bar in lane 6. The white bar in each lane represents the yield of minus strand product (relative quantity given below the graph). The associated black bar represents the amount of minus strand product after correction for the product derived from uncharged template (background-corrected; relative quantity listed below the graph).

4.3.3 Aminoacylation and eEF1A•GTP interaction also repress minus strand synthesis from non-viral RNAs

By introducing point mutations into the anticodon and acceptor stem pseudoknot, it has been possible to produce infectious TYMV RNA for which the aminoacylation identity has been switched from valine to methionine (Dreher et al., 1996). Using the TLS derived from this RNA (TY-Met-TLS RNA) as RdRp template permitted an assessment of the influence of the identity of the esterified amino acid on minus strand synthesis in our assays. After adjustment for the background contributed by uncharged template RNAs, minus strand synthesis was reduced about 3-fold after methionylation and to background levels in the presence of eEF1A•GTP (Fig. 4.3B). These results were similar to those obtained with the valylatable TY83 RNA (Fig. 4.3A).

Eggplant mosaic tymovirus genomic RNA has a valylatable TLS similar to that of TYMV RNA, but its affinity for eEF1A•GTP has been estimated to be 28 times lower than that of valyl-TYMV RNA (K_d of 57 nM cf. 2 nM) (Dreher and Goodwin, 1998). The weaker interaction involving the EMV TLS is thought to be due to differences in the construction of the T-stem. As a consequence of the weaker affinity, we expected the repression of minus strand synthesis from valyl-EMV-TLS RNA to require higher levels of eEF1A•GTP. This expectation is confirmed in Fig. 4.4. Strong repression of valyl-TY83 RNA was observed at an eEF1A:RNA ratio of 1.5 (lane 5), while minus strand synthesis from valyl-EMV-TLS RNA was little affected at this ratio (lane 11). Some repression was observed at an eEF1A:RNA ratio of 7.4 (lane 12), but much greater repression of valyl-TY83 RNA template activity was observed at this level of eEF1A•GTP (lane 6).
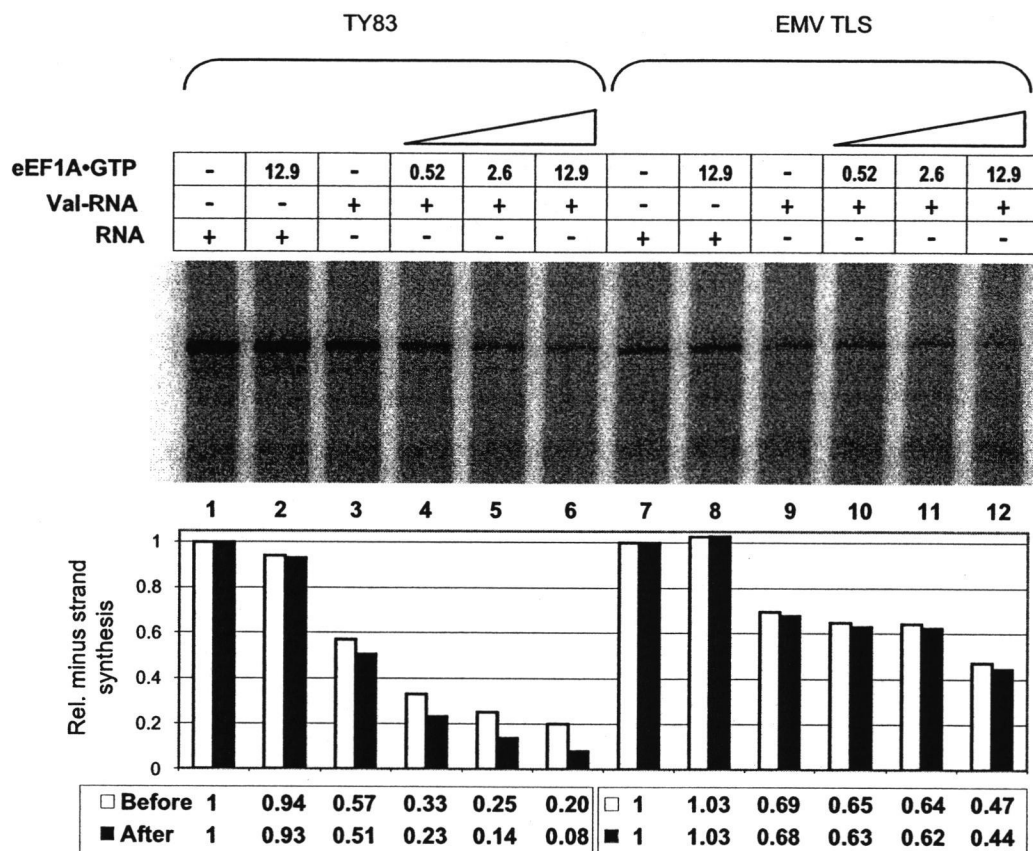
Fig. 4.4. Higher levels of eEF1A•GTP needed to repress minus strand synthesis from EMV TLS RNA.
Minus strand assays and their quantitation from duplicate experiments are presented as in Fig. 4.3, using the indicated RNAs in the free and valylated form (1.75 pmol) as templates in the presence of varying levels of eEF1A•GTP as indicated (pmoles).

In order to further explore the effect of different amino acids and the generality of eEF1A•GTP repression, we examined minus strand synthesis using tRNA[Ala], tRNA[Phe], and tRNA[His] transcripts as templates. Consistent with the major role of the 3´-CCA initiation box in controlling minus strand synthesis by TYMV RdRp (Deiman et al., 1998; Singh and Dreher, 1998), unmodified tRNAs synthesized in vitro can be active templates. Mature, fully modified, tRNAs are poor templates, probably because of the

presence of modified bases (Singh and Dreher, 1997). For each of the tRNAs tested, a decrease of minus strand synthesis was observed after aminoacylation (Fig. 4.5, lanes 2) and especially when aminoacyl-RNAs were tested in the presence of eEF1A•GTP (Fig. 4.5, lanes 3). Similar decreases in template activity were observed for tRNAs after aminoacylation with their cognate amino acids alanine, phenylalanine, and histidine (Fig. 4.5A, B, C, lanes 2), despite the different chemical nature and size of their side chains. Note that the percentage of non-histidylated tRNA^{His} (Fig. 4.5C, lane 4) was overestimated from acid-urea gel analysis because of the greater sensitivity to deacylation during gel analysis of the histidyl compared to other aminoacyl ester linkages (Hentzen et al., 1972).

A tRNA^{Ala}

	1	2	3	4
□ Before	1	0.52	0.30	0.29
■ After	1	0.31	0.01	

B tRNA^{Phe}

	1	2	3	4
□ Before	1	0.46	0.25	0.10
■ After	1	0.40	0.17	

C tRNA^{His}

	1	2	3	4
□ Before	1	0.25	0.11	0.31*
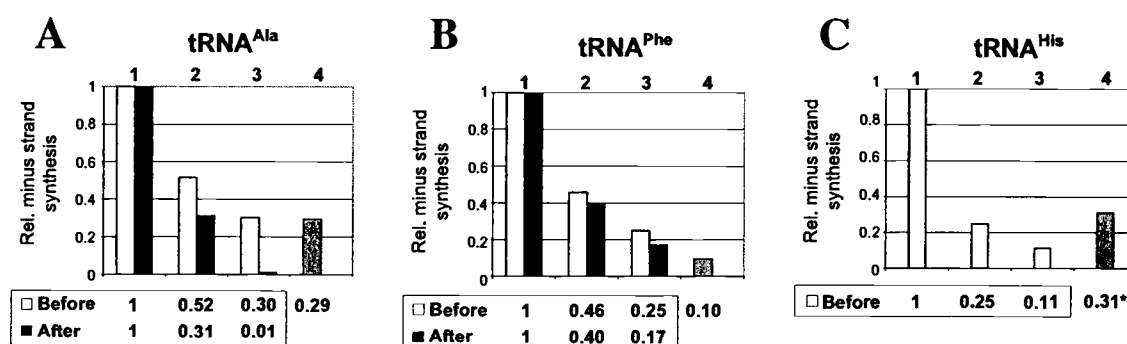
Fig. 4.5. Repression of minus strand synthesis from non-viral RNA templates charged with various amino acids.
The quantitations of minus strand assays from duplicate experiments are presented as in Fig. 4.3, using the indicated unmodified tRNA transcripts (1 or 2 pmol) as templates (lanes 1). In adjacent lanes, RNAs were aminoacylated with their cognate amino acid (lanes 2) and were preincubated with eEF1A•GTP (10 pmol; lanes 3). Lanes 4 represent the proportion of non-aminoacylated RNA present. The asterisk in (C) indicates overestimation of the proportion of uncharged RNA due to the sensitivity of histidyl-tRNA^{His} to deacylation (see text); consequently, no background correction was applied to the tRNA^{His} experiment.

4.4 Discussion

Our genetic and biochemical studies on TYMV have led us to the minus strand repression model as explaining an important role of tRNA mimicry (Dreher, 1999; Filichkin et al., 2000). Point mutations of the valine identity elements that destroyed valylatability (Tsai and Dreher, 1991) or switched identity to methionine (Dreher et al., 1996) indicated a requirement for aminoacylation rather than a specific interaction with valyl-tRNA synthetase or some other protein that contacts the valine identity nucleotides. Given the abundance of eEF1A•GTP in cells and its high affinity for valyl-TYMV RNA (Dreher and Goodwin, 1998), these results implicated eEF1A•GTP interaction as a critical outcome of tRNA mimicry. Binding as it does at the 3′ terminus, one might imagine eEF1A•GTP acting as a transcription factor directing TYMV RdRp to its initiation site at the 3′ end, or alternatively as a repressor blocking the access of the RdRp. The former scenario (Hall, 1979) was inspired by the presence of EF-Tu (the bacterial homolog of eEF1A) as a subunit of the replicase (RdRp) of Qβ bacteriophage (Blumenthal and Carmichael, 1979). However, because minus strand synthesis in vitro from TY83 RNA template by TYMV RdRp is independent of tRNA mimicry (Singh and Dreher, 1998), the idea that eEF1A serves as a transcription factor or in some other capacity to promote minus strand synthesis can be rejected. This conclusion is supported by results showing that aminoacylation is not required for the infectivity of certain variant TYMV genomes (Goodwin et al., 1997; Filichkin et al., 2000) and indeed aminoacylation has not been absolutely conserved among the tymoviruses (Dreher and Goodwin, 1998). If eEF1A•GTP serves a repressor function towards minus strand synthesis, we have proposed that another ligand, presumably a host protein, substitutes as the repressor for those tymoviral genomes incapable of aminoacylation (Dreher, 1999).

Our experiments here have shown that eEF1A•GTP is indeed capable of repressing minus strand synthesis originating from the TYMV TLS. The effect is entirely dependent on prior aminoacylation of the RNA (Fig. 4.3), indicating that eEF1A•GTP has no direct effect (positive or negative) on the activity of TYMV RdRp. There is no evidence that the TYMV RdRp complex includes eEF1A as a subunit in analogy with Qβ

replicase (Joshi et al., 1986; Pulikowska et al., 1988). We consider repression to occur by simple steric interference, in direct relation to the proportion of template molecules bound by eEF1A•GTP. Repression of minus strand synthesis templated by valyl-TY83 RNA, which binds eEF1A•GTP with a K_d of 2 nM, occurred at lower concentrations of eEF1A•GTP than were needed to repress synthesis templated by EMV TLS RNA ($K_d =$ 57 nM)(Fig. 4.4). eEF1A•GTP would appear to be a highly effective choice as a repressor in vivo because of its high affinity for valyl-TYMV RNA, abundance in the cell, and binding contact directly with the 3′ CCA terminus (Nissen et al., 1995; Dreher et al., 1999) that serves as the site of minus strand initiation (Singh and Dreher, 1997).

Minus strand repression was confirmed with a number of other aminoacylated RNA templates, both viral and non-viral, that included four amino acid specificities other than valine (Figs. 4.3B and 5). In each case, the residual signal produced by the RdRp in the presence of eEF1A•GTP can be explained by the presence of some non-aminoacylated template that we have not been able to avoid. Taking this background signal into account, eEF1A•GTP is seen to be a potent repressor of minus strand synthesis upon binding to aminoacylated templates.

Interestingly, the addition of an amino acid to the 3′ CCA terminus of templates was itself found to inhibit minus strand synthesis by TYMV RdRp (Figs. 4.3 and 4.5). Because eEF1A•GTP activity is not detectable in our RdRp preparations, this effect is unrelated to eEF1A•GTP repression. Perhaps the presence of the amino acid close to the site of initiation interferes with proper loading of the template into the initiation pocket of the RdRp. Amino acids with widely differing sidechains (alanine, valine, methionine, histidine, phenylalanine) resulted in roughly similar inhibition (2 to 4-fold).

A repressed state of minus strand synthesis can clearly only exist transiently during the viral infection. It might conceivably occur initially before sufficient viral RdRp has been produced by translation of the inoculum RNA, or it might occur late to produce a switch from minus strand to plus strand synthesis as has been observed for some viruses (e.g., Ishikawa et al., 1991). The former scenario is the more attractive, since it seems unlikely that early eEF1A•GTP interaction can be avoided and unlikely that eEF1A•GTP levels,

access to viral RNA or affinity for viral RNA would increase sufficiently during infection so as to substantially increase the binding to aminoacylated viral RNA. Further, we have seen no evidence that minus strand synthesis ceases earlier than plus strand synthesis during TYMV infections in protoplasts (B. Bradel and T. Dreher, unpublished). In response to the efficiency of valylation and eEF1A•GTP binding, we expect that inoculum RNAs released into the cytoplasm become rapidly valylated and incorporated into ternary complexes with eEF1A•GTP. eEF1A•GTP binding is then likely to persist until viral gene expression has proceeded to the point when sufficient TYMV RdRp complexes exist to compete with eEF1A•GTP for access to the 3′-end or when genomic RNAs have been recruited to the vesicular sites of viral replication (Prod'homme et al., 2001; Schwartz et al., 2002) that are likely to be free of competing eEF1A•GTP. Together with the expected absence of valyl-tRNA synthetase from the replication vesicles, viral RNAs would rapidly become deacylated and fully active as templates.

Supported by the results reported here, we propose that before the onset of viral RNA replication, TYMV RNA exists in a state that is repressed for involvement in replication because of eEF1A•GTP binding. This same state appears to be necessary for maximal translational gene expression, since we demonstrate in the accompanying paper (Matsuda and Dreher, 2004) that the TYMV TLS serves as a translational enhancer in cells and that this enhancement requires aminoacylation and probably eEF1A•GTP interaction. The presence and absence of eEF1A•GTP bound to the TLS may act as a switch between the dual roles of the viral RNA in translation and replication, ensuring that these processes are coordinated to act sequentially rather than simultaneously on an RNA molecule.

The repression of minus strand synthesis may be a common strategy for positive strand RNA viruses to prevent premature initiation of RNA replication before adequate gene expression has occurred. In the case of *Alfalfa mosaic virus*, the viral coat protein binds to the 3′-terminal region of the genomic RNA and inhibits minus strand synthesis in vitro by the viral RdRp (Houwing and Jaspars, 1986; Olsthoorn et al., 1999). Coat protein must be available for binding to the viral 3′-termini in order to initiate an infection, and this interaction seems to be necessary for enhanced translation (Neeleman

et al., 2001). This regulation is analogous to the situation we have described for TYMV, with 3′-binding and dissociation by coat protein instead of eEF1A•GTP effecting a simultaneous switch between translation and replication (Bol, 2003). For other viruses, the default structure of the viral RNA includes an inherently inaccessible base-paired 3′-end, which may serve to delay the onset of replication until a conformational change, perhaps triggered by interaction with viral replication proteins, makes the 3′-end available for replication (Koev et al., 2002). Minus strand repression could also be a feature of the replication scheme of double-stranded RNA viruses, where mRNAs transcribed at the beginning of the infection are used as templates for the production of double-stranded genomes after their initial role in translation. Rotavirus NSP3 protein has been shown to enhance translation by binding the 3′ terminal nucleotides (Piron et al., 1998), which are also required for minus strand initiation (Chen et al., 2001a). Subject to whether NSP3 exists in the subcellular compartment where RNA synthesis is occurring (Chen et al., 2001a), it has been suggested that NSP3 could interfere with minus strand synthesis (Deo et al., 2002) in a repression like that we have observed with eEF1A•GTP and TYMV RNA.

4.5   Materials and methods

4.5.1   Template preparation for negative strand synthesis

T7 transcriptional templates for making TY83, TY-Met-TLS, *Escherichia coli* tRNA^{His} and EMV-TLS RNAs were generated by PCR using reverse primers containing nucleotides modified with 2′-O-methyl groups at the two 5′-most positions in order to minimize non-templated 3′ nucleotide addition by T7 RNA polymerase (Kao et al., 1999). TY-Met-TLS RNA corresponds to TY-U55/C54/A53(L1=UU) RNA described by Dreher et al. (1996). *E. coli* tRNA^{Ala} and yeast tRNA^{Phe} were transcribed from *Bst*NI-linearized pCA0 and pYF0, respectively (Pleiss and Uhlenbeck, 2001). RNAs were transcribed with T7 RNA polymerase and purified through 6% denaturing PAGE as described (Tretheway et al., 2001). Final RNA concentrations were determined by spectrophotometry.

4.5.2 Aminoacylation of RNA transcripts

RNA transcripts were charged under the following conditions using purified phenylalanyl- and histidyl-tRNA synthetase from yeast and alanyl-tRNA synthetase from *E. coli*, or valyl- or methionyl-tRNA synthetase activities present in a partially purified wheat germ extract (Dreher et al., 1992). Valylation was performed in 25 mM Tris-HCl (pH 8.0), 2 mM $MgCl_2$, 1mM ATP, 0.1 mM spermine and 50 μM valine (30°C for 30 min); phenylalanylation in 10 mM HEPES (pH 7.5), 15 mM $MgCl_2$, 25 mM KCl, 2 mM ATP, 4 mM DTT and 10 μM phenylalanine (37°C for 15 min); methionylation in 25 mM Tris-HCl (pH 8.5), 7.5 mM $MgCl_2$, 0.5 mM ATP, 1mM DTT and 40 μM methionine (30°C for 30 min); alanylation in 30 mM HEPES-KOH (pH 7.5), 30 mM KCl, 15 mM $MgCl_2$, 2 mM ATP, 4 mM DTT and 25 μM alanine (30 °C for 30 min); histidylation in 60 mM Tris-HCl (pH 7.5), 10 mM $MgCl_2$, 30 mM KCl, 2.5 mM ATP, 5 mM DTT and 15 μM histidine (30°C for 45 min).

Aminoacylation reactions were terminated with SDS and EDTA, followed by acidification with excess sodium acetate (pH 5.2) to reduce deacylation. Following phenol extraction and ethanol precipitation, RNAs were redissolved in 0.1 M sodium acetate (pH 5.2) containing 8 M urea, and were preparatively separated by electrophoresis (4°C for 9 hrs) on 6.5% polyacrylamide gels (19:1 acrylamide: bisacrylamide) containing 8 M urea in 0.1 M sodium acetate (pH 5.2) (Varshney et al., 1991). These acid-urea gels permitted assessment of the extent of aminoacylation (see Fig. 4.2). RNAs were visualized by staining with methylene blue in 0.1 M sodium acetate (pH 5.2) at 4°C. Bands of interest were excised, eluted in 30 mM sodium acetate (pH 5.2) containing 0.1% SDS and 1 mM EDTA at 4°C with constant shaking for 8 hrs, and recovered by ethanol precipitation. The aminoacylated RNAs were redissolved in 5 mM NaOAc (pH 5.2) and stored in aliquots at -80°C. The integrity and concentration of all RNAs were determined by comparison with a standard curve prepared by running a series of appropriate RNAs with known concentrations on 6% denaturing PAGE and staining with methylene blue.

Valine was intentionally deacylated from [³H]valyl-TY83 RNA by incubation in 50 mM Tris-HCl (pH 9.0), 0.1% SDS, 1 mM EDTA at 37°C for 10 hours, before recovery by ethanol precipitation. Deacylation was monitored by counting TCA-precipitable [³H]valine.

4.5.3 Minus strand synthesis assays with TYMV RdRp

Partially purified TYMV RdRp was prepared from TYMV-infected Chinese cabbage and treated with micrococcal nuclease as described (Singh and Dreher, 1997) to remove endogenous RNAs. Minus strand synthesis assays (25 μl) contained 21.5 μl of treated RdRp in final conditions of 40 mM Tris-HCl (pH 8.0), 8 mM KCl, 10 mM MgCl₂, 0.4% Lubrol PX (Sigma), 0.5 mM ATP, UTP and GTP, 1 μM [α-³²P]CTP (400 Ci/mmol), 10 mM DTT, 1 μg actinomycin D and 10U of ribonuclease inhibitor (RNasin, Promega). In addition, reactions contained template RNAs (e.g., RNA, RNA + eEF1A•GTP, valyl-RNA, deacylated valyl-RNA, or valyl-RNA + eEF1A•GTP) that had been added in 2.5 μl of EF buffer (see below).

To limit transcription to one round per template, reactions were initiated by incubation at 14°C for 3 min in the absence of ATP. After addition of ATP and polyethylene sulfonate (PES, Aldrich) (20 μg in 1 μl), incubation was continued at 30°C for 12 min.

Reactions were stopped by two phenol/chloroform extractions and products were recovered by ethanol precipitation. Products were analyzed by 12% native PAGE as described (Singh and Dreher, 1997), including treatment with ribonuclease in high salt to verify the synthesis of complementary strand RNA. The radiolabeled products were visualized by phosphorimagery (Molecular Dynamics).

4.5.4 Preincubation of templates with eEF1A•GTP and determination of ternary complexes by ribonuclease protection assay

Purified wheat germ eEF1A (Dreher et al., 1999) was activated by incubation with 40 μM GTP in EF buffer [40 mM HEPES (pH 7.5), 100 mM NH₄Cl, 10 mM MgCl₂, 1 mM DTT and 25% (v/v) glycerol] at 30°C for 20 min. Wheat germ eEF1A•GTP (typically 10

pmol in 1.25 μl for each RdRp reaction) was added to the same volume of RNA template in EF buffer containing 40 μM GTP, and incubated on ice for 15 min before adding to 22.5 μl of TYMV RdRp reaction mixture.

To assess ternary complex formation between eEF1A•GTP and aminoacylated RNA under the RdRp reaction conditions, RNase protection assays (Dreher et al., 1999) were performed with valyl-TY83 RNA in complete 25 μl TYMV RdRp reactions, except that [α-^{32}P]CTP was omitted.

4.6 Acknowledgments

4.7 References

Ahlquist, P. (2002) RNA-dependent RNA polymerases, viruses, and RNA silencing. *Science*, **296**, 1270-1273.

Barrera, I., Schuppli, D., Sogo, J.M. and Weber, H. (1993) Different mechanisms of recognition of bacteriophage Q beta plus and minus strand RNAs by Q beta replicase. *J Mol Biol*, **232**, 512-521.

Barton, D.J., Morasco, B.J. and Flanegan, J.B. (1999) Translating ribosomes inhibit poliovirus negative-strand RNA synthesis. *J Virol*, **73**, 10104-10112.

Barton, D.J., O'Donnell, B.J. and Flanegan, J.B. (2001) 5' cloverleaf in poliovirus RNA is a cis-acting replication element required for negative-strand synthesis. *EMBO J*, **20**, 1439-1448.

Blumenthal, T. and Carmichael, G.G. (1979) RNA replication: function and structure of Q beta-replicase. *Annu Rev Biochem*, **48**, 525-548.

Bol, J. (2003) *Alfalfa mosaic virus*: coat protein-dependent initiation of infection. *Molecular Plant Pathology*, **4**, 1-8.

Chen, D., Barros, M., Spencer, E. and Patton, J.T. (2001a) Features of the 3'-consensus sequence of rotavirus mRNAs critical to minus strand synthesis. *Virology*, **282**, 221-229.

Chen, J., Noueiry, A. and Ahlquist, P. (2001b) Brome mosaic virus Protein 1a recruits viral RNA2 to RNA replication through a 5' proximal RNA2 signal. *J Virol*, **75**, 3207-3219.

de Smit, M.H., Gultyaev, A.P., Hilge, M., Bink, H.H., Barends, S., Kraal, B. and Pleij, C.W. (2002) Structural variation and functional importance of a D-loop-T-loop interaction in valine-accepting tRNA-like structures of plant viral RNAs. *Nucleic Acids Res*, **30**, 4232-4240.

Deiman, B.A., Koenen, A.K., Verlaan, P.W. and Pleij, C.W. (1998) Minimal template requirements for initiation of minus-strand synthesis in vitro by the RNA-dependent RNA polymerase of turnip yellow mosaic virus. *J Virol*, **72**, 3965-3972.

Deo, R.C., Groft, C.M., Rajashankar, K.R. and Burley, S.K. (2002) Recognition of the rotavirus mRNA 3' consensus by an asymmetric NSP3 homodimer. *Cell*, **108**, 71-81.

Dreher, T.W., Tsai, C.H., Florentz, C. and Giegé, R. (1992) Specific valylation of turnip yellow mosaic virus RNA by wheat germ valyl-tRNA synthetase determined by three anticodon loop nucleotides. *Biochemistry*, **31**, 9183-9189.

Dreher, T.W., Tsai, C.H. and Skuzeski, J.M. (1996) Aminoacylation identity switch of turnip yellow mosaic virus RNA from valine to methionine results in an infectious virus. *Proc Natl Acad Sci U S A*, **93**, 12212-12216.

Dreher, T.W. and Goodwin, J.B. (1998) Transfer RNA mimicry among tymoviral genomic RNAs ranges from highly efficient to vestigial. *Nucleic Acids Res*, **26**, 4356-4364.

Dreher, T.W. (1999) Functions of the 3'-untranslated regions of positive strand RNA viral genomes. *Annu Rev Phytopathol*, **37**, 151-174.

Dreher, T.W., Uhlenbeck, O.C. and Browning, K. (1999) Quantitative assessment of EF-1a-GTP binding to aminoacyl-tRNA, aminoacyl-viral RNA and tRNA shows close correspondence to the RNA binding properties of EF-Tu. *J. Biol. Chem.*, **274**, 666-672.

Filichkin, S.A., Bransom, K.L., Goodwin, J.B. and Dreher, T.W. (2000) The infectivities of turnip yellow mosaic virus genomes with altered tRNA mimicry are not dependent on compensating mutations in the viral replication protein. *J Virol*, **74**, 8368-8375.

Gamarnik, A. and Andino, R. (1998) Switch from translation to RNA replication in a positive-stranded RNA virus. *Genes and Development*, **12**, 2293-2304.

Goodwin, J.B., Skuzeski, J.M. and Dreher, T.W. (1997) Characterization of chimeric turnip yellow mosaic virus genomes that are infectious in the absence of aminoacylation. *Virology*, **230**, 113-124.

Hall, T.C. (1979) Transfer RNA-like structures in viral genomes. *Int Rev Cytol*, **60**, 1-26.

Hentzen, D., Mandel, P. and Garel, J.P. (1972) Relation between aminoacyl-tRNA stability and the fixed amino acid. *Biochim Biophys Acta*, **281**, 228-232.

Houwing, C.J. and Jaspars, E.M.J. (1986) Coat protein blocks the in vitro transcription of the virion RNAs of alfalfa mosaic virus. *FEBS Letters*, **209**, 284-288.

Ishikawa, M., Meshi, T., Ohno, T. and Okada, Y. (1991) Specific cessation of minus-strand RNA accumulation at an early stage of tobacco mosaic virus infection. *J Virol*, **65**, 861-868.

Jacobs, B.L. and Langland, J.O. (1996) When two strands are better than one: the mediators and modulators of the cellular responses to double-stranded RNA. *Virology*, **219**, 339-349.

Joshi, R.L., Ravel, J.M. and Haenni, A.L. (1986) Interaction of turnip yellow mosaic virus Val-RNA with eukaryotic elongation factor EF-1α. Search for a function. *EMBO J*, **5**, 1143-1148.

Kao, C., Zheng, M. and Rudisser, S. (1999) A simple and efficient method to reduce nontemplated nucleotide addition at the 3 terminus of RNAs transcribed by T7 RNA polymerase. *RNA*, **5**, 1268-1272.

Koev, G., Liu, S., Beckett, R. and Miller, W.A. (2002) The 3prime prime or minute-terminal structure required for replication of Barley yellow dwarf virus RNA contains an embedded 3prime prime or minute end. *Virology*, **292**, 114-126.

Kolakofsky, D. and Weissmann, C. (1971a) Possible mechanism for transition of viral RNA from polysome to replication complex. *Nat New Biol*, **231**, 42-46.

Kolakofsky, D. and Weissmann, C. (1971b) Qβ replicase as repressor of Qβ RNA-directed protein synthesis. *Biochim Biophys Acta*, **246**, 596-599.

Matsuda, D. and Dreher, T.W. (2004) The tRNA-like structure of *Turnip yellow mosaic virus* RNA is a 3′-translational enhancer. *Virology* **in press**.

Neeleman, L., Olsthoorn, R.C., Linthorst, H.J. and Bol, J.F. (2001) Translation of a nonpolyadenylated viral RNA is enhanced by binding of viral coat protein or polyadenylation of the RNA. *Proc Natl Acad Sci U S A*, **98**, 14286-14291.

Nissen, P., Kjeldgaard, M., Thirup, S., Polekhina, G., Reshetnikova, L., Clark, B.F. and Nyborg, J. (1995) Crystal structure of the ternary complex of Phe-tRNA[Phe], EF-Tu, and a GTP analog. *Science*, **270**, 1464-1472.

Olsthoorn, R.C., Mertens, S., Brederode, F.T. and Bol, J.F. (1999) A conformational switch at the 3' end of a plant virus RNA regulates viral replication. *EMBO J*, **18**, 4856-4864.

Piron, M., Vende, P., Cohen, J. and Poncet, D. (1998) Rotavirus RNA-binding protein NSP3 interacts with eIF4GI and evicts the poly(A) binding protein from eIF4F. *EMBO J*, **17**, 5811-5821.

Pleiss, J.A. and Uhlenbeck, O.C. (2001) Identification of thermodynamically relevant interactions between EF-Tu and backbone elements of tRNA. *J Mol Biol*, **308**, 895-905.

Prod'homme, D., Le Panse, S., Drugeon, G. and Jupin, I. (2001) Detection and subcellular localization of the turnip yellow mosaic virus 66K replication protein in infected cells. *Virology*, **281**, 88-101.

Pulikowska, J., Wojtaszek, P., Korcz, A., Michalski, Z., Candresse, T. and Twardowski, T. (1988) Immunochemical properties of elongation factors 1 of plant origin. *Eur J Biochem*, **171**, 131-136.

Rietveld, K., Van Poelgeest, R., Pleij, C.W., Van Boom, J.H. and Bosch, L. (1982) The tRNA-like structure at the 3' terminus of turnip yellow mosaic virus RNA. Differences and similarities with canonical tRNA. *Nucleic Acids Res*, **10**, 1929-1946.

Schwartz, M., Chen, J., Janda, M., Sullivan, M., den Boon, J. and Ahlquist, P. (2002) A positive-strand RNA virus replication complex parallels form and function of retrovirus capsids. *Mol Cell*, **9**, 505-514.

Singh, R.N. and Dreher, T.W. (1997) Turnip yellow mosaic virus RNA-dependent RNA polymerase: initiation of minus strand synthesis in vitro. *Virology*, **233**, 430-439.

Singh, R.N. and Dreher, T.W. (1998) Specific site selection in RNA resulting from a combination of nonspecific secondary structure and -CCR- boxes: initiation of minus strand synthesis by turnip yellow mosaic virus RNA-dependent RNA polymerase. *RNA*, **4**, 1083-1095.

Tretheway, D.M., Yoshinari, S. and Dreher, T.W. (2001) Autonomous role of 3'-terminal CCCA in directing transcription of RNAs by Qβ replicase. *J Virol*, **75**, 11373-11383.

Tsai, C.H. and Dreher, T.W. (1991a) Turnip yellow mosaic virus RNAs with anticodon loop substitutions that result in decreased valylation fail to replicate efficiently. *J Virol*, **65**, 3060-3067.

Tsai, C.H. and Dreher, T.W. (1991b) Turnip yellow mosaic virus RNAs with anticodon loop substitutions that result in decreased valylation fail to replicate efficiently. *J Virol*, **65**, 3060-3067.

Uhlenbeck, O.C. (1995) Keeping RNA happy. *RNA*, **1**, 4-6.

van Duin, J. (1988) Single-stranded RNA bacteriophages. In: The Bacteriophages, Vol 1, ed. R. Calendar, Plenum Press, NY, pp. 117-166.

Varshney, U., Lee, C.P. and RajBhandary, U.L. (1991) Direct analysis of aminoacylation levels of tRNAs in vivo. Application to studying recognition of *Escherichia coli* initiator tRNA mutants by glutaminyl-tRNA synthetase. *J Biol Chem*, **266**, 24712-24718.

Chapter 5 The Valine Anticodon and Valylatability of *Peanut Clump Virus* RNAs are Not Essential but Provide a Modest Competitive Advantage in Plants

Daiki Matsuda, Patrice Dunoyer, Odile Hemmer, Christiane Fritsch and Theo W. Dreher

5.1   Abstract

The role of valine aminoacylation of the two genomic RNAs of *Peanut clump virus* (PCV) was studied by comparing the amplification *in vivo* of RNAs with GAC, GΔC or CCA anticodons in the tRNA-like structure (TLS) present at the 3´-end of each viral RNA. The PCV RNA1 TLS of isolate PCV2 possesses a GAC anticodon and is capable of highly efficient valylation, whereas the RNA2 TLS has a GΔC anticodon that does not support valylation. The presence in RNA1 of GΔC or CCA anticodons that conferred non-valylatability resulted in about 2 to 3-fold and 12 to 25-fold reduction, respectively, in RNA accumulations in tobacco BY-2 protoplasts inoculated with the RNA1 variants together with wild type RNA2(GΔC). No differences in RNA levels were observed among protoplasts inoculated with the three variant RNA2s in the presence of wild type RNA1(GAC). All combinations of valylatable and non-valylatable RNAs 1 and 2 were similarly infectious in *Nicotiana benthamiana* plants, and viral RNAs accumulated to similar levels; all input TLS sequences were present unchanged in apical leaves. In direct competition experiments in *N.benthamiana* plants, however, both RNA1 and RNA2 with GAC valylatable anticodons outcompeted the non-valylatable variants. We conclude that valylation provides a small but significant replicational advantage to both PCV RNAs. Sequence analysis of the TLS from RNA2 of a second PCV isolate, PO2A, revealed the presence of an intact GAC valine anticodon, suggesting that the differential valylation of the genomic RNAs of isolate PCV2 is not a general characteristic of PCV.

5.2   Introduction

The recent sequencing of the genomes of several fungus-transmitted rod-shaped viruses (furo- and furo-like viruses) has revealed members of the *Pecluvirus, Furovirus* and *Pomovirus* genera to possess genomic RNAs with a tRNA-like structure (TLS) at the 3´-end of the 3´-untranslated region (Goodwin and Dreher, 1998) (Shirako and Wilson, 1999). All of these TLSs can be specifically and efficiently aminoacylated with valine,

and thus are functionally related in their *in vitro* properties to the TLSs of tymoviruses (Goodwin and Dreher, 1998). The TLSs of the furoviruses and pomoviruses are indeed closely related in structure to the TLSs of *Turnip yellow mosaic virus* (TYMV) and other tymoviruses, while the TLSs of *Peanut clump* and *Indian peanut clump* pecluviral RNAs have a 42 nucleotide insert between the aminoacyl acceptor/TΨ and anticodon/D halves of a TYMV-like TLS (Fig. 5.1; Goodwin, 1998). A unique aspect of the TLSs of the two PCV genomic RNAs is the association of a valine anticodon and efficient valine acceptance with the TLS of RNA1, but the absence of both from the TLS of RNA2 due to a single nucleotide deletion (Fig. 5.1; Manohar et al., 1993; Goodwin and Dreher, 1998). Such differential aminoacylation properties have not been previously described for a plant virus, and suggested the existence of RNA component-specific regulation of some aspect of the virus replication cycle in a way that is sensitive to the aminoacylation status of the RNA.

Apart from the tymoviruses and furo-like viruses mentioned above, aminoacylatable TLSs are also found in the genomes of bromoviruses, cucumoviruses, hordeiviruses and tobamoviruses (Mans, Pleij, and Bosch, 1991). The functions of TLSs in viral biology have been studied in the TYMV and *Brome mosaic virus* (BMV) systems, by studying the effects of mutations that decrease or effectively abolish the aminoacylation capacity of the viral RNA. Point mutations in the CAC valine anticodon of the genomic RNA of TYMV (a monopartite virus) resulted in parallel losses of *in vitro* valine binding and replication in protoplasts (Tsai and Dreher, 1991). Because valine identity is strongly centered on the middle and 3´ anticodon nucleotides (Dreher et al., 1992), single or double mutations at these positions decrease valine charging to background levels. Such mutant genomic RNAs are non-infectious to Chinese cabbage plants, and replicate to trace levels (≤0.2% of wild type) in protoplasts (Tsai and Dreher, 1991), demonstrating the importance of an intact valine anticodon. Conversion of aminoacylation identity from valine to methionine, in part by mutation of the anticodon, further demonstrated that efficient aminoacylation rather than the presence of a valine anticodon is required for infectivity and amplification in protoplasts (Dreher, Tsai, and

Skuzeski, 1996). Although we have founds means to circumvent the requirement for aminoacylation with chimeric TYMV genomes bearing heterologous 3´-termini (Goodin et al., 1997; Filichkin et al., 2000), wild type TYMV RNA clearly has a strong requirement for efficient aminoacylation.
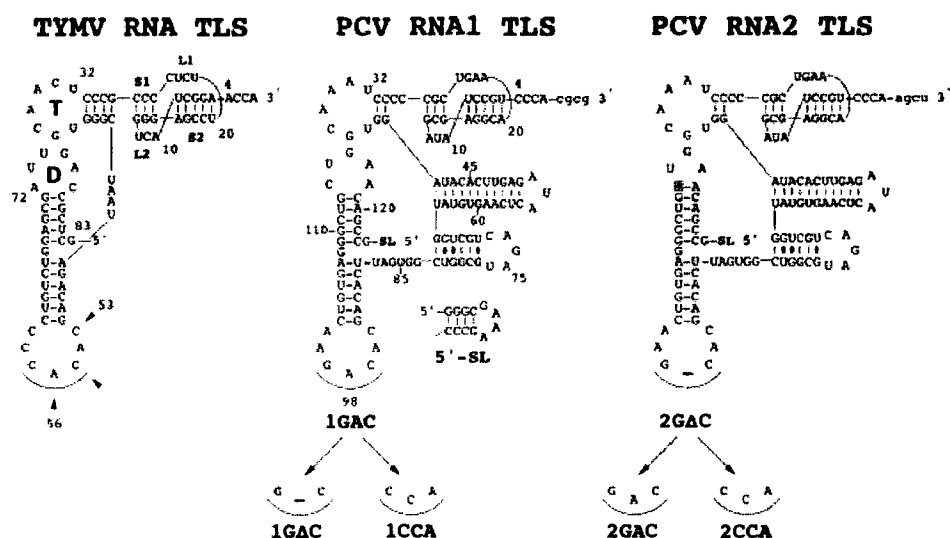
Fig. 5.1 Sequences and proposed secondary structures of TYMV and PCV TLSs. The main structural features of the TLSs are depicted on the TYMV structure: T and D loops analogous to those of tRNAs, the acceptor/T arm pseudoknot indicated by helical segments S1 and S2 and connecting loops L1 and L2, and the major valine identity nucleotides (arrowheads) in the anticodon loop (anticodon underlined), which are recognized by valyl-tRNA synthetase. The nucleotide in reverse shading in the PCV RNA2 TLS is one of the two nucleotides that differ from the PCV RNA1 TLS sequence. The other difference, a single nucleotide deletion in the anticodon of PCV RNA2, is shown with a dash. The stem/loop (5´-SL) structure shown beside the PCV RNA1 TLS is present at the 5´ end of the PCV RNA1 and 2 TLS RNAs used for *in vitro* valylation assays, and is represented by "SL" in each structure. Nucleotides shown in lower case at the 3´ ends of the PCV RNA 1 and 2 TLSs are of non-viral origin, derived from the *Mlu*I and *Hind*III linearization, respectively, of plasmid templates used to make the infectious transcripts used in *in vivo* replication experiments. Those nucleotides are not present in the SLTLS transcripts used for valylation assays. During plant cell inoculation, the additional nucleotides are thought to be removed by exonuclease action and repair of the 3´-CCA by CCA nucleotidyltransferase, or by internal initiation during minus strand synthesis. The mutations introduced into the RNA1 and RNA2 anticodons are indicated below the structures. TLS nucleotides are numbered from the 3´ A of the viral sequences.

Experiments with BMV, whose three genomic RNAs have near-identical TLSs that accept tyrosine, have also utilized mutations designed to specifically decrease the RNA's aminoacylation efficiency (Dreher and Hall, 1988). However, since the tyrosine identity elements within the BMV TLS have not been mapped, strong point mutations of the type used with TYMV RNA were not available and the role of aminoacylation has not been so clearly identified. The presence of aminoacylation mutations on RNA3, which does not encode essential replication proteins, has little if any influence on RNA amplification (Dreher, Rao, and Hall, 1989; Rao and Hall, 1991). On the other hand, marked decreases in viral RNA amplification in protoplasts result when these mutations are present on RNA1 (A.L.N. Rao, pers. commun.; Duggal, 1994 #769} or RNA2 }(Rao and Hall, 1991), which encode essential RNA replication proteins. These observations suggest that the role of aminoacylation in a multipartite virus can differ among the genomic RNAs. This could be a consequence of the increased debilitation of a replication defect in an RNA component that itself encodes an essential replication protein (an RNA replicated *in cis*) compared to the same defect in an RNA not encoding an essential protein (an RNA replicated *in trans*).

Peanut clump virus (PCV) was chosen as an excellent system for further studying the role of aminoacylation in a multipartite virus, with likely differential effects of aminoacylation on RNAs replicated *in cis* and *in trans*. Because of the similarity of the PCV TLS to that from TYMV, strong point mutations with known effects on valylation were available. A differential role for aminoacylation of RNA1 and RNA2 in the bipartite PCV genome was suggested by the existence of an intact GAC valine anticodon in RNA1 (Herzog et al., 1994) but an incomplete GΔC anticodon in RNA2 (Fig. 5.1) (Manohar et al., 1993). The PCV RNA1 TLS can be valylated as efficiently as the TYMV TLS and tRNAVal, but virtually no valylation was detected for the RNA2 TLS(Goodwin and Dreher, 1998). PCV RNA1 (5897 nt) encodes all the essential viral replication proteins and is able to replicate independently in protoplasts (Herzog et al., 1998). PCV RNA2 (4503 nt) encodes proteins involved in viral spread through the plant and probably in fungus transmission (Herzog et al., 1998).

In order to address the role of valylation in the bipartite genome of PCV, we have compared the amplification of viral RNAs in protoplasts and plants after inoculation with valylation-proficient and -deficient variants of both genomic RNAs. We find that valylatability is not essential for infectivity, although valylatable RNAs 1 and 2 are able to outcompete non-valylatable RNAs during virus amplification in plants. These results differ sharply from the effects of similar mutations in TYMV. Our results also indicate that the differential valylatability of PCV RNAs 1 and 2 does not serve a critical regulatory function in plants and is not characteristic of all *Pecluvirus* isolates.

5.3   Materials and methods

5.3.1   Preparation of wild type and mutant genomic RNAs.

A 380 bp fragment containing the 3´-TLS of PCV RNA1 was subcloned from pPC1, which contains full-length infectious RNA1 sequences (Herzog et al., 1998), into the phagemid pLITMUS39 (New England Biolabs) using *Nhe*I and *Mlu*I restriction enzymes. The corresponding 358 bp RNA2 fragment from pPC2 (Herzog et al., 1998) was subcloned using *Spe*I and *Hind*III. Single-stranded dU-containing encapsidated DNA was prepared using M13K07 helper phage, and oligonucleotide-directed mutagenesis was performed as described (Kunkel, Roberts, and Zakour, 1987). The following mutagenic deoxy oligomers, with anticodon sequences underlined, were used (note that the RNA1 and RNA2 sequences were cloned in opposite orientations): AAGTGTCGT<u>GC</u>TTGACACTCCCGA and AAGTGTCGT<u>TGG</u>TTGACACTCCCGA for mutation of the RNA1 TLS to GAC and CCA anticodons, respectively; GAGTGTCAA<u>GAC</u>ACGACACTTAGTGGCT and GAGTGTCAA<u>CCA</u>ACGACACTTAGTGGCT for mutation of the RNA2 TLS to GAC and CCA anticodons, respectively. After sequencing the entire subcloned fragments, each mutated sequence was returned to the full-length genomic clones using the restriction sites mentioned above.

After linearization of pPC1 and its derivatives with *Mlu*I, and pPC2 and its derivatives with *Hind*III, 5´-capped genomic transcripts were made using T7 RNA polymerase (Herzog et al., 1998).

5.3.2 Aminoacylation analysis.

To test the valine acceptance after mutation of the anticodon, 136/135 nt long RNAs comprising the TLS adjacent to a heterologous stem/loop (PCV1-SLTLS and PCV2-SLTLS and their variants; Fig. 5.1) were prepared by T7 transcription from PCR generated template DNA as described (Goodwin and Dreher, 1998). Valine acceptance was assessed by incubation with partially purifed wheat germ valyl-tRNA synthetase in TM buffer [25 mM Tris HCl (pH 8.0), 2 mM $MgCl_2$, 1 mM ATP, 0.1 mM spermidine] and 10 μM [3H]valine at 30°C (Goodwin and Dreher, 1998).

5.3.3 Inoculation and analysis of protoplasts and plants.

Protoplasts were prepared from *Nicotiana tabacum* suspension cell line BY-2 (Koiwai, Noguchi, and Tamaki, 1971), and 1x106 protoplasts were inoculated by electroporation with 5 μg each of capped RNA1 and RNA2 transcripts as described (Herzog et al., 1998). Total nucleic acids were extracted 48 h post inoculation.

Nicotiana benthamiana plants were grown to 2-3 fully expanded leaves and each plant was inoculated with 200 μl containing 5 μg each of capped RNA1 and RNA2 transcripts in 5 mM sodium phosphate (pH 7.5) and 0.03 % macaloid.

At 11 days post inoculation (dpi), apical and inoculated leaves were harvested and frozen in liquid nitrogen. RNA was extracted from 200 mg of frozen, ground leaf powder. To prepare total RNA, the powder was extracted with 600 μl of ice-cold buffer A [200 mM Tris-HCl (pH 9), 400 mM KCl, 35 mM $MgCl_2$, 25 mM EGTA, and 200 mM sucrose], and the recovered RNA was extracted with phenol/chloroform and ethanol precipitated.

Positive and negative sense genomic RNAs were detected in Northern blots after electrophoresis through 1% agarose gels. The strand-specific 32P-labeled RNA probes represented the 3´-most 124 nt of RNA1 for detecting the negative strands of both RNA1 and 2, and the complementary sequence for detecting the positive strands of both RNA1 and 2. The riboprobes were made by transcription with T7 RNA polymerase from PCR-generated products. Northern blots were analyzed (Herzog et al., 1998) and quantitated with a phosphorimager (Fuji BAS1000).

5.3.4 Sequence analysis of progeny RNA isolated from infected plants.

Total RNA was extracted from 200 mg of *N. benthamiana* leaves as described above. The RNAs were 3´ polyadenylated using *E. coli* poly(A) polymerase (Gibco-BRL), and subjected to RT-PCR, using T35GG to prime reverse transcription and as the downstream PCR primer. To amplify RNA1 and RNA2 3´-sequences, the upstream primers AGCGAGAAACTCTGTTGGCT and CATAGCTTTTGCATCCTACTAC, respectively, were used. This resulted in amplification of a 436/435 bp product from RNA1 and a 373/372 bp product from RNA2. The specificity of these amplifications was verified with test template mixtures.

Gel purified PCR products were sequenced by automated fluorescent dye-terminator sequencing (Model 373, Applied Biosystems) using the primer GCGAGCCATAGAGCACGGTT for both RNA1 and RNA2 products; this oligo primes 247/246 nt from the 3´-terminus.

When analyzing RNA from plants inoculated with mixed RNA sequences, the relative amounts of the competing sequences were determined by comparing the areas of peaks in the fluorescent dye trace. For competition involving a GΔC anticodon, in which there is a 1 nt shift between the two sequences downstream of the anticodon, three or four well-isolated downstream peaks were used for area comparison. For competition between sequences with GAC and CCA anticodons, the first nucleotide of the anticodon was compared.

5.4 Results

5.4.1 Valylation mutants of PCV RNAs 1 and 2.

In order to investigate the role of valylation in PCV, mutations were introduced into the anticodons of the RNA1 and RNA2 TLSs, permitting the influence of GAC, GΔC or CCA anticodons (Fig. 5.1) to be tested for each genomic RNA. A GAC anticodon, as present in the wild type sequence of RNA1 of PCV (isolate PCV2; Herzog et al., 1994), results in highly efficient valylation. A GΔC anticodon, present in the wild type sequence of PCV RNA2 (isolate PCV2; Manohar et al., 1993), lacks the central nucleotide of the anticodon and directs virtually no valylation: the V_{max}/K_m for valylation of the PCV RNA2 TLS is 7.6x10-4 relative to that for the RNA1 TLS (Goodwin and Dreher, 1998). A CCA anticodon in the structurally related TYMV TLS results in a similar loss of valylatability (Tsai and Dreher, 1991). This anticodon sequence was chosen because of its strong effect on viral replication in the TYMV system. Inoculation of Chinese cabbage protoplasts with genomic RNA bearing a CCA anticodon led to $\leq$0.002 times the levels of coat protein accumulated after inoculation with wild type TYMV RNA, and the mutant RNA was not infectious in plants (Tsai and Dreher, 1991). Interconversion between the GAC, GΔC and CCA anticodons by mutation during plant inoculation experiments is unlikely in view of the deletion or double substitutions distinguishing these anticodons.

Before observing the effects of mutated anticodons of the RNAs *in planta*, the *in vitro* valylation properties of each mutant RNA were examined. As previously (Goodwin and Dreher, 1998), valylation was tested in the context of the short SLTLS RNAs with 3'-CCA termini shown in Fig. 5.1; these RNAs are transcribed from PCR-amplified templates and have a stable stem/loop at the 5'-end of the TLS that includes sequences conducive to T7 transcription. Both the RNA1 and RNA2 TLSs with a GAC anticodon were efficiently valylated by wheat germ valyl-tRNA synthetase (Fig. 5.2), confirming the dominant role of the anticodon in specifying valylation. The RNA2 nucleotide

substitution in the D stem/loop (Fig. 5.1) evidently does not interfere with the folding of a TLS conformation able to support efficient valylation.

None of the SLTLS RNAs with GΔC and CCA anticodons showed valylation above background (Fig. 5.2), consistent with previous experience with PCV RNA2 SLTLS (GΔC anticodon)(Goodwin and Dreher, 1998) and TYMV RNA mutants (CCA anticodon; Tsai and Dreher, 1991).

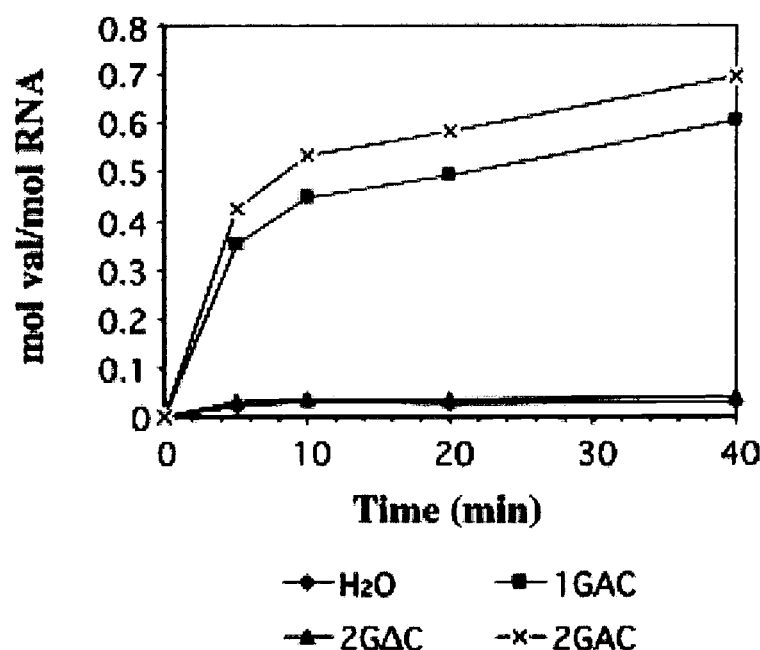**Fig. 5.2 Comparison of the *in vitro* valylation profiles of PCV RNA1 and 2 TLSs with GAC, GΔC and CCA anticodons.**
RNAs comprising the TLS and the additional 5'-stem/loop (SLTLS RNAs as shown in Fig. 1) were valylated with wheat germ valyl-tRNA synthetase in TM buffer. The valylation profiles of SLTLS RNAs 1GΔC, 1CCA and 2CCA coincided with that of the water control, and are omitted from the graph for reasons of clarity.

5.4.2 RNA accumulation in protoplasts is affected by anticodon mutations in RNA1 but not in RNA2.

BY-2 tobacco protoplasts were inoculated with all combinations of the valylatable and non-valylatable capped genomic transcripts. Since RNA1 is sufficient to replicate independently in protoplasts, replication of the RNA1 mutants was also studied without RNA2 co-inoculation. Total RNA was extracted from protoplasts 48 h post-inoculation, and RNA1 and RNA2 were detected by Northern blot hybridization using a 124 nt riboprobe complementary to the PCV TLSs. The use of a probe that hybridizes equally to both genomic RNAs enabled a direct comparison of RNA1 and RNA2 levels.

When RNA1 was inoculated alone (Fig. 5.3, lanes 1-3), or when RNAs 1 and 2 were co inoculated (Fig. 5.3, lanes 4-12), the viral RNA accumulations were determined by the anticodon sequence of RNA1, decreasing in the order GAC>GΔC>CCA. Thus, inoculations with the non valylatable RNA1 mutants resulted in lower levels of RNA accumulation as compared to those with the valylatable RNA1 (compare lanes 1, 4, 7 and 10 with the rest). Interestingly, RNA1+RNA2 inoculations including RNA 1CCA resulted in substantially lower viral RNA accumulations (14 to 24-fold reduction relative to RNA 1GAC) than inoculations including RNA 1GΔC (2.0 to 3.6 fold reduction) (Fig. 5.3, lanes 4-12). When RNA1 was inoculated alone, the non-valylatable mutants (especially RNA 1GΔC) accumulated to even lower levels relative to RNA 1GAC (Fig. 5.3, lanes 1 3). Perhaps the encapsidation function provided by RNA2 plays a role in preventing the degradation of genomic RNA, especially when the levels are sub-normal.

In contrast to the RNA1 mutations, there was no apparent influence of the RNA2 anticodon sequence on the accumulation of viral RNAs in protoplasts. Similar accumulations were observed for all three RNA1+RNA2 inoculations involving RNA 1GAC (Fig. 5.3, lanes 4, 7 and 10), RNA 1GΔC (Fig. 5.3, lanes 5, 8 and 11), or RNA 1CCA (Fig. 5.3, lanes 6, 9 and 12). Thus, the role of valylation appears to differ between RNA1 and RNA2, reminiscent of the differential effects of aminoacylation mutations in the three BMV RNAs (Duggal, Lahser, and Hall, 1994).
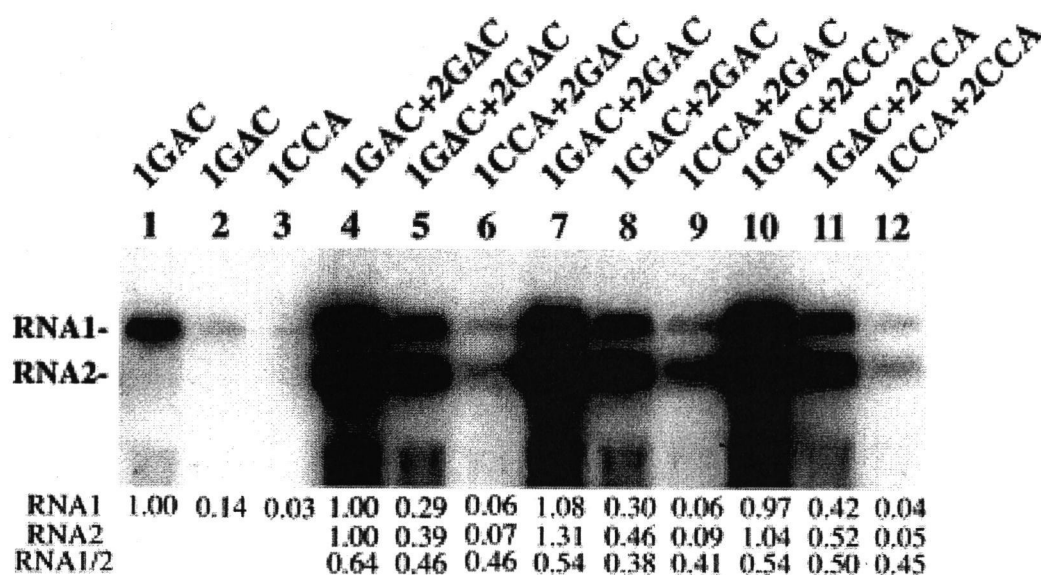
Fig. 5.3 Northern blot analysis of PCV RNAs with GAC, GΔC and CCA anticodons amplified in tobacco BY-2 protoplasts.
Protoplasts (1x106) were inoculated with the RNA1 variants or with all possible combinations of RNA1 and 2 transcripts as indicated above each lane. At 48 h.p.i., total RNAs were extracted, separated on a 1% agarose gel, and the viral RNAs were detected by Northern hybridization using a riboprobe complementary to the 3´ most 124 nt whose sequences are almost identical in RNA1 and 2. The positions of RNA 1 and 2 are indicated at left. The relative accumulations of RNA1 and RNA2, as well as the RNA1/RNA2 ratios, are shown beneath each lane (averages of 3 independent inoculations).

The ratio of RNA1 to RNA2 varied little among the permuted RNA1+RNA2 inoculations, although this ratio is up to 40% higher in infections with RNA 1GAC compared to the other RNA1 variants (Fig. 5.3, lanes 4, 7, and 10 cf. 5-6, 8-9 and 11-12). The valylatability of the PCV RNAs is clearly not an important determinant of the RNA1:RNA2 ratio. Likewise, no differences in the ratios of minus to plus strands were observed for either RNA1 or RNA2 among the various inoculations (not shown). In summary, the protoplast inoculations indicate that the valylatability of RNA1 enhances

the overall amplification of PCV RNAs in BY-2 cells, with no apparent specific effects on plus or minus RNA1 or RNA2 accumulation.

5.4.3   No effects of the anticodon mutations observed in whole plants.

Nicotiana benthamiana plants, systemic hosts for PCV, were inoculated with the same combinations of RNA1+RNA2 used above. Surprisingly in view of the protoplast results, symptoms developed at similar times (6 to 8 d.p.i.) and to similar severities in all inoculated plants. At 11 d.p.i., total RNA was extracted from apical leaves, and the viral genomic RNAs were detected by Northern blotting (Fig. 5.4). Similar levels of viral RNA were present in all plants, with at most only a slight reduction in RNA1 accumulations for infections including non-valylatable RNA1 relative to those with RNA 1GAC (Fig. 5.4, lanes 2-3, 5-6 and 8-9 cf. lanes 1, 4 and 7). No systematic differences were observed in RNA2 accumulations among the various infections. Note that, for unknown reasons, RNA1:RNA2 levels are typically lower in whole plant extracts than in protoplast extracts (Herzog et al., 1998).

To determine whether any mutations were introduced into the TLSs of the viral RNAs amplified in plants, the sequences of the 3´-terminal 234 nts (233 nts for GΔC RNAs) were derived by sequencing PCR products amplified after polyadenylation and reverse transcription. RNA1 and RNA2 sequences were specifically amplified by this procedure. All amplified RNA1 and RNA2 sequences perfectly matched the inoculated sequences, both in the anticodon and throughout the analyzed 3´-region (not shown). These results clearly demonstrate that the valylation properties do not measurably affect PCV infectivity and the amplification of viral RNAs in *N. benthamiana* plants. The reasons for the differential effects produced by inoculation of protoplasts and plants with non-valylatable RNA1 are not clear.
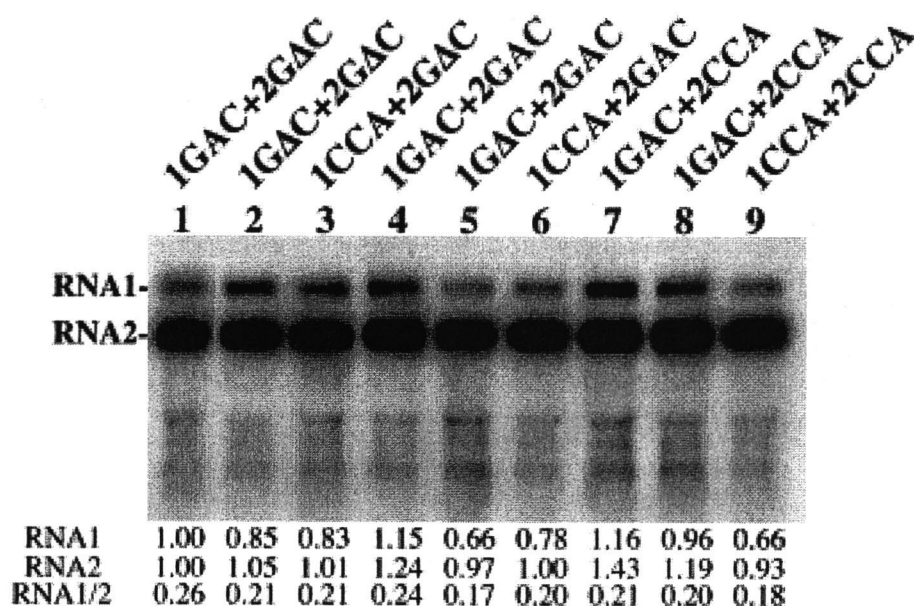
Fig. 5.4 Northern blot analysis of PCV RNAs with GAC, GΔC and CCA anticodons amplified in *N. benthamiana* plants.
The indicated RNA1+2 combinations (as in Fig. 3) were inoculated onto *N. benthamiana* plants. Total RNAs were extracted at 11 d.p.i., separated on a 1% agarose gel, and the positive strands of the viral RNA genome were detected by Northern hybridization as in Fig. 3. The positions of RNAs 1 and 2 are indicated at left. The relative accumulations of RNA1 and RNA2, as well as the RNA1/RNA2 ratios, are shown beneath each lane.

5.4.4 *Competition experiments in plants indicate an advantage for valylation of both RNA1 and RNA2.*

In order to explore further a possible role of valylation in *N. benthamiana* plants and the difference from the results obtained with protoplasts, co-inoculations involving two RNA1 or two RNA2 variants (together with the other wild type genomic RNA) were conducted, permitting direct competition between the two genotypes to occur *in planta*. At 11 d.p.i., both apical and inoculated leaves were collected separately for total RNA extraction and 3´-sequencing of RNA1 and RNA2 as described above. Mixed sequences involving the GΔC anticodon were readily evident in the fluorescent dye trace generated

by the automated sequencer, with a clear transition from a single sequence to a mixed sequence occurring at the anticodon (Fig. 5.5). By sequencing known mixtures of GAC and GΔC or CCA and GΔC DNAs in the ratios 5:1, 2:1 and 1:1, we verified that isolated nucleotides downstream of the anticodon could be used to estimate the allele ratio by determining the extent of peak splitting into a doublet; the relative peak areas of each peak in the doublet were proportional to the input GAC:GΔC ratios. Thus, three or four peaks in the fluorescence profile (Fig. 5.5), which became doublets when both 3 nt (GAC or CCA) and 2 nt (GΔC) anticodons were present, were used to estimate the ratio of alleles present in the viral RNAs extracted from the plants. The identification of mixed sequences containing GAC and CCA anticodons relied on the sequence of the anticodon triplet alone. Test mixtures verified that both alleles in a mixture with a GAC:CCA ratio (1:1) could be detected.

Analysis of the progeny from inoculations with RNAs 1GAC+1GΔC+2GΔC and RNAs 1GAC+1CCA+2GΔC revealed the valylatable RNA 1GAC to be at a competitive advantage over non-valylatable RNA1 (Table 5.1). The advantage over RNA 1GΔC was very slight, with a 1GAC/1GΔC ratio of 1.4 in inoculated leaves and 2.4 in apical leaves. The increased dominance of RNA 1GAC in apical compared with inoculated leaves suggests that true selection is occurring, rather than the 1GAC/1GΔC ratio perhaps being determined by a slight excess of RNA 1GAC in the inoculum. Marked preference for the amplification of RNA 1GAC over RNA 1CCA was observed, however, with selective amplification of RNA 1GAC in inoculated leaves and no RNA 1CCA detectable in apical leaves. In both cases, the RNA2 sequences were verified to be unchanged for the inoculated GΔC anticodon. These experiments have revealed the same GAC>GΔC >CCA ranking of amplification capacity among RNA1 variants as observed in protoplasts.

Transition starts here

120   130

3 T GT CA A [G A C] AC N AC A C T N A G N G GC T

Mixed peaks of black(G) and red(T)

Red(T) and blue(C)

T_{24} C_{19} C_{14} G_6
(1:2.2)   (1:1.9)   (1:3.0)   (1:2.4)

200   210
; N   GA AN   G G AN   GA TN T C C   T C
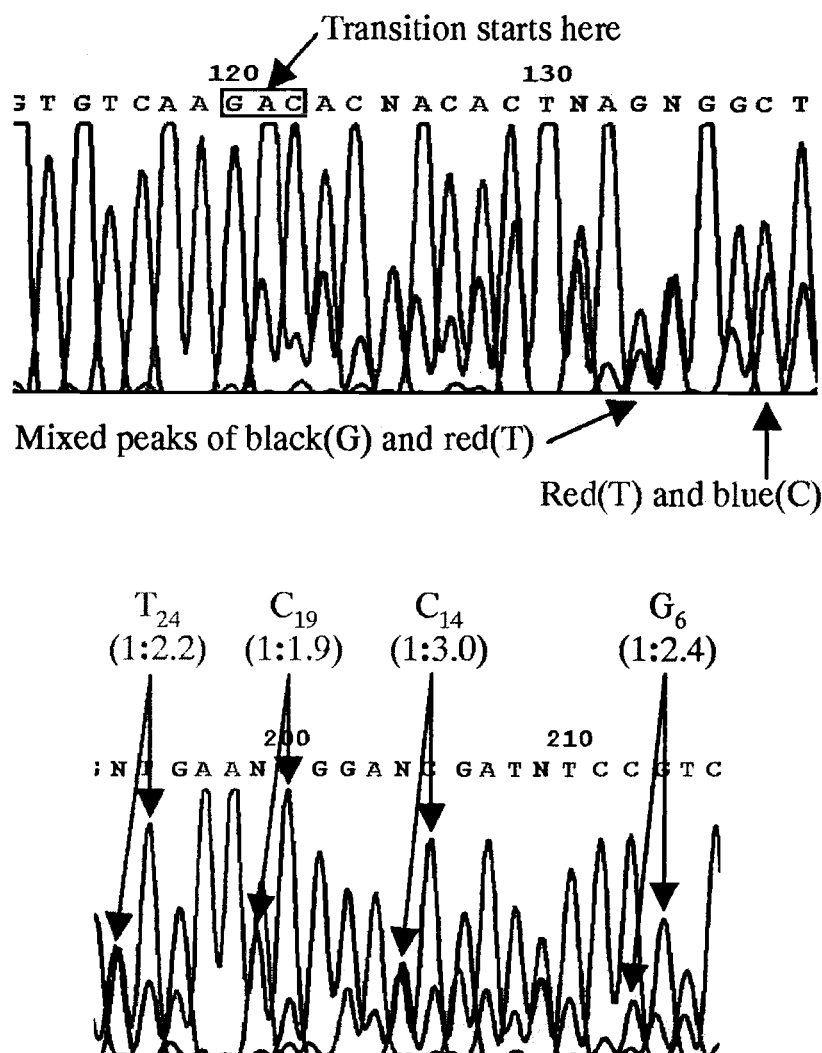
Fig. 5.5 A sequence profile of the RNA1 from apical leaves of the mixed inoculations of wild type RNA 1GAC and RNA 1GΔC.

The sequence profile was obtained from the RT-PCR products whose template RNAs had been extracted from the inoculated and apical leaves of a *N. benthamiana* plant 11 d.p.i. with an equal amount of the 5′-capped RNA 1GAC and RNA 1GΔC transcripts. No mixed nucleotide peak was observed in the profile upstream of the second nucleotide of the anticodon (boxed, upper panel), where the signal of A overlaps with that of C. The one-nucleotide-shifted peaks (examples of such red and blue doublets are indicated to the right of the upper panel) were evident throughout the remaining viral sequence. The doublet peak areas representing G6, C14, C19, and T24 shown in the lower panel (refer to Fig. 1) were measured and used to estimate the ratio of wild type to mutant RNA in the extract.

Competition between RNA 2GΔC and RNA 2GAC or RNA 2CCA (in the presence of RNA 1GAC) was also followed. RNA 2GAC was strongly favored over the wild type RNA 2GΔC, which accumulated 7 times less than RNA 2GAC in inoculated leaves and was not detected in apical leaves (Table 5.1). This result clearly indicates that RNA 2GAC has a replicative advantage over the natural RNA 2GΔC of PCV isolate PCV2. After co-inoculation of the two non-valylatable variants of RNA2 (2GΔC and 2CCA), RNA 2CCA was moderately more abundant than RNA 2GΔC in both inoculated and apical leaves (Table 1).

No mutations in the TLS outside the anticodon were observed in any of the progeny RNAs isolated from plants.

Table 5.1 Direct competition between RNA1 and RNA2 variants with different anticodon sequences in *N. benthamiana* plants[1]

RNA in Competition	Anticodon sequence		RNA ratio (WT/Mutant)	
	WT	Mutant	Inoculated leaves	Apical leaves
RNA1[2]	1GAC	1GΔC	1.4	2.4
	1GAC	1CCA	8.1	Only GAC[4]
RNA2[3]	2GΔC	2GAC	0.14	Only GAC[4]
	2GΔC	2CCA	0.70	0.45

[1] RNAs were extracted 11 d.p.i., polyadenylated and subjected to RT-PCR, amplifying the 3′-234 nts, which were sequenced by fluorescent dye terminator methodology (see Fig. 5). The ratios of anticodon sequences were determined as described in the text.
[2] The indicated variants of RNA1 were coinoculated with wild type RNA2 (GAC).
[3] The indicated variants of RNA2 were coinoculated with wild type RNA1 (GAC).
[4] The detection limit for a minor sequence is about 10% of the predominant sequence.

5.4.5 A GAC anticodon is present in the RNA2 TLS of PCV isolate PO2A.

The indication from our competition experiments that valylatability of RNA2 should be a selection criterion in the evolution and maintenance of PCV suggests that isolate PCV2 is not an optimized strain. In order to see whether RNA2 in another PCV strain has the expected GAC anticodon, we sequenced the 3′ untranslated region of RNA2 from strain PO2A (GenBank accession number AJ277545). The origin of strain PO2A has been described Manohar *et al.* (Manohar et al., 1993). The only difference from RNA2 of strain PCV2 in the 3′-200 nucleotides (i.e., including the entire TLS) is the presence in strain PO2A of a GAC instead of GΔC anticodon. This result makes it clear that there is no fundamental requirement for a GΔC anticodon in the RNA2 TLS of PCV.

5.5 Discussion

Protoplast and plant experiments with valylatable and non-valylatable PCV RNAs 1 and 2 have clearly demonstrated that the GAC valine anticodon and the capacity for efficient valylation are not essential properties for the amplification of either RNA1 or RNA2, nor for PCV infectivity in general. This result constrasts sharply with results from the TYMV system, in which the loss of valylatability through mutation of the valine anticodon — including mutation to the same CCA anticodon as studied in this paper with PCV — abrogated infectivity (Tsai and Dreher, 1991). Nevertheless, while non-valylatable PCV mutants supported efficient infections in plants (Fig. 5.4), clear replicational advantages were observed for the valylatable RNA1 (P1GAC) over the two non valylatable variants both in *N. tabacum* BY-2 protoplasts (Fig. 5.3) and in competition experiments in *N. benthamiana* plants (Fig. 5.5, Table 1). A similar replicational advantage of the RNA 2GAC allele was also observed in the plant competition experiments (Table 1), even though the natural sequence of RNA2 of the PCV2 isolate of PCV is a GΔC anticodon (Manohar et al., 1993).

We conclude that an intact valine anticodon and the resultant valylatability are mildly advantageous attributes to both of the PCV genomic RNAs, perhaps more so for

RNA1, although the protoplast and whole plant experiments differ on this point, for unknown reasons that may be related to the specific host cell. Our protoplast results indicating a greater role for valylation in RNA1 than in RNA2 are reminiscent of results from the BMV system, in which non aminoacylation mutations are more critical in RNA1 and in RNA2 than in RNA3 (Duggal, Lahser, and Hall, 1994). BMV RNA1 and PCV RNA1 both encode essential replication proteins whose action may be at least partially *cis*-limited, acting preferentially (presumably at the earliest stages of an infection) on the replication of RNA1 itself. Aminoacylation may play a role in this process, and so be more crucial for those RNAs of a multipartite virus that are replicated *in cis* than those replicated *in trans* (BMV RNA3 and PCV RNA2). There is no information on what mechanistic role valylation plays in the replication of PCV, nor on whether that role is similar, though less crucial, than the postulated role of valylation in the regulated suppression of minus strand synthesis in the TYMV system (Dreher, 1999).

Curiosity about the significance of the differential valylation of RNA1 and 2 from the PCV2 isolate was a major incentive in conducting these studies. Protoplast inoculations failed to detect any effect of RNA valylatability on the accumulation of positive or negative sense RNA1 or RNA2, and thus on RNA1/RNA2 ratios (Fig. 5.3 and not shown). We had imagined that differential valylatability might have evolved because of an involvement in the fine regulation of viral RNA synthesis. However, the plant competition experiments make it clear that a valylatable RNA2 with a GAC anticodon is at a competitive advantage over the GΔC anticodon of RNA2 of isolate PCV2, at least in *N. benthamiana* plants. In this regard, the sequences of other PCV or Indian PCV isolates should be informative. Indeed, we find that RNA2 from PCV isolate PO2A possesses a GAC instead of GΔC anticodon. The same is true of RNA2 from the closely related *Indian peanut clump virus*, L serotype (Naidu et al., 2000), whose RNA1 contains a valylatable TLS very similar to that of PCV RNA (Miller et al., 1996; Goodwin and Dreher, 1998).

It thus appears that a GΔC anticodon has become fixed in RNA2 of the PCV2 isolate by a replicational error, and that differential valylation is not an important

biological trait nor a defining characteristic of the *Pecluviridae*. The survival of this mutation is indicative of the minor role played by valylation in the PCV system, especially in the case of RNA2. Nevertheless, sufficient advantage is conferred during infections in *N. benthamiana* plants for the selection of RNAs 1 and 2 with intact GAC valine anticodons that are capable of efficient valylation. Further studies are needed to determine whether this selective advantage is mechanistically related to the crucial role of valylation in TYMV.

4.6 Acknowledgments

4.7 References

Dreher, T. W., and Hall, T. C. (1988). Mutational analysis of the tRNA mimicry of brome mosaic virus RNA. Sequence and structural requirements for aminoacylation and 3'-adenylation. *J Mol Biol* **201**, 41-55.

Dreher, T. W., Rao, A. L., and Hall, T. C. (1989). Replication in vivo of mutant brome mosaic virus RNAs defective in aminoacylation. *J Mol Biol* **206**, 425-38.

Dreher, T. W., Tsai, C. H., Florentz, C., and Giege, R. (1992). Specific valylation of turnip yellow mosaic virus RNA by wheat germ valyl-tRNA synthetase determined by three anticodon loop nucleotides. *Biochemistry* **31**, 9183-9.

Dreher, T. W., Tsai, C. H., and Skuzeski, J. M. (1996). Aminoacylation identity switch of turnip yellow mosaic virus RNA from valine to methionine results in an infectious virus. *Proc Natl Acad Sci U S A* **93**, 12212-6.

Dreher, T. W. (1999). Functions of the 3'-Untranslated Regions of Positive Strand Rna Viral Genomes. *Annu Rev Phytopathol* **37**, 151-174.

Duggal, R., Lahser, F. C., and Hall, T. C. (1994). Cis-acting sequences in the replication of plant viruses with plus-sense RNA genomes. *Annu Rev Phytopathol* **32**, 287-309.

Filichkin, S. A., Bransom, K. L., Goodwin, J. B., and Dreher, T. W. (2000). The infectivities of turnip yellow mosaic virus genomes with altered tRNA mimicry are not dependent on compensating mutations in the viral replication protein. *J Virol* **74**, 8368-75.

Goodin, M. M., Schlagnhaufer, B., Weir, T., and Romaine, C. P. (1997). Characterization of an RNA-dependent RNA polymerase activity associated with La France isometric virus. *J Virol* **71,** 2264-9.

Goodwin, J. B., and Dreher, T. W. (1998). Transfer RNA mimicry in a new group of positive-strand RNA plant viruses, the furoviruses: differential aminoacylation between the RNA components of one genome. *Virology* **246,** 170-8.

Herzog, E., Guilley, H., Manohar, S. K., Dollet, M., Richards, K., Fritsch, C., and Jonard, G. (1994). Complete nucleotide sequence of peanut clump virus RNA 1 and relationships with other fungus-transmitted rod-shaped viruses. *J Gen Virol* **75,** 3147-55.

Herzog, E., Hemmer, O., Hauser, S., Meyer, G., Bouzoubaa, S., and Fritsch, C. (1998). Identification of genes involved in replication and movement of peanut clump virus. *Virology* **248,** 312-22.

Koiwai, A., Noguchi, M., and Tamaki, E. (1971). Changes in the amino acid composition of tobacco cells in suspension culture. *Phytochemistry* **10,** 561-566.

Kunkel, T. A., Roberts, J. D., and Zakour, R. A. (1987). Rapid and efficient site-specific mutagenesis without phenotypic selection. *Methods Enzymol* **154,** 367-82.

Manohar, S. K., Guilley, H., Dollet, M., Richards, K., and Jonard, G. (1993). Nucleotide sequence and genetic organization of peanut clump virus RNA 2 and partial characterization of deleted forms. *Virology* **195,** 33-41.

Mans, R. M., Pleij, C. W., and Bosch, L. (1991). tRNA-like structures. Structure, function and evolutionary significance. *Eur J Biochem* **201,** 303-24.

Miller, J. S., Wesley, S. V., Naidu, R. A., Reddy, D. V., and Mayo, M. A. (1996). The nucleotide sequence of RNA-1 of Indian peanut clump furovius. *Arch Virol* **141,** 2301-12.

Naidu, R. A., Miller, J. S., Mayo, M. A., Wesley, S. V., and Reddy, A. S. (2000). The nucleotide sequence of *Indian peanut clump virus* RNA 2: Sequence comparisons among pecluviruses. *Archives of Virology* **In press.**

Rao, A. L. N., and Hall, T. C. (1991). Interference in trans with brome mosaic virus replication by RNA-2 bearing aminoacylation-deficient mutants. *Virology* **180,** 16-22.

Shirako, Y., and Wilson, T. M. A., Eds. (1999). Furoviruses. Encyclopedia of Virology. Edited by A. Granoff, and R. Webster: Academic Press.

Tsai, C. H., and Dreher, T. W. (1991). Turnip yellow mosaic virus RNAs with anticodon loop substitutions that result in decreased valylation fail to replicate efficiently. *J Virol* **65,** 3060-7.

Chapter 6 <u>CONCLUSIONS</u>

6.1 Two new roles of the TYMV TLS

In this thesis, I have reported two new roles of the TYMV TLS in the viral infection: translation enhancement and repression of minus strand synthesis. In addition to the previously known role of the TLS as a telomere that maintains the intact 3´-CCA terminus (Dreher et al., 1989; Rao et al., 1989; Dreher, 1999), the discovery of these two new functions has expanded the importance of the TLS in the virus lifecycle.

Translation is a vital process in which a positive strand RNA virus synthesizes viral proteins, such as replication proteins, which will be used in subsequent steps for the successful amplification of the viral genome. Since many viral RNAs lack a 5´-cap and/or poly(A) tail in their genomic RNA, viral translation enhancers appear generally necessary to support the efficient translation of the viral RNAs. Using a luciferase reporter system in cowpea protoplasts, we found that the TYMV 3´-terminal 109 nts function as a translation enhancer (Chapter 2; Matsuda and Dreher, 2004). This function was found to be in synergistic relationship with the 5´-cap, implying that the two termini of the RNA may physically interact. This is the case with a 5´-cap and poly(A) tail, which also show a synergistic functional relationship (Gallie, 1991), and which physically interact via a protein bridge (Jacobson, 1996; Sachs et al., 1997; Gallie, 1998). Importantly, the TYMV translation enhancement function is largely supported by the efficient valylatability of the 3´-TLS, and apparently by the subsequent eEF1A interaction.

Recently, an alternative role of the TYMV TLS in translation was proposed (Barends et al., 2003). This so called "Trojan horse" model of TYMV translation postulates that the TYMV TLS can drive translation initiation in vitro specifically of ORF206 in a cap-independent manner. Interestingly, the authors reported that neither the valylation status of the TYMV TLS nor the TLS portion downstream of the anticodon loop is important for the postulated unique mode of p206 translation initiation. In direct contradiction to the model, using a luciferase reporter system in protoplasts, we have demonstrated that the 5´-cap has a strong positive effect on the translation of both p206 and p69 (Chapter 3). Moreover, deletion of the 3´-UTR resulted in comparable decreases

in the expression of both p206 and p69. Therefore, although appealing and interesting, the Trojan horse model of TYMV TLS function is not supported by the in vivo results.

In the bipartite PCV (Chapter 5; Matsuda et al., 2000) and tripartite BMV (Dreher et al., 1989; Rao and Hall, 1991; Duggal et al., 1994), the introduction of a non-aminoacylatable TLS was found to be less influential in RNA amplification when the TLS was placed in the trans-replicating RNAs than in the cis-replicating RNAs. Previously, in BMV, the 3′-terminal 151 nts harboring the TLS were shown to provide translation enhancement in protoplasts (Gallie and Kobayashi, 1994). Aminoacylation-controlled translation enhancement would provide an explanation for the stronger effects on the replication of RNAs encoding key proteins needed for the early stages of an infection. The minimal effect of the non-aminoacylatable TLSs in the trans-replicating PCV RNA2 and BMV RNA3 may be related to their encoded proteins being of less primary importance in RNA amplification. Unlike replication proteins, these proteins are not necessarily expressed immediately in order to kick off virus replication, and thus, low levels of protein expression can be tolerated.

Again, this hypothesis is based on the assumption that the PCV and BMV TLSs function as 3′-translation enhancers that are controlled by their aminoacylatabilities. In the near future, this point must be examined and the search for the TLS-dependent 3′-translation enhancement should also be expanded to other TLS-carrying viruses. An in vitro RNase protection assay did not detect interaction of [^{3}H]valine-charged PCV TLS with eEF1A•GTP (Goodwin and Dreher, 1998). If we find aminoacylation of the PCV TLS can control gene expression, we may need to re-investigate the PCV TLS•eEF1A interaction by using other methods, such as fluorescence measurement with BIAcore.

The argument that sufficient levels of replication protein expression are required for efficient virus replication is consistent with observations from the tripartite AMV. Polyadenylation of replication protein–encoding RNA1 partially circumvented the requirement of CP for efficient RNA amplification (Neeleman et al., 2001). Inoculum that included polyadenylated AMV RNA1 increased viral replication in protoplasts by about 50-fold, while polyadenylation of RNA2 and 3 did not result in significant changes.

Thus, the low level of non-poly(A) tailed RNA1 translation was a "bottleneck" for efficient viral replication.

Although translation may directly relate importance of aminoacylatability with its effect on RNA encoding replication protein, it is likely that the aminoacylatability of replication protein-encoding RNAs also affects the other steps in virus replication, which eventually influence amplification of plus strands and thus expression of replication protein. Indeed, eEF1A was found to be involved in controlling TYMV minus strand synthesis (Chapter 4; Matsuda et al., 2004). Weiland and Dreher (1993) showed that helper TYMV RNA encoding the replication protein is preferentially replicated compared to an RNA encoding a non-functional, mutant replication protein when they were coinoculated in protoplasts. This strong cis-preferential replication indicates that the genomic RNA undergoing translation must be the one that becomes a template for minus strand synthesis, rather than serving only for providing viral proteins to RNAs destined for replication. Thus, traffic control is required between ribosomes and newly synthesized RdRp, since simultaneous translation and minus strand synthesis on an RNA molecule are incompatible processes, as has been shown with poliovirus (Gamarnik and Andino, 1998) and bacteriophage Qβ (Kolakofsky and Weissmann, 1971a, 1971b). Demonstrating that interaction of eEF1A•GTP with aminoacylated RNA represses minus strand synthesis in vitro in a concentration dependent manner (Chapter 4; Matsuda et al., 2004), we propose that eEF1A plays dual roles in translation enhancement and traffic control by stopping RdRp from prematurely accessing the initiation site.

The transition from translation to replication may be achieved via displacement of eEF1A with newly synthesized RdRp when it reaches a critical concentration. Simultaneously or alternatively, as proposed for BMV (Noueiry and Ahlquist, 2003), TYMV RNAs may be physically sequestered from translational machineries to the chloroplast peripheral vesicles where TYMV RNA amplification is thought to occur (Bové and Bové, 1985; Garnier, 1986; Prod'homme et al., 2001).

The eEF1A-dependent repression of minus strand synthesis is considered to take place in early stages of replication for the following two reasons: 1) the TYMV TLS is an

exceedingly efficient substrate for the cellular tRNA enzymes, CCA-NTase, ValRS, and eEF1A (Dreher and Goodwin, 1998), suggesting that eEF1A association should occur rapidly after the TYMV RNA enters the cell; 2) there is no indication of a late cessation of minus strand synthesis during TYMV infections in protoplasts (B. Bradel and T. Dreher, unpublished) such as exists in some viruses prior to cessation of plus strand synthesis (Sawicki and Sawicki, 1980; Sawicki et al., 1981; Ishikawa et al., 1991).

Complementing the results presented in Chapter 4 showing that eEF1A can repress minus strand synthesis in vitro, there is evidence that eEF1A does not play a previously postulated role (Hall, 1979) in promoting minus stand synthesis: 1) the 3´-terminal 28 nts, which lack the anticodon stem-loop (thus no aminoacylation nor aminoacylation-dependent eEF1A interaction occurs), demonstrated similar minus strand template activity in vitro to the 3´-terminal 254 nt RNA (Singh and Dreher, 1997; Deiman et al., 1998); 2) the TYMV chimeric viruses with non-aminoacylatable TLSs incapable of interacting with eEF1A were found to be infectious (Goodwin et al., 1997; Filichkin et al., 2000); 3) eEF1A•GTP binds very tightly to the valylated TYMV TLS (Dreher and Goodwin, 1998; Dreher et al., 1999); and 4) no detectable eEF1A was found in TYMV replicase preparation from TYMV-infected leaves (Pulikowska et al., 1988), Minus strand repression or a default state in which the 3´-end is inaccessible to replicase may be a common function in RNA viruses, indicated by a growing body of reports on bacteriophage Qβ (Kolakofsky and Weissmann, 1971a; Kolakofsky and Weissmann, 1971b), AMV (Houwing and Jaspars, 1986; Olsthoorn et al., 1999), *Tombusvirus* (Pogany et al., 2003), rotavirus (Deo et al., 2002) and *Luteovirus* (Koev et al., 2002).

6.2   Future directions

Since the functions in translation enhancement and minus strand repression are coincident in TYMV, it is difficult to study the individual processes in vivo. However, chimeric TYMV genomes with a modified TMV 3´-UTR may provide a useful system to study these two functions separately. These genomic RNAs (TYMC-XX and YY) have the TMV UPD3 (see Fig. 1.2.D) and non-aminoacylatable TMV TLSs that are modified

with a TYMV-like anticodon and acceptor stem (Goodwin et al., 1997; Filichkin et al., 2000). Interestingly, substitution of the valine anticodon sequence of CAC with CGC (TYMC-XX(CGC)) resulted in significantly lower viral replication in protoplasts (Gopinath and T. Dreher, unpublished). Assuming that translation enhancement should be provided by TMV UPD3 (Leathers et al., 1993), poor replication of TYMC-XX(CGC) might result from disruption of minus strand repression. However, since these chimeric RNAs are non-aminoacylatable, eEF1A does not interact with the 3´-terminus. Therefore, some other factor(s) must replace the function of eEF1A as a minus strand repressor. Following the confirmation of efficient translation of TYMC-XX(CGC), the protein interacting with the 3´-terminus should be identified by electrophoretic mobility shift assay using protoplast extracts or performing reversible chemical-crosslinking in infected protoplasts.

Another issue that must be resolved in the future is the translation enhancement of ELV RNA. In the genus *Tymovirus*, ELV is an interesting deviation from the rest of the members because of the presence of a vestigial TLS lacking an anticodon stem loop. Therefore, ELV TLS cannot be charged with valine (nor with any other amino acid) and cannot be bound by eEF1A•GTP (Dreher and Goodwin, 1998). Although the TYMV chimeric variant with the ELV TLS is somewhat attenuated (about 25% CP accumulation in protoplasts relative to wild type TYMV), it is infectious in plants. By contrast, the anticodon point mutation (CAC to CGC) renders wild type TYMV non-infectious (Tsai and Dreher, 1991). Therefore, the ELV TLS should possess features for translation enhancement and minus strand repression that are different than the TYMV TLS. From the point of view of understanding translation enhancement and minus strand repression, we are interested in identifying factors interacting with the ELV TLS.

In order to investigate the mechanism of the TYMV 3´-translation enhancement, the role of eEF1A interaction with the TYMV TLS should be confirmed in vivo in the future. In addition to continued attempts to develop eEF1A interaction mutations, eEF1A can be tethered to a non-TYMV 3´-UTR, using bacteriophage λ antiterminator protein N interacting with RNA box B (Tan and Frankel, 1995). This approach was successfully

used to study the ribosome recruitment function of eIF4E in HeLa cells (De Gregorio et al., 2001). Interestingly, eEF1A was UV-cross linked to the TMV UPD3 (Zeenko et al., 2002), which is responsible for the TMV 3´-translation enhancement (Leathers et al., 1993). Thus, the possible similarities of the roles of eEF1A in the TYMV and TMV 3´-translation enhancement can be explored in the future.

Finally, studies in Chapter 3 regarding the mechanism of expression of ORF69 and ORF206 should be extended further. Several approaches can be considered to study the mechanisms. Those approaches include replacement of the entire 5´-UTR with a non-viral sequence of similar length, introduction of a stable stem loop structure within 12 nts from the 5´-terminus to see if ribosomes are loaded at the 5´-terminus, alteration of initiation context strength for ORF69 and ORF206, introduction of other initiation codon mutations, alteration of the length of the phylogenetically conserved 4 nts spacer between the two initiation codons, and examination of the effect of the secondary structure located downstream of the initiation codons.

Bibliography

Ahlquist, P., Noueiry, A. O., Lee, W. M., Kushner, D. B., and Dye, B. T. (2003). Host factors in positive-strand RNA virus genome replication. *J Virol* **77,** 8181-6.

Ahlquist, P. (2002) RNA-dependent RNA polymerases, viruses, and RNA silencing. *Science,* **296,** 1270-1273

Allen, E., Wang, S., and Miller, W. A. (1999). Barley yellow dwarf virus RNA requires a cap-independent translation sequence because it lacks a 5' cap. *Virology* **253,** 139-44.

Andersen, G. R., Nissen, P., and Nyborg, J. (2003). Elongation factors in protein biosynthesis. *Trends Biochem Sci* **28,** 434-41.

Andino, R., Rieckhof, G. E., and Baltimore, D. (1990). A functional ribonucleoprotein complex forms around the 5' end of poliovirus RNA. *Cell* **63,** 369-80.

Andino, R., Rieckhof, G. E., Achacoso, P. L., and Baltimore, D. (1993). Poliovirus RNA synthesis utilizes an RNP complex formed around the 5'-end of viral RNA. *EMBO J* **12,** 3587-98.

Arts, G. J., Kuersten, S., Romby, P., Ehresmann, B., and Mattaj, I. W. (1998). The role of exportin-t in selective nuclear export of mature tRNAs. *EMBO J* **17,** 7430-41.

Baim, S. B., and Sherman, F. (1988). mRNA structures influencing translation in the yeast Saccharomyces cerevisiae. *Mol Cell Biol* **8,** 1591-601.

Barends, S., Bink, H. H., van den Worm, S. H., Pleij, C. W., and Kraal, B. (2003). Entrapping ribosomes for viral translation: tRNA mimicry as a molecular Trojan horse. *Cell* **112,** 123-9.

Barrera, I., Schuppli, D., Sogo, J.M. and Weber, H. (1993) Different mechanisms of recognition of bacteriophage Q beta plus and minus strand RNAs by Q beta replicase. *J Mol Biol,* **232,** 512-521.

Barton, D.J., Morasco, B.J. and Flanegan, J.B. (1999) Translating ribosomes inhibit poliovirus negative-strand RNA synthesis. *J Virol,* **73,** 10104-10112.

Barton, D. J., O'Donnell, B. J., and Flanegan, J. B. (2001). 5' cloverleaf in poliovirus RNA is a cis-acting replication element required for negative-strand synthesis. *EMBO J* **20,** 1439-48.

Bi, X., and Goss, D. J. (2000). Wheat germ poly(A)-binding protein increases the ATPase and the RNA helicase activity of translation initiation factors eIF4A, eIF4B, and eIF-iso4F. *J Biol Chem* **275,** 17740-6.

Bink, H. H., Hellendoorn, K., van der Meulen, J., and Pleij, C. W. (2002). Protonation of non-Watson-Crick base pairs and encapsidation of turnip yellow mosaic virus RNA. *Proc Natl Acad Sci U S A* **99,** 13465-70.

Blumenthal, T., Landers, T. A., and Weber, K. (1972). Bacteriophage Qß replicase contains the protein biosynthesis elongation factors EF Tu and EF Ts. *Proc Natl Acad Sci U S A* **69,** 1313-7.

Blumenthal, T. and Carmichael, G.G. (1979) RNA replication: function and structure of Q beta-replicase. *Annu Rev Biochem,* **48,** 525-548

Bohnsack, M. T., Regener, K., Schwappach, B., Saffrich, R., Paraskeva, E., Hartmann, E., and Gorlich, D. (2002). Exp5 exports eEF1A via tRNA from nuclei and synergizes with other transport pathways to confine translation to the cytoplasm. *EMBO J* **21,** 6205-15.

Bol, J. (2003). alfalfa mosaic virus: coat protein-dependent initiation of infection. *Molecular Plant Pathology* **4,** 1-8.

Bové, J. M., and Bové, C. (1985). Turnip yellow mosaic virus RNA replication on the chloroplast envelope. *Physiol Vég* **23.**

Boyer, J. C., Zaccomer, B., and Haenni, A. L. (1993). Electrotransfection of turnip yellow mosaic virus RNA into Brassica leaf protoplasts and detection of viral RNA products with a non-radioactive probe. *J Gen Virol* **74** (**Pt 9**), 1911-7.

Bozarth, C. S., Weiland, J. J., and Dreher, T. W. (1992). Expression of ORF-69 of turnip yellow mosaic virus is necessary for viral spread in plants. *Virology* **187,** 124-30.

Bransom, K. L., Weiland, J. J., Tsai, C. H., and Dreher, T. W. (1995). Coding density of the turnip yellow mosaic virus genome: roles of the overlapping coat protein and p206-readthrough coding regions. *Virology* **206,** 403-12.

Bransom, K. L., Wallace, S. E., and Dreher, T. W. (1996). Identification of the cleavage site recognized by the turnip yellow mosaic virus protease. *Virology* **217,** 404-6.

Briand, J. P., Jonard, G., Guilley, H., Richards, K., and Hirth, L. (1977). Nucleotide sequence (n=159) of the amino-acid-accepting 3'-OH extremity of turnip-yellow-mosaic-virus RNA and the last portion of its coat-protein cistron. *Eur J Biochem* **72,** 453-63.

Briand, J. P., Keith, G., and Guilley, H. (1978). Nucleotide sequence at the 5′extremity of turnip yellow mosaic virus genome RNA. *Prc. Natl. Acad. Sci. (USA)* **75,** 3168-3172.

Brown, D., and Gold, L. (1995). Selection and characterization of RNAs replicated by Q beta replicase. *Biochemistry* **34,** 14775-82.

Brown, D., and Gold, L. (1996). RNA replication by Q beta replicase: a working model. *Proc Natl Acad Sci U S A* **93,** 11558-62.

Browning, K. S. (1996). The plant translational apparatus. *Plant Mol Biol* **32,** 107-44.

Calado, A., Treichel, N., Muller, E. C., Otto, A., and Kutay, U. (2002). Exportin-5-mediated nuclear export of eukaryotic elongation factor 1A and tRNA. *EMBO J* **21,** 6216-24.

Caldas, T. D., El Yaagoubi, A., and Richarme, G. (1998). Chaperone properties of bacterial elongation factor EF-Tu. *J Biol Chem* **273,** 11478-82.

Canady, M. A., Larson, S. B., Day, J., and McPherson, A. (1996). Crystal structure of turnip yellow mosaic virus. *Nat Struct Biol* **3,** 771-81.

Castagnetti, S., Hentze, M. W., Ephrussi, A., and Gebauer, F. (2000). Control of oskar mRNA translation by Bruno in a novel cell-free system from Drosophila ovaries. *Development* **127,** 1063-8.

Chapman, M. R., and Kao, C. C. (1999). A minimal RNA promoter for minus-strand RNA synthesis by the brome mosaic virus polymerase complex. *J Mol Biol* **286,** 709-20.

Chen, D., and Patton, J. T. (2000). De novo synthesis of minus strand RNA by the rotavirus RNA polymerase in a cell-free system involves a novel mechanism of initiation. *RNA* **6,** 1455-67.

Chen, D., Barros, M., Spencer, E. and Patton, J.T. (2001a) Features of the 3'-consensus sequence of rotavirus mRNAs critical to minus strand synthesis. *Virology*, **282**, 221-229.

Chen, J., Noueiry, A., and Ahlquist, P. (2001b). Brome mosaic virus Protein 1a recruits viral RNA2 to RNA replication through a 5' proximal RNA2 signal. *J Virol* **75**, 3207-19.

Chizhikov, V., and Patton, J. T. (2000). A four-nucleotide translation enhancer in the 3'-terminal consensus sequence of the nonpolyadenylated mRNAs of rotavirus. *RNA* **6**, 814-25.

Choi, Y. G., Dreher, T. W., and Rao, A. L. (2002). tRNA elements mediate the assembly of an icosahedral RNA virus. *Proc Natl Acad Sci U S A* **99**, 655-60.

Condeelis, J. (1995). Elongation factor 1 alpha, translation and the cytoskeleton. *Trends Biochem Sci* **20**, 169-70.

Dasgupta, R., and Kaesberg, P. (1982). Complete nucleotide sequences of the coat protein messenger RNAs of brome mosaic virus and cowpea chlorotic mottle virus. *Nucleic Acids Res* **10**, 703-13.

De Gregorio, E., Baron, J., Preiss, T., and Hentze, M. W. (2001). Tethered-function analysis reveals that eIF4E can recruit ribosomes independent of its binding to the cap structure. *RNA* **7**, 106-13.

de Smit, M. H., Gultyaev, A. P., Hilge, M., Bink, H. H., Barends, S., Kraal, B., and Pleij, C. W. (2002). Structural variation and functional importance of a D-loop-T-loop interaction in valine-accepting tRNA-like structures of plant viral RNAs. *Nucleic Acids Res* **30**, 4232-40.

Deiman, B. A., Verlaan, P. W., and Pleij, C. W. (2000). In vitro transcription by the turnip yellow mosaic virus RNA polymerase: a comparison with the alfalfa mosaic virus and brome mosaic virus replicases. *J Virol* **74**, 264-71.

Deiman, B. A. L. M., Koenen, A. K., Verlaan, P. W. G., and Pleij, C. W. A. (1998). Minimal template requirements for initiation of minus-strand synthesis in vitro by the RNA-dependent RNA polymerase of turnip yellow mosaic virus. *J Virol* **72**, 3965-72.

Deo, R. C., Groft, C. M., Rajashankar, K. R., and Burley, S. K. (2002). Recognition of the rotavirus mRNA 3' consensus by an asymmetric NSP3 homodimer. *Cell* **108**, 71-81.

Deutscher, M.P. (1982). tRNA nucleotidyltransferase. *The Enzymes* 15, 183-215.

Dever, T. E., Costello, C. E., Owens, C. L., Rosenberry, T. L., and Merrick, W. C. (1989). Location of seven post-translational modifications in rabbit elongation factor 1 alpha including dimethyllysine, trimethyllysine, and glycerylphosphorylethanolamine. *J Biol Chem* **264**, 20518-25.

Dever, T. E. (2002). Gene-specific regulation by general translation factors. *Cell* **108**, 545-56.

Diez, J., Ishikawa, M., Kaido, M., and Ahlquist, P. (2000). Identification and characterization of a host protein required for efficient template selection in viral RNA replication. *Proc Natl Acad Sci U S A* **97**, 3913-8.

Ding, S. W., Howe, J., Keese, P., Mackenzie, A., Meek, D., Osorio-Keese, M., Skotnicki, M., Srifah, P., Torronen, M., and Gibbs, A. (1990). The tymobox, a sequence shared by most tymoviruses: its use in molecular studies of tymoviruses. *Nucleic Acids Res* **18,** 1181-7.

Dreher, T. W., and Hall, T. C. (1988a). Mutational analysis of the tRNA mimicry of brome mosaic virus RNA. Sequence and structural requirements for aminoacylation and 3'-adenylation. *J Mol Biol* **201,** 41-55.

Dreher, T. W., and Hall, T. C. (1988b). Mutational analysis of the sequence and structural requirements in brome mosaic virus RNA for minus strand promoter activity. *J Mol Biol* **201,** 31-40.

Dreher, T. W., Rao, A. L., and Hall, T. C. (1989). Replication in vivo of mutant brome mosaic virus RNAs defective in aminoacylation. *J Mol Biol* **206,** 425-38.

Dreher, T. W., Tsai, C. H., Florentz, C., and Giege, R. (1992). Specific valylation of turnip yellow mosaic virus RNA by wheat germ valyl-tRNA synthetase determined by three anticodon loop nucleotides. *Biochemistry* **31,** 9183-9.

Dreher, T. W., Tsai, C. H., and Skuzeski, J. M. (1996). Aminoacylation identity switch of turnip yellow mosaic virus RNA from valine to methionine results in an infectious virus. *Proc Natl Acad Sci U S A* **93,** 12212-6.

Dreher, T. W., and Goodwin, J. B. (1998). Transfer RNA mimicry among tymoviral genomic RNAs ranges from highly efficient to vestigial. *Nucleic Acids Res* **26,** 4356-64.

Dreher, T. W. (1999). Functions of the 3'-Untranslated Regions of Positive Strand Rna Viral Genomes. *Annu Rev Phytopathol* **37,** 151-174.

Dreher, T. W., Uhlenbeck, O. C., and Browning, K. S. (1999). Quantitative assessment of EF-1alpha.GTP binding to aminoacyl-tRNAs, aminoacyl-viral RNA, and tRNA shows close correspondence to the RNA binding properties of EF-Tu. *J Biol Chem* **274,** 666-72.

Dreher, T. W. (2001). Tymoviruses. *In* "Encyclopedia of Plant Pathology" (O. C. Maloy, and D. Murray, Eds.), pp. 1051-1054. John Wiley & Sons, New York.

Duggal, R., Lahser, F. C., and Hall, T. C. (1994). Cis-acting sequences in the replication of plant viruses with plus-sense RNA genomes. *Annu Rev Phytopathol* **32,** 287-309.

Dumas, P., Moras, D., Florentz, C., Giege, R., Verlaan, P., Van Belkum, A., and Pleij, C. W. (1987). 3-D graphics modelling of the tRNA-like 3'-end of turnip yellow mosaic virus RNA: structural and functional implications. *J Biomol Struct Dyn* **4,** 707-28.

Dunoyer, P., Pfeffer, S., Fritsch, C., Hemmer, O., Voinnet, O., and Richards, K. E. (2002). Identification, subcellular localization and some properties of a cysteine-rich suppressor of gene silencing encoded by peanut clump virus. *Plant J* **29,** 555-67.

Ehrenfeld, E. (1996). Initiation of translation by picornavirus RNAs. *In* "Translational control" (J. W. B. Hershey, M. B. Mathew, and N. Sonenberg, Eds.), pp. 549-573. Cols Spring Harbor Laboratory Press, Cold Spring Harbor, N. Y.

Erhardt, M., Stussi-Garaud, C., Guilley, H., Richards, K. E., Jonard, G., and Bouzoubaa, S. (1999). The first triple gene block protein of peanut clump virus localizes to the plasmodesmata during virus infection. *Virology* **264,** 220-9.

Fajardo, J. E., and Shatkin, A. J. (1990). Translation of bicistronic viral mRNA in transfected cells: regulation at the level of elongation. *Proc Natl Acad Sci U S A* **87,** 328-32.

Felden, B., Florentz, C., Giege, R., and Westhof, E. (1996). A central pseudoknotted three-way junction imposes tRNA-like mimicry and the orientation of three 5' upstream pseudoknots in the 3' terminus of tobacco mosaic virus RNA. *RNA* **2,** 201-12.

Filichkin, S. A., Bransom, K. L., Goodwin, J. B., and Dreher, T. W. (2000). The infectivities of turnip yellow mosaic virus genomes with altered tRNA mimicry are not dependent on compensating mutations in the viral replication protein. *J Virol* **74,** 8368-75.

Florentz, C., and Giegé, R. (1995). tRNA-like structures in plant viral RNAs. *In* "tRNA: Structure, Biosynthesis, and Function" (D. Söll, and U. L. RajBhandary, Eds.), pp. 141-163. ASM Press, Washington, D.C.

Frolov, I., and Schlesinger, S. (1996). Translation of Sindbis virus mRNA: analysis of sequences downstream of the initiating AUG codon that enhance translation. *J Virol* **70,** 1182-90.

Futterer, J., and Hohn, T. (1996). Translation in plants--rules and exceptions. *Plant Mol Biol* **32,** 159-89.

Gallie, D. R., Sleat, D. E., Watts, J. W., Turner, P. C., and Wilson, T. M. (1987a). A comparison of eukaryotic viral 5'-leader sequences as enhancers of mRNA expression in vivo. *Nucleic Acids Res* **15,** 8693-711.

Gallie, D. R., Sleat, D. E., Watts, J. W., Turner, P. C., and Wilson, T. M. (1987b). The 5'-leader sequence of tobacco mosaic virus RNA enhances the expression of foreign gene transcripts in vitro and in vivo. *Nucleic Acids Res* **15,** 3257-73.

Gallie, D. R., and Walbot, V. (1990). RNA pseudoknot domain of tobacco mosaic virus can functionally substitute for a poly(A) tail in plant and animal cells. *Genes Dev* **4,** 1149-57.

Gallie, D. R. (1991). The cap and poly(A) tail function synergistically to regulate mRNA translational efficiency. *Genes Dev* **5,** 2108-16.

Gallie, D. R., and Kobayashi, M. (1994). The role of the 3'-untranslated region of non-polyadenylated plant viral mRNAs in regulating translational efficiency. *Gene* **142,** 159-65.

Gallie, D. R., Ling, J., Niepel, M., Morley, S. J., and Pain, V. M. (2000). The role of 5'-leader length, secondary structure and PABP concentration on cap and poly(A) tail function during translation in Xenopus oocytes. *Nucleic Acids Res* **28,** 2943-53.

Gallie, D. R. (2002). The 5'-leader of tobacco mosaic virus promotes translation through enhanced recruitment of eIF4F. *Nucleic Acids Res* **30,** 3401-11.

Gamarnik, A. V., and Andino, R. (1997). Two functional complexes formed by KH domain containing proteins with the 5' noncoding region of poliovirus RNA. *RNA* **3**, 882-92.

Gamarnik, A. V., and Andino, R. (1998). Switch from translation to RNA replication in a positive-stranded RNA virus. *Genes Dev* **12**, 2293-304.

Gamarnik, A. V., and Andino, R. (2000). Interactions of viral protein 3CD and poly(rC) binding protein with the 5' untranslated region of the poliovirus genome. *J Virol* **74**, 2219-26.

Gargouri, R., Joshi, R. L., Bol, J. F., Astier-Manifacier, S., and Haenni, A. L. (1989). Mechanism of synthesis of turnip yellow mosaic virus coat protein subgenomic RNA in vivo. *Virology* **171**, 386-93.

Garnier, M., Candresse, T., and Bove, J.M. (1986). Immunocytochimical localization of TYMV-coded structural and nonstructural proteins by the Portein A-gold techneque. *Virology* **151**, 100-109.

Gonen, H., Smith, C. E., Siegel, N. R., Kahana, C., Merrick, W. C., Chakraburtty, K., Schwartz, A. L., and Ciechanover, A. (1994). Protein synthesis elongation factor EF-1 alpha is essential for ubiquitin-dependent degradation of certain N alpha-acetylated proteins and may be substituted for by the bacterial elongation factor EF-Tu. *Proc Natl Acad Sci U S A* **91**, 7648-52.

Goodwin, J. B., Skuzeski, J. M., and Dreher, T. W. (1997). Characterization of chimeric turnip yellow mosaic virus genomes that are infectious in the absence of aminoacylation. *Virology* **230**, 113-24.

Goodwin, J. B., and Dreher, T. W. (1998). Transfer RNA mimicry in a new group of positive-strand RNA plant viruses, the furoviruses: differential aminoacylation between the RNA components of one genome. *Virology* **246**, 170-8.

Grosshans, H., Hurt, E., and Simos, G. (2000). An aminoacylation-dependent nuclear tRNA export pathway in yeast. *Genes Dev* **14**, 830-40.

Guilley, H., and Briand, J. P. (1978). Nucleotide sequence of turnip yellow mosaic virus coat protein mRNA. *Cell* **15**, 113-22.

Guo, L., Allen, E., and Miller, W. A. (2000). Structure and function of a cap-independent translation element that functions in either the 3' or the 5' untranslated region. *RNA* **6**, 1808-20.

Guo, L., Allen, E. M., and Miller, W. A. (2001). Base-pairing between untranslated regions facilitates translation of uncapped, nonpolyadenylated viral RNA. *Mol Cell* **7**, 1103-9.

Haenni, A. L., Joshi, S., and Chapeville, F. (1982). tRNA-like structures in the genomes of RNA viruses. *Prog Nucleic Acid Res Mol Biol* **27**, 85-104.

Hall, T. C. (1979). Transfer RNA-like structures in viral genomes. *Int Rev Cytol* **60**, 1-26.

Hann, L. E., and Gehrke, L. (1995). mRNAs containing the unstructured 5' leader sequence of alfalfa mosaic virus RNA 4 translate inefficiently in lysates from poliovirus-infected HeLa cells. *J Virol* **69**, 4986-93.

Hann, L. E., Webb, A. C., Cai, J. M., and Gehrke, L. (1997). Identification of a competitive translation determinant in the 3' untranslated region of alfalfa mosaic virus coat protein mRNA. *Mol Cell Biol* **17**, 2005-13.

Hatta, T., Bullivant, S., and Matthews, R. E. (1973). Fine structure of vesicles induced in chloroplasts of Chinese cabbage leaves by infection with turnip yellow mosaic virus. *J Gen Virol* **20**, 37-50.

Hatta, T., and Matthews, R. E. (1974). The sequence of early cytological changes in Chinese cabbage leaf cells following systemic infection with turnip yellow mosaic virus. *Virology* **59**, 383-96.

Hellen, C. U., and Sarnow, P. (2001). Internal ribosome entry sites in eukaryotic mRNA molecules. *Genes Dev* **15**, 1593-612.

Hellendoorn, K., Michiels, P. J., Buitenhuis, R., and Pleij, C. W. (1996). Protonatable hairpins are conserved in the 5'-untranslated region of tymovirus RNAs. *Nucleic Acids Res* **24**, 4910-7.

Hellendoorn, K., Verlaan, P. W., and Pleij, C. W. (1997). A functional role for the conserved protonatable hairpins in the 5' untranslated region of turnip yellow mosaic virus RNA. *J Virol* **71**, 8774-9.

Hemmer, O., Dunoyer, P., Richards, K., and Fritsch, C. (2003). Mapping of viral RNA sequences required for assembly of peanut clump virus particles. *J Gen Virol* **84**, 2585-94.

Hentzen, D., Mandel, P. and Garel, J.P. (1972) Relation between aminoacyl-tRNA stability and the fixed amino acid. *Biochim Biophys Acta*, **281**, 228-232

Herold, J., and Andino, R. (2001). Poliovirus RNA replication requires genome circularization through a protein-protein bridge. *Mol Cell* **7**, 581-91.

Herzog, E., Guilley, H., Manohar, S. K., Dollet, M., Richards, K., Fritsch, C., and Jonard, G. (1994). Complete nucleotide sequence of peanut clump virus RNA 1 and relationships with other fungus-transmitted rod-shaped viruses. *J Gen Virol* **75**, 3147-55.

Herzog, E., Guilley, H., and Fritsch, C. (1995). Translation of the second gene of peanut clump virus RNA 2 occurs by leaky scanning in vitro. *Virology* **208**, 215-25.

Herzog, E., Hemmer, O., Hauser, S., Meyer, G., Bouzoubaa, S., and Fritsch, C. (1998). Identification of genes involved in replication and movement of peanut clump virus. *Virology* **248**, 312-22.

Hirth, L., and Givord, L. (1985). Tymoviruses. *In* "The Plant Viruses" (R. Koenig, Ed.), Vol. 3. 163-212 vols. Plenum Press, New York, NY.

Hotokezaka, Y., Tobben, U., Hotokezaka, H., Van Leyen, K., Beatrix, B., Smith, D. H., Nakamura, T., and Wiedmann, M. (2002). Interaction of the eukaryotic elongation factor 1A with newly synthesized polypeptides. *J Biol Chem* **277**, 18545-51.

Houwing, C. J., and Jaspars, E. M. J. (1986). Coat protein blocks the in vitro transcription of the virion RNAs of alfalfa mosaic virus. *FEBS Letters* **209**, 284-288.

Hull, R. (2002). "Matthew's Plant Virology." Fourth ed., Academic Press, Inc., San Diego.

Ishikawa, M., Meshi, T., Ohno, T. and Okada, Y. (1991) Specific cessation of minus-strand RNA accumulation at an early stage of tobacco mosaic virus infection. *J Virol*, **65**, 861-868.

Ishikawa, M., Diez, J., Restrepo-Hartwig, M., and Ahlquist, P. (1997). Yeast mutations in multiple complementation groups inhibit brome mosaic virus RNA replication

and transcription and perturb regulated expression of the viral polymerase-like gene. *Proc Natl Acad Sci U S A* **94**, 13810-5.

Jacobs, B.L. and Langland, J.O. (1996) When two strands are better than one: the mediators and modulators of the cellular responses to double-stranded RNA. *Virology*, **219**, 339-349.

Jacobson, A. (1996). Poly(A) metabolism and translation: the closed-loop model. *In* "Translational control" (J. Hershey, Mathews, MB, Sonenberg, N, Ed.), pp. 451-480. Cold Spring Harbor Laboratory Press.

Jacobson, A., and Peltz, S. W. (1996). Interrelationships of the pathways of mRNA decay and translation in eukaryotic cells. *Annu Rev Biochem* **65**, 693-739.

Janda, M., and Ahlquist, P. (1998). Brome mosaic virus RNA replication protein 1a dramatically increases in vivo stability but not translation of viral genomic RNA3. *Proc Natl Acad Sci U S A* **95**, 2227-32.

Jaspars, E. M. (1999). Genome activation in alfamo- and ilarviruses. *Arch Virol* **144**, 843-63.

Jobling, S. A., and Gehrke, L. (1987). Enhanced translation of chimaeric messenger RNAs containing a plant viral untranslated leader sequence. *Nature* **325**, 622-5.

Jobling, S. A., Cuthbert, C. M., Rogers, S. G., Fraley, R. T., and Gehrke, L. (1988). In vitro transcription and translational efficiency of chimeric SP6 messenger RNAs devoid of 5' vector nucleotides. *Nucleic Acids Res* **16**, 4483-98.

Johnston, J. C., and Rochon, D. M. (1996). Both codon context and leader length contribute to efficient expression of two overlapping open reading frames of a cucumber necrosis virus bifunctional subgenomic mRNA. *Virology* **221**, 232-9.

Joshi, C. P., Zhou, H., Huang, X., and Chiang, V. L. (1997). Context sequences of translation initiation codon in plants. *Plant Mol Biol* **35**, 993-1001.

Joshi, R., and Haenni, A. (1986). Search for tRNA-like properties in tomato aspermy virus RNA. *FEBS Letters* **194**, 157-194.

Joshi, S., Haenni, A. L., Hubert, E., Huez, G., and Marbaix, G. (1978). In vivo aminoacylation and 'processing' of turnip yellow mosaic virus RNA in Xenopus laevis oocytes. *Nature* **275**, 339-41.

Joshi, S., Chapeville, F., and Haenni, A. L. (1982). Turnip yellow mosaic virus RNA is aminoacylated *in vivo* in Chinese cabbage leaves. *EMBO J* **1**, 935-938.

Juszczuk, M., Paczkowska, E., Sadowy, E., Zagorski, W., and Hulanicka, D. M. (2000). Effect of genomic and subgenomic leader sequences of potato leafroll virus on gene expression. *FEBS Lett* **484**, 33-6.

Kadare, G., David, C., and Haenni, A. L. (1996). ATPase, GTPase, and RNA binding activities associated with the 206-kilodalton protein of turnip yellow mosaic virus. *J Virol* **70**, 8169-74.

Kao, C. C., and Sun, J. H. (1996). Initiation of minus-strand RNA synthesis by the brome mosaicvirus RNA- dependent RNA polymerase: use of oligoribonucleotide primers. *J Virol* **70**, 6826-30.

Kao, C., Zheng, M. and Rudisser, S. (1999) A simple and efficient method to reduce nontemplated nucleotide addition at the 3 terminus of RNAs transcribed by T7 RNA polymerase. *RNA*, **5**, 1268-1272.

Kawaguchi, R., and Bailey-Serres, J. (2002). Regulation of translational initiation in plants. *Curr Opin Plant Biol* **5,** 460-5.

Kim, C. H., Kao, C. C., and Tinoco, I., Jr. (2000). RNA motifs that determine specificity between a viral replicase and its promoter. *Nat Struct Biol* **7,** 415-23.

Klovins, J., Berzins, V., and van Duin, J. (1998). A long-range interaction in Qbeta RNA that bridges the thousand nucleotides between the M-site and the 3' end is required for replication. *RNA* **4,** 948-57.

Koev, G., Liu, S., Beckett, R., and Miller, W. A. (2002). The 3prime prime or minute-terminal structure required for replication of Barley yellow dwarf virus RNA contains an embedded 3prime prime or minute end. *Virology* **292,** 114-26.

Koh, D. C., Wong, S. M., and Liu, D. X. (2003). Synergism of the 3'-untranslated region and an internal ribosome entry site differentially enhances the translation of a plant virus coat protein. *J Biol Chem* **278,** 20565-73.

Koiwai, A., Noguchi, M., and Tamaki, E. (1971). Changes in the amino acid composition of tobacco cells in suspension culture. *Phytochemistry* **10,** 561-566.

Kolakofsky, D., and Weissmann, C. (1971a). Possible mechanism for transition of viral RNA from polysome to replication complex. *Nat New Biol* **231,** 42-6.

Kolakofsky, D., and Weissmann, C. (1971b). Qβ replicase as repressor of Qβ RNA-directed protein synthesis. *Biochim Biophys Acta* **246,** 596-9.

Kolk, M. H., van der Graaf, M., Wijmenga, S. S., Pleij, C. W., Heus, H. A., and Hilbers, C. W. (1998). NMR structure of a classical pseudoknot: interplay of single- and double-stranded RNA. *Science* **280,** 434-8.

Koonin, E. V., and Dolja, V. V. (1993). Evolution and taxonomy of positive-strand RNA viruses: implications of comparative analysis of amino acid sequences. *Crit Rev Biochem Mol Biol* **28,** 375-430.

Kozak, M. (1986a). Point mutations define a sequence flanking the AUG initiator codon that modulates translation by eukaryotic ribosomes. *Cell* **44,** 283-92.

Kozak, M. (1986b). Influences of mRNA secondary structure on initiation by eukaryotic ribosomes. *Proc Natl Acad Sci U S A* **83,** 2850-4.

Kozak, M. (1987). An analysis of 5'-noncoding sequences from 699 vertebrate messenger RNAs. *Nucleic Acids Res* **15,** 8125-48.

Kozak, M. (1989). Circumstances and mechanisms of inhibition of translation by secondary structure in eucaryotic mRNAs. *Mol Cell Biol* **9,** 5134-42.

Kozak, M. (1991a). Structural features in eukaryotic mRNAs that modulate the initiation of translation. *J Biol Chem* **266,** 19867-70.

Kozak, M. (1991b). A short leader sequence impairs the fidelity of initiation by eukaryotic ribosomes. *Gene Expr* **1,** 111-5.

Kozak, M. (1995). Adherence to the first-AUG rule when a second AUG codon follows closely upon the first. *Proc Natl Acad Sci U S A* **92,** 2662-6.

Kozak, M. (1997). Recognition of AUG and alternative initiator codons is augmented by G in position +4 but is not generally affected by the nucleotides in positions +5 and +6. *EMBO J* **16,** 2482-92.

Kozak, M. (1999). Initiation of translation in prokaryotes and eukaryotes. *Gene* **234,** 187-208.

Kudlicki, W., Coffman, A., Kramer, G., and Hardesty, B. (1997). Renaturation of rhodanese by translational elongation factor (EF) Tu. Protein refolding by EF-Tu flexing. *J Biol Chem* **272,** 32206-10.

Kunkel, T. A., Roberts, J. D., and Zakour, R. A. (1987). Rapid and efficient site-specific mutagenesis without phenotypic selection. *Methods Enzymol* **154,** 367-82.

L'Italien, J. J., and Laursen, R. A. (1979). Location of the site of methylation in elongation factor Tu. *FEBS Lett* **107,** 359-62.

Lau, N. C., Lim, L. P., Weinstein, E. G., and Bartel, D. P. (2001). An abundant class of tiny RNAs with probable regulatory roles in *Caenorhabditis elegans. Science* **294,** 858-62.

Le, H., Browning, K. S., and Gallie, D. R. (2000). The phosphorylation state of poly(A)-binding protein specifies its binding to poly(A) RNA and its interaction with eukaryotic initiation factor (eIF) 4F, eIFiso4F, and eIF4B. *J Biol Chem* **275,** 17452-62.

Leathers, V., Tanguay, R., Kobayashi, M., and Gallie, D. R. (1993). A phylogenetically conserved sequence within viral 3' untranslated RNA pseudoknots regulates translation. *Mol Cell Biol* **13,** 5331-47.

Lesemann, D. (1977). Virus group-specific and virus-specific cytological alterations induced by members of the tymovirus group. *Phytopath Z* **90,** 315-321.

Lie, Y. S., and Macdonald, P. M. (1999). Translational regulation of oskar mRNA occurs independent of the cap and poly(A) tail in Drosophila ovarian extracts. *Development* **126,** 4989-96.

Lim, L. P., Lau, N. C., Weinstein, E. G., Abdelhakim, A., Yekta, S., Rhoades, M. W., Burge, C. B., and Bartel, D. P. (2003). The microRNAs of Caenorhabditis elegans. *Genes Dev* **17,** 991-1008.

Loesch-Fries, L. S., and Hall, T. C. (1982). *In vivo* aminoacylation of brome mosaic and barley stripe mosaic virus RNAs. *Nature* **298,** 771-773.

Lopez-Valenzuela, J. A., Gibbon, B. C., Hughes, P. A., Dreher, T. W., and Larkins, B. A. (2003). eEF1A Isoforms Change in Abundance and Actin-Binding Activity during Maize Endosperm Development. *Plant Physiol* **133,** 1285-95.

Luo, Y., and Goss, D. J. (2001). Homeostasis in mRNA initiation: wheat germ poly(A)-binding protein lowers the activation energy barrier to initiation complex formation. *J Biol Chem* **276,** 43083-6.

Macdonald, P. (2001). Diversity in translational regulation. *Curr Opin Cell Biol* **13,** 326-331.

Mangus, D.A., Evans, M.C. and Jacobson, A. (2003). Poly(A)-binding proteins: multifunctional scaffolds for the post-transcriptional control of gene expression. *Genome Biol* **4,** 223.

Manohar, S. K., Guilley, H., Dollet, M., Richards, K., and Jonard, G. (1993). Nucleotide sequence and genetic organization of peanut clump virus RNA 2 and partial characterization of deleted forms. *Virology* **195,** 33-41.

Mans, R. M., Pleij, C. W., and Bosch, L. (1991). tRNA-like structures. Structure, function and evolutionary significance. *Eur J Biochem* **201,** 303-24.

Markham, R., and Smith, K. M. (1946). A new crystalline plant virus. *Nature* **157,** 300.

Martelli, G. P., Sabanadzovic, S., Abou-Ghanem Sabanadzovic, N., Edwards, M. C., and Dreher, T. (2002). The family Tymoviridae. *Arch Virol* **147**, 1837-46.

Matthews, R. (1991). "Plant Virology." Third ed., Academic Press, Inc., San Diego.

Matthews, R. E. (1981). Portraits of viruses: turnip yellow mosaic virus. *Intervirology* **15**, 121-44.

Matsuda, D., Dunoyer, P., Hemmer, O., Fritsch, C., and Dreher, T. W. (2000). The valine anticodon and valylatability of Peanut clump virus RNAs are not essential but provide a modest competitive advantage in plants. *J Virol* **74**, 8720-5.

Matsuda, D., and Dreher, T. W. (2004). The tRNA-like structure of Turnip yellow mosaic virus RNA is a 3´-translational enhancer. *Virology* **in press**.

Matsuda, D., Yoshinari, S., and Dreher, T. W. (2004). eEF1A binding to aminoacylated viral RNA represses minus strand synthesis by TYMV RNA-dependent RNA polymerase. *Virology* **in press**.

Mendez, R., and Richter, J. D. (2001). Translational control by CPEB: a means to the end. *Nat Rev Mol Cell Biol* **2**, 521-9.

Meshi, T., Ohno, T., Iba, H., and Okada, Y. (1981). Nucleotide sequence of a cloned cDNA copy of TMV (cowpea strain) RNA, including the assembly origin, the coat protein cistron, and the 3' non- coding region. *Mol Gen Genet* **184**, 20-5.

Meulewaeter, F., Danthinne, X., Van Montagu, M., and Cornelissen, M. (1998). 5'- and 3'-sequences of satellite tobacco necrosis virus RNA promoting translation in tobacco. *Plant J* **14**, 169-76.

Miller, J. S., Wesley, S. V., Naidu, R. A., Reddy, D. V., and Mayo, M. A. (1996). The nucleotide sequence of RNA-1 of Indian peanut clump furovius. *Arch Virol* **141**(12), 2301-12.

Miller, W. A., Bujarski, J. J., Dreher, T. W., and Hall, T. C. (1986). Minus-strand initiation by brome mosaic virus replicase within the 3' tRNA-like structure of native and modified RNA templates. *J Mol Biol* **187**, 537-46.

Miranda, G., Schuppli, D., Barrera, I., Hausherr, C., Sogo, J. M., and Weber, H. (1997). Recognition of bacteriophage Qbeta plus strand RNA as a template by Qbeta replicase: role of RNA interactions mediated by ribosomal proteins S1 and host factor. *J Mol Biol* **267**, 1089-103.

Morch, M. D., Boyer, J. C., and Haenni, A. L. (1988). Overlapping open reading frames revealed by complete nucleotide sequencing of turnip yellow mosaic virus genomic RNA. *Nucleic Acids Res* **16**, 6157-73.

Munshi, R., Kandl, K. A., Carr-Schmid, A., Whitacre, J. L., Adams, A. E., and Kinzy, T. G. (2001). Overexpression of translation elongation factor 1A affects the organization and function of the actin cytoskeleton in yeast. *Genetics* **157**, 1425-36.

Naidu, R. A., Miller, J. S., Mayo, M. A., Wesley, S. V., and Reddy, A. S. (2000). The nucleotide sequence of Indian peanut clump virus RNA 2: sequence comparisons among pecluviruses. *Arch Virol* **145**, 1857-66.

Neeleman, L., Olsthoorn, R. C., Linthorst, H. J., and Bol, J. F. (2001). Translation of a nonpolyadenylated viral RNA is enhanced by binding of viral coat protein or polyadenylation of the RNA. *Proc Natl Acad Sci U S A* **98**, 14286-91.

Nissen, P., Kjeldgaard, M., Thirup, S., Polekhina, G., Reshetnikova, L., Clark, B. F., and Nyborg, J. (1995). Crystal structure of the ternary complex of Phe-tRNAPhe, EF-Tu, and a GTP analog. *Science* **270**, 1464-72.

Noueiry, A. O., and Ahlquist, P. (2003). Brome Mosaic Virus RNA Replication: Revealing the Role of the Host in RNA Virus Replication. *Annu Rev Phytopathol*.

Ohlmann, T., Rau, M., Pain, V. M., and Morley, S. J. (1996). The C-terminal domain of eukaryotic protein synthesis initiation factor (eIF) 4G is sufficient to support cap-independent translation in the absence of eIF4E. *Embo J* **15**, 1371-82.

Olsthoorn, R. C., Mertens, S., Brederode, F. T., and Bol, J. F. (1999). A conformational switch at the 3' end of a plant virus RNA regulates viral replication. *EMBO J* **18**, 4856-64.

Osman, T. A., Hemenway, C. L., and Buck, K. W. (2000). Role of the 3' tRNA-like structure in tobacco mosaic virus minus-strand RNA synthesis by the viral RNA-dependent RNA polymerase In vitro. *J Virol* **74**, 11671-80.

Pause, A., Methot, N., Svitkin, Y., Merrick, W. C., and Sonenberg, N. (1994). Dominant negative mutants of mammalian translation initiation factor eIF-4A define a critical role for eIF-4F in cap-dependent and cap-independent initiation of translation. *EMBO J* **13**, 1205-15.

Pelletier, J., and Sonenberg, N. (1988). Internal initiation of translation of eukaryotic mRNA directed by a sequence derived from poliovirus RNA. *Nature* **334**, 320-5.

Peranen, J., Laakkonen, P., Hyvonen, M., and Kaariainen, L. (1995). The alphavirus replicase protein nsP1 is membrane-associated and has affinity to endocytic organelles. *Virology* **208**, 610-20.

Pestova, T. V., Kolupaeva, V. G., Lomakin, I. B., Pilipenko, E. V., Shatsky, I. N., Agol, V. I., and Hellen, C. U. (2001). Molecular mechanisms of translation initiation in eukaryotes. *Proc Natl Acad Sci U S A* **98**, 7029-36.

Petrushenko, Z. M., Budkevich, T. V., Shalak, V. F., Negrutskii, B. S., and El'skaya, A. V. (2002). Novel complexes of mammalian translation elongation factor eEF1A.GDP with uncharged tRNA and aminoacyl-tRNA synthetase. Implications for tRNA channeling. *Eur J Biochem* **269**, 4811-8.

Piron, M., Vende, P., Cohen, J., and Poncet, D. (1998). Rotavirus RNA-binding protein NSP3 interacts with eIF4GI and evicts the poly(A) binding protein from eIF4F. *EMBO J* **17**, 5811-21.

Pleij, C. W., Rietveld, K., and Bosch, L. (1985). A new principle of RNA folding based on pseudoknotting. *Nucleic Acids Res* **13**, 1717-31.

Pleiss, J.A. and Uhlenbeck, O.C. (2001) Identification of thermodynamically relevant interactions between EF-Tu and backbone elements of tRNA. *J Mol Biol*, **308**, 895-905.

Pogany, J., Fabian, M. R., White, K. A., and Nagy, P. D. (2003). A replication silencer element in a plus-strand RNA virus. *EMBO J* **22**, 5602-11.

Poncet, D., Laurent, S., and Cohen, J. (1994). Four nucleotides are the minimal requirement for RNA recognition by rotavirus non-structural protein NSP3. *EMBO J* **13**, 4165-73.

Preiss, T., Muckenthaler, M. and Hentze, M.W. (1998). Poly(A)-tail-promoted translation in yeast: implications for translational control. *RNA* **4**, 1321-1331.

Preiss, T., and Hentze, M. W. (1999). From factors to mechanisms: translation and translational control in eukaryotes. *Curr Opin Genet Dev* **9**, 515-21.

Prod'homme, D., Le Panse, S., Drugeon, G., and Jupin, I. (2001). Detection and subcellular localization of the turnip yellow mosaic virus 66K replication protein in infected cells. *Virology* **281**, 88-101.

Prod'homme, D., Jakubiec, A., Tournier, V., Drugeon, G., and Jupin, I. (2003). Targeting of the turnip yellow mosaic virus 66K replication protein to the chloroplast envelope is mediated by the 140K protein. *J Virol* **77**, 9124-35.

Pulikowska, J., Wojtaszek, P., Korcz, A., Michalski, Z., Candresse, T., and Twardowski, T. (1988). Immunochemical properties of elongation factors 1 of plant origin. *Eur J Biochem* **171**, 131-6.

Qu, F., and Morris, T. J. (2000). Cap-independent translational enhancement of turnip crinkle virus genomic and subgenomic RNAs. *J Virol* **74**, 1085-93.

Ranjith-Kumar, C. T., Zhang, X., and Kao, C. C. (2003). Enhancer-like activity of a brome mosaic virus RNA promoter. *J Virol* **77**, 1830-9.

Rao, A. L., Dreher, T. W., Marsh, L. E., and Hall, T. C. (1989). Telomeric function of the tRNA-like structure of brome mosaic virus RNA. *Proc Natl Acad Sci U S A* **86**, 5335-9.

Rao, A. L. N., and Hall, T. C. (1991). Interference in trans with brome mosaic virus replication by RNA-2 bearing aminoacylation-deficient mutants. *Virology* **180**, 16-22.

Rao, A. L. N., and Hall, T. C. (1993). Recombination and polymerase error facilitate restoration of infectivity in brome mosaic virus. *J Virol* **67**, 969-979.

Restrepo-Hartwig, M., and Ahlquist, P. (1999). Brome mosaic virus RNA replication proteins 1a and 2a colocalize and 1a independently localizes on the yeast endoplasmic reticulum. *J Virol* **73**, 10303-9.

Rietveld, K., Van Poelgeest, R., Pleij, C. W., Van Boom, J. H., and Bosch, L. (1982). The tRNA-like structure at the 3' terminus of turnip yellow mosaic virus RNA. Differences and similarities with canonical tRNA. *Nucleic Acids Res* **10**, 1929-46.

Rogers, G. W., Jr., Richter, N. J., and Merrick, W. C. (1999). Biochemical and kinetic characterization of the RNA helicase activity of eukaryotic initiation factor 4A. *J Biol Chem* **274**, 12236-44.

Rohozinski, J., and Hancock, J. M. (1996). Do light-induced pH changes within the chloroplast drive turnip yellow mosaic virus assembly? *J Gen Virol* **77**, 163-5.

Rozanov, M. N., Drugeon, G., and Haenni, A. L. (1995). Papain-like proteinase of turnip yellow mosaic virus: a prototype of a new viral proteinase group. *Arch Virol* **140**, 273-88.

Rudinger, J., Florentz, C., and Giege, R. (1994). Histidylation by yeast HisRS of tRNA or tRNA-like structure relies on residues -1 and 73 but is dependent on the RNA context. *Nucleic Acids Res* **22**, 5031-7.

Sachs, A. B., Davis, R. W., and Kornberg, R. D. (1987). A single domain of yeast poly(A)-binding protein is necessary and sufficient for RNA binding and cell viability. *Mol Cell Biol* **7**, 3268-76.

Sachs, A. B. (1993). Messenger RNA degradation in eukaryotes. *Cell* **74**, 413-21.

Sachs, A. B., Sarnow, P., and Hentze, M. W. (1997). Starting at the beginning, middle, and end: translation initiation in eukaryotes. *Cell* **89**, 831-8.

Sagliocco, F. A., Vega Laso, M. R., Zhu, D., Tuite, M. F., McCarthy, J. E., and Brown, A. J. (1993). The influence of 5'-secondary structures upon ribosome binding to mRNA during translation in yeast. *J Biol Chem* **268**, 26522-30.

Sarnow, P. (2003). Viral internal ribosome entry site elements: novel ribosome-RNA complexes and roles in viral pathogenesis. *J Virol* **77**, 2801-6.

Sawicki, D. L., and Sawicki, S. G. (1980). Short-lived minus-strand polymerase for Semliki Forest virus. *J Virol* **34**, 108-18.

Sawicki, D. L., Sawicki, S. G., Keranen, S., and Kaariainen, L. (1981). Specific Sindbis virus-coded function for minus-strand RNA synthesis. *J Virol* **39**, 348-58.

Schirawski, J., Planchais, S., and Haenni, A. L. (2000a). An improved protocol for the preparation of protoplasts from an established Arabidopsis thaliana cell suspension culture and infection with RNA of turnip yellow mosaic tymovirus: a simple and reliable method. *J Virol Methods* **86**, 85-94.

Schirawski, J., Voyatzakis, A., Zaccomer, B., Bernardi, F., and Haenni, A. L. (2000b). Identification and functional analysis of the turnip yellow mosaic tymovirus subgenomic promoter. *J Virol* **74**, 11073-80.

Schwartz, M., Chen, J., Janda, M., Sullivan, M., den Boon, J. and Ahlquist, P. (2002) A positive-strand RNA virus replication complex parallels form and function of retrovirus capsids. *Mol Cell*, **9**, 505-514.

Senear, A. W., and Steitz, J. A. (1976). Site-specific interaction of Qbeta host factor and ribosomal protein S1 with Qbeta and R17 bacteriophage RNAs. *J Biol Chem* **251**, 1902-12.

Shaw, G., and Kamen, R. (1986). A conserved AU sequence from the 3' untranslated region of GM-CSF mRNA mediates selective mRNA degradation. *Cell* **46**, 659-67.

Shirako, Y., and Wilson, T. M. A., Eds. (1999). Furoviruses. Encyclopedia of Virology. Edited by A. Granoff, and R. Webster: Academic Press.

Singh, R. N., and Dreher, T. W. (1997). Turnip yellow mosaic virus RNA-dependent RNA polymerase: initiation of minus strand synthesis in vitro. *Virology* **233**, 430-9.

Singh, R. N., and Dreher, T. W. (1998). Specific site selection in RNA resulting from a combination of nonspecific secondary structure and -CCR- boxes: initiation of minus strand synthesis by turnip yellow mosaic virus RNA-dependent RNA polymerase. *RNA* **4**, 1083-95.

Slusher, L. B., Gillman, E. C., Martin, N. C., and Hopper, A. K. (1991). mRNA leader length and initiation codon context determine alternative AUG selection for the yeast gene MOD5. *Proc Natl Acad Sci U S A* **88**, 9789-93.

Sonenberg, N., Morgan, M. A., Merrick, W. C., and Shatkin, A. J. (1978). A polypeptide in eukaryotic initiation factors that crosslinks specifically to the 5'-terminal cap in mRNA. *Proc Natl Acad Sci U S A* **75**, 4843-7.

Sutic, D. D., Ford, R. E., and Tosic, M. T. (1999). Handbook of plant virus diseases, pp. 232-234. CRC Press, Boca Raton, Fla.

Svitkin, Y. V., Pause, A., Haghighat, A., Pyronnet, S., Witherell, G., Belsham, G. J., and Sonenberg, N. (2001). The requirement for eukaryotic initiation factor 4A (eIF4A) in translation is in direct proportion to the degree of mRNA 5' secondary structure. *RNA* **7**, 382-94.

Tan, R., and Frankel, A. D. (1995). Structural variety of arginine-rich RNA-binding peptides. *Proc Natl Acad Sci U S A* **92**, 5282-6.

Tanguay, R. L., and Gallie, D. R. (1996a). Isolation and characterization of the 102-kilodalton RNA-binding protein that binds to the 5' and 3' translational enhancers of tobacco mosaic virus RNA. *J Biol Chem* **271**, 14316-22.

Tanguay, R. L., and Gallie, D. R. (1996b). The effect of the length of the 3'-untranslated region on expression in plants. *FEBS Lett* **394**, 285-8.

Tarun, S. Z. and Sachs, A. B. (1995). A common function for mRNA 5´ and 3´ ends in translation initiation in yeast. *Genes Develop* **9**, 2997-3007.

Tarun, S. Z., Jr., and Sachs, A. B. (1996). Association of the yeast poly(A) tail binding protein with translation initiation factor eIF-4G. *EMBO J* **15**, 7168-77.

Thouvenel, J. C., Dollet, M., and Fauquet, C. (1976). Some properties of Peanut Clump, a newly discovered virus. *Annu. Appl. Biol.* **84**, 311-320.

Thouvenel, J. C., Fauquet, C., and Dollet, M. (1978). Transmission par la graine du virus du clump de l'arachide. *Oléagineux* **33**, 503-504.

Tomashevskaya, O., Solovyev, A., Karpova, O., Fedorkin, O., Rodionova, N., Morozov, S., and Atabekov, J. (1993). Effects of sequence elements in the potato virus X RNA 5' non-translated alpha beta-leader on its translation enhancing activity. *J Gen Virol* **74**, 2717-2724

Tretheway, D. M., Yoshinari, S., and Dreher, T. W. (2001). Autonomous role of 3'-terminal CCCA in directing transcription of RNAs by Qbeta replicase. *J Virol* **75**, 11373-83.

Tsai, C. H., and Dreher, T. W. (1991). Turnip yellow mosaic virus RNAs with anticodon loop substitutions that result in decreased valylation fail to replicate efficiently. *J Virol* **65**, 3060-7.

Tsai, C. H., and Dreher, T. W. (1992). Second-site suppressor mutations assist in studying the function of the 3' noncoding region of turnip yellow mosaic virus RNA. *J Virol* **66**, 5190-9.

Turner, R. L., Glynn, M., Taylor, S. C., Cheung, M. K., Spurr, C., Twell, D., and Foster, G. D. (1999). Analysis of a translational enhancer present within the 5'-terminal sequence of the genomic RNA of potato virus S. *Arch Virol* **144**, 1451-61.

Uchida, N., Hoshino, S., Imataka, H., Sonenberg, N., and Katada, T. (2002). A novel role of the mammalian GSPT/eRF3 associating with poly(A)-binding protein in Cap/Poly(A)-dependent translation. *J Biol Chem* **277**, 50286-92.

Uhlenbeck, O.C. (1995) Keeping RNA happy. *RNA*, **1**, 4-6.

van Belkum, A., Cornelissen, B., Linthorst, H., Bol, J., Pley, C., and Bosch, L. (1987). tRNA-like properties of tobacco rattle virus RNA. *Nucleic Acids Res* **15**, 2837-50.

Vende, P., Piron, M., Castagne, N., and Poncet, D. (2000). Efficient translation of rotavirus mRNA requires simultaneous interaction of NSP3 with the eukaryotic translation initiation factor eIF4G and the mRNA 3' end. *J Virol* **74**, 7064-71.

Varshney, U., Lee, C.P. and RajBhandary, U.L. (1991) Direct analysis of aminoacylation levels of tRNAs in vivo. Application to studying recognition of *Escherichia coli* initiator tRNA mutants by glutaminyl-tRNA synthetase. *J Biol Chem*, **266**, 24712-24718.

Vlot, A. C., Neeleman, L., Linthorst, H. J., and Bol, J. F. (2001). Role of the 3'-untranslated regions of alfalfa mosaic virus RNAs in the formation of a transiently expressed replicase in plants and in the assembly of virions. *J Virol* **75**, 6440-9.

Wang, L., and Wessler, S. R. (2001). Role of mRNA secondary structure in translational repression of the maize transcriptional activator Lc(1,2). *Plant Physiol* **125**, 1380-7.

Wang, S., Browning, K. S., and Miller, W. A. (1997). A viral sequence in the 3'-untranslated region mimics a 5' cap in facilitating translation of uncapped mRNA. *EMBO J* **16**, 4107-16.

Wang, S., Guo, L., Allen, E., and Miller, W. A. (1999). A potential mechanism for selective control of cap-independent translation by a viral RNA sequence in cis and in trans. *RNA* **5**, 728-38.

Weiland, J. J., and Dreher, T. W. (1989). Infectious TYMV RNA from cloned cDNA: effects in vitro and in vivo of point substitutions in the initiation codons of two extensively overlapping ORFs. *Nucleic Acids Res* **17**, 4675-87.

Weiland, J. J., and Dreher, T. W. (1993). Cis-preferential replication of the turnip yellow mosaic virus RNA genome. *Proc Natl Acad Sci U S A* **90**, 6095-9.

Wells, D. R., Tanguay, R. L., Le, H., and Gallie, D. R. (1998a). HSP101 functions as a specific translational regulatory protein whose activity is regulated by nutrient status. *Genes Dev* **12**, 3236-51.

Wells, S. E., Hillner, P. E., Vale, R. D., and Sachs, A. B. (1998b). Circularization of mRNA by eukaryotic translation initiation factors. *Mol Cell* **2**, 135-40.

Wentz, M. J., Patton, J. T., and Ramig, R. F. (1996). The 3'-terminal consensus sequence of rotavirus mRNA is the minimal promoter of negative-strand RNA synthesis. *J Virol* **70**, 7833-41.

Wesley, S. V., Mayo, M. A., Jolly, C. A., Naidu, R. A., Reddy, D. V., Jana, M. K., and Parnaik, V. K. (1994). The coat protein of Indian peanut clump virus: relationships with other furoviruses and with barley stripe mosaic virus. *Arch Virol* **134**, 271-8.

Williams, M. A., and Lamb, R. A. (1989). Effect of mutations and deletions in a bicistronic mRNA on the synthesis of influenza B virus NB and NA glycoproteins. *J Virol* **63**, 28-35.

Wu, B., and White, K. A. (1999). A primary determinant of cap-independent translation is located in the 3'-proximal region of the tomato bushy stunt virus genome. *J Virol* **73**, 8982-8.

Wu, X., Xu, Z., and Shaw, J. G. (1994). Uncoating of tobacco mosaic virus RNA in protoplasts. *Virology* **200,** 256-62.

Yoshinari, S., and Dreher, T. W. (2000). Internal and 3' RNA initiation by Qβ replicase directed by CCA boxes. *Virology* **271,** 363-370.

Yoshinari, S., Nagy, P. D., Simon, A. E., and Dreher, T. W. (2000). CCA initiation boxes without unique promoter elements support in vitro transcription by three viral RNA-dependent RNA polymerases. *RNA* **6,** 698-707.

Zeenko, V. V., Ryabova, L. A., Spirin, A. S., Rothnie, H. M., Hess, D., Browning, K. S., and Hohn, T. (2002). Eukaryotic elongation factor 1A interacts with the upstream pseudoknot domain in the 3' untranslated region of tobacco mosaic virus RNA. *J Virol* **76,** 5678-91.